FACULTY OF SCIENCE AND TECHNOLOGY

MASTER'S THESIS

Study programme / specialisation: Offshore Field Development Technology, 3011	The *(**spring**/autumn)* semester, *2023* **Open** / Confidential
Author: Nikita Viazikov	
Supervisor at UiS: Professor Ove Tobias Gudmestad Co-supervisor: External supervisor(s):	
Thesis title: Methods for in-line diagnostics of in-field pipelines during subsea production with application(s)	
Credits (ECTS): 30 ECTS	
Keywords: OLGA, PVTSim, pipeline, ILI, flow assurance, hydrates, pig, smart pigging, multiphase flow	Pages: 70 + appendix: 39 Stavanger, *15.06.2023*

Table of contents

1. Executive summary

This thesis serves as a comprehensive study incorporating smart pigging technology and software modeling applications for flow assurance purposes, with a special emphasis on subsea pipelines.

In the modeling chapters, OLGA and PVTSim software packages were used to build a model of a hypothetical subsea pipeline, which is based on the example of the Kirinskoye gas condensate field.

The constructed dynamic model addresses several crucial aspects of pipeline flow assurance, namely:

1) Hydrate formation zones within a pipeline: their location diagnostics and mitigation via continuous inhibitor injection;

2) Estimation of the required slugcatcher unit's capacity for liquid collection and water disposal.

As a result of the simulations and their analysis, the following goals were achieved:

1) The hydrate formation zone within the pipeline is located and the optimal solution to mitigate the issue is proposed and justified based on the multiple hydrate formation simulations' results. The environmental effect of the solution for the hydrate problem mitigation is also taken into account, and the minimization of its ecological imprint is justified.

2) Liquid surge volumes for the cases of stabilized operational conditions and pig run are modeled in relation to the two project-proposed flow values within the pipeline: $2{,}64 \cdot 10^6$ m^3/day and $3{,}5 \cdot 10^6$ m^3/day, respectively. All of the cases modeled are proven to lie within the slugcatcher's liquid receiving capacity. The optimal value of flow for the system is proposed and justified.

3) Pig run velocities for both flow value cases considered are calculated. It is concluded that in both pig runs an intelligent pig of any physical measurement principle considered in the thesis can be implemented without a reduction in the quality of measurements.

2. Introduction

2.1. Background

Transporting a large volume of crude, natural gas, condensate, and refined products, pipeline networks are crucial for the petroleum industry overall. And, being the only way to maintain continuous flow within the system, in-field pipelines are taking a core role.

As with any other equipment, pipelines require regular diagnostics and maintenance to avoid critical situations that might cause a wide range of troubles, starting from unplanned downtime to very loss of structural integrity. All those problems might be caused thanks to several factors including corrosion and reduction or complete clogging of the cross-sectional area.

The question of proper diagnostics of all the troubles named becomes especially important when it comes to the subsea field development, where access to the pipelines' outer wall is either severely hampered or even completely impossible due to trenching protection. Presently, in this kind of operations environment, the means of in-line pipe diagnostics and modeling are representing the most accurate and reliable tools of diagnostics available.

2.2. Objective

This Master's thesis scope is centered around in-line pipe corrosion diagnostics via smart pigging and the software modeling of the operations related to it. As well as software modeling of water, hydrate, paraffin, and/or asphaltene accumulation, which will also define the frequency of the conventional (non-smart) pigging required to maintain the pipeline's safe operations state.

The modeling in this work is conducted for a hypothetical pipeline, which is defined based on the actual pipeline data from Kirinskoye gas condensate field. The conducted modeling covers the problem of hydrate formation in the pipeline system, as well as selects an optimal solution for the given case; it also covers the operational problems related to the liquid being held up along the pipeline and its removal process via pigging; pig velocity limitations for the intelligent runs are considered.

2.3. Definitions

Bubble point – the temperature at which the first vapor bubble appears out of a liquid mixture made of two or more components.

Cloud point – the temperature below which solution loses its transparency due to the emulsion formation in “liquid-liquid” systems or the formation of a sol/suspension in “liquid-solid” systems.

Colligative properties – are the properties of chemical solutions that are dependent on the number of molecules in the solvent and regardless of the molecules’ nature.

Ferromagnetic material – a material that is noticeably attracted to magnets due to its magnetic permeability. Magnetic permeability defines the induced magnetization in the vicinity of another magnet's field.

Sour corrosion – corrosion mechanism based on the primary presence of H_2S in the feed stream; requires water to be presented for the corrosion reaction to appear; CO_2 can also be presented in small quantities but will not be the main corrosion driver in this case.

Sweet corrosion – corrosion mechanism based on the primary presence of CO_2 in the feed stream; requires water to be presented for the corrosion reaction to appear.

2.4. Abbreviations

EMAT	Electromagnetic acoustic transducer
FBE	Fusion-bonded epoxy
GCF	Gas condensate field
IEC	Inspection eddy current
ILI	In-line inspection
MEG	Mono-Ethylene Glycol
MFL	Magnetic flux leakage
NDT	Non-destructive testing
PE	Polyethylene
PPM	Parts per million
PT	Pressure and temperature
ROV	Remotely operated vehicle
SP	Subsea pipeline
UT	Ultrasonic test
WAT	Wax appearance temperature

3. Subsea pipelines' specifics

The requirements for the design, construction, and operation of subsea pipelines (further SP) have their own specific features in comparison to onshore ones. Those features are defined by numerous factors, among which are **[1]**:

1. Buoyancy
2. On bottom stability and needs for trenching
3. Aggressive sea media
4. Absence of intermediate compressor stations
5. Effects of winds, currents, and waves
6. Bottom bathymetry
7. Impacts with anchors and trawl-boards, needs for protection
8. In freezing waters - lack of year-round access for inspection and maintenance, etc.

One of the main attributes of an SP, undoubtedly, is represented by severely hampered access to the pipelines' outer wall due to its subsea placement. It might be aggravated even further by the presence of the concrete weight coating, trenching protection, and by the limited navigable period in freezing waters.

As of today, the combination of the factors described above leaves practically no alternatives for industry professionals to conduct diagnostics of SPs via any other methods but in-line ones, which are mainly represented by smart-pigging solutions.

The most distinct differences in in-line diagnostics for an SP compared to an on-shore pipeline are hidden behind the pig movement trajectory: if possible, a "circular" pig trajectory will be implemented, which would require two parallel lines of identical inner diameter. This pigging scheme allows both inserting and catching the pig in an easily accessible point, such as a shoreline pig launching and receiving unit. However, this pigging scheme is not always an option due to several reasons, the most unavoidable of which is limited time and funds in the early stage of the field development.

In the early stage of field development, the production company always needs to start commercial development as soon as possible. Since constructing a two-line production SP requires a significant amount of both time and investments, the field's production process is, almost as a rule, starting with a one-line SP. This makes the "linear" pigging trajectory the only option applicable, where the pig will be inserted through a special loading chamber in the area of the subsea manifold.

4. Subsea pipelines flow assurance

Flow assurance is a crucial part of the hydrocarbon industry's midstream ecosystem. It refers to the set of practices and technologies that aim to ensure the continuous and safe transportation of hydrocarbons: from a wellhead to a refining facility as well as from a refining facility to an end-customer, both of which are mainly conducted via a pipeline network.

In terms of subsea development in particular, SPs are serving as the only way to deliver the hydrocarbons produced from a subsea field to a refining facility, whether the last one is an offshore or an onshore one. In this case, flow assurance is conducted via pipelines' transient modeling and regular surveying to constantly monitor the rate of corrosion and its severeness, as well as water, hydrate, paraffine, and asphaltene accumulation within the pipeline. It also includes measures against the build-up of the factors named, the most important of which are: maintaining the desired Pressure and Temperature (PT) conditions within the system, injection of inhibitors, and mechanical intervention.

4.1. Corrosion

For a subsea pipeline, as for any other one, corrosion can be divided into two types relative to its wall: an internal and an external one, respectively.

Whereas the external corrosion for a subsea pipeline during its operational stage of life is represented exclusively by water corrosion, the internal one might be caused due to several factors, the most important amongst which are: condensed water, CO_2, and H_2S. The factors named will be discussed in the chapter's sections related to them.

It is also worth mentioning that in terms of industry-scale trends related to the pipelines' corrosion, and SPs corrosion data in particular, the three following dependencies can be identified **[2]**:

1) Pipelines of a larger diameter are less subjected to corrosion in comparison with the smaller diameter ones. This trend is explained due to the fact that most of the small-diameter pipelines in the industry are the in-field ones and the feed transported by them is much more corrosively aggressive than for the larger-diameter ones, which are much more commonly used as the gathering and export pipelines.

2) The frequency of corrosion-related failures is directly dependent on a pipeline wall thickness: the thicker the wall – the less likely its structural integrity to be compromised by the corrosion before the critical spot will be noticed during a planned survey.

3) Due to the combination of high and even conductivity of the surrounding seawater, combined with modern multilayer coating and cathodic protection, SPs are much less susceptible to external corrosion than onshore pipelines.

4.1.1. Water corrosion

Out of all the substances coming into contact with a pipeline during its lifecycle, water is the one that causes the most problems, since it is capable of corroding the pipe by itself and, simultaneously, plays a key role in CO_2 and H_2S corrosion mechanisms.

Pipeline internal corrosion is not spread equally along its length. The zone subjected to the most severe corrosion is always located a couple of kilometers downstream from the pipeline's starting point. In this area, the temperature drop becomes sufficient to cause condensation for most of the water particles in the stream. In the industry's practice, it was observed that after reaching its peak rate in this zone, the corrosion rate tends to fade as the stream flows further down the pipe. This effect is taking place due to the further reduction of the stream's temperature, which significantly reduces the internal corrosion rate.

For the SPs, as well as for the onshore ones, the most efficient way to prevent all the water-related corrosion processes are to remove as much water from the feed contents as technologically and economically possible for every case. For this purpose, most of the recently developed subsea fields are equipped with subsea separators that are capable of stripping water from both gas and oil crude streams. Although most of the water is being removed by this measure, some water particles will still be presented in the feed stream, and, especially for the gas fields, it creates a significant problem, which is being solved via scheduled pigging runs.

Regarding external corrosion: subsea pipelines rarely suffer from the loss of their structural integrity and/or loss of containment due to it. Present-day subsea pipelines are, almost as a rule, covered with multi-layer protection, which includes both thermal insulation and, in some cases, concrete coating. All the coating layers applied contribute to the reduction of the pipeline's outer wall's chance to be exposed to seawater. However, if all the coating protection layers were breached, and the pipeline's wall made direct contact with the surrounding water, the sacrificial anodes, connected to the pipe, are starting their job as a part of the cathodic protection system.

Cathodic protection has a significant and easily-calculatable corrosion-preventative capacity. This fact, combined with the regular ROV-based visual inspection, allows the industry engineers to plan replacement schedules for the sacrificial elements upfront for months, thus almost nullifying the effect of the external water-related corrosion on a subsea pipeline.

4.1.2. CO_2 corrosion

Pure CO_2 in its liquid and gaseous states does not inflict metal corrosion. However, as soon as there are some water particles covering the steel surface, the following reaction takes place:

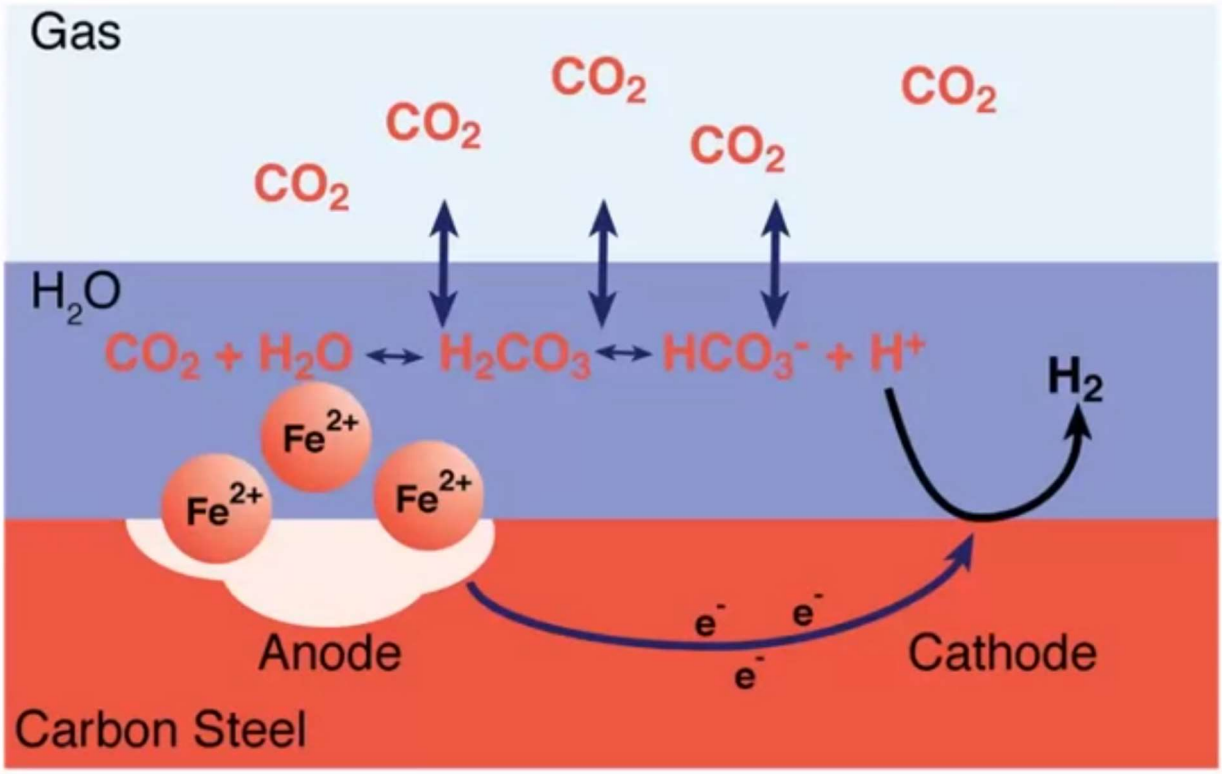

Figure 1. CO_2 (Sweet) corrosion mechanism

Source: "Protecting the World: Oilfield corrosion and control - Sweet corrosion", The University of Manchester lecture course on Coursera, [3].

As can be seen from Figure 1, CO_2 dissolving in water initially forms a weak Carbonic acid. This acid, although corrosive by itself, almost immediately dissolves, leaving H^+ atoms, thus causing the Cathodic reaction on the inner surface of the pipeline's wall. There are plenty of parameters affecting the corrosion reaction rate in this case **[3]**:

- CO_2 partial pressure;
- Fluid chemistry / pH / flow;
- Steel chemistry and microstructure;
- Temperature and the presence of microscales.

The last parameter requires some clarification to be provided: up to temperatures of approximately 70°C, the corrosion rate is constantly growing with an increase in temperature. However, above this temperature threshold, crystals of Siderite ($FeCO_3$) are starting to form on the carbon steel's surface. Those crystals do not only cover the steel's surface, thus protecting it from reaction with H^+ atoms but also, being of a non-conductive nature, reducing the areas which might have served as potential anodes to the corrosion reaction.

The sweet corrosion might result in multiple metal loss defects, the most frequent of which are: uniform corrosion, pitting, and mesa corrosion.

4.1.3. H_2S corrosion

The mechanism of H_2S corrosion (also known as sour corrosion) is essentially identical to the sweet corrosion mechanism: hydrogen sulfide in an absolutely dry feed is also non-corrosive by itself. However, as soon as the water is presented, the following reaction takes place:

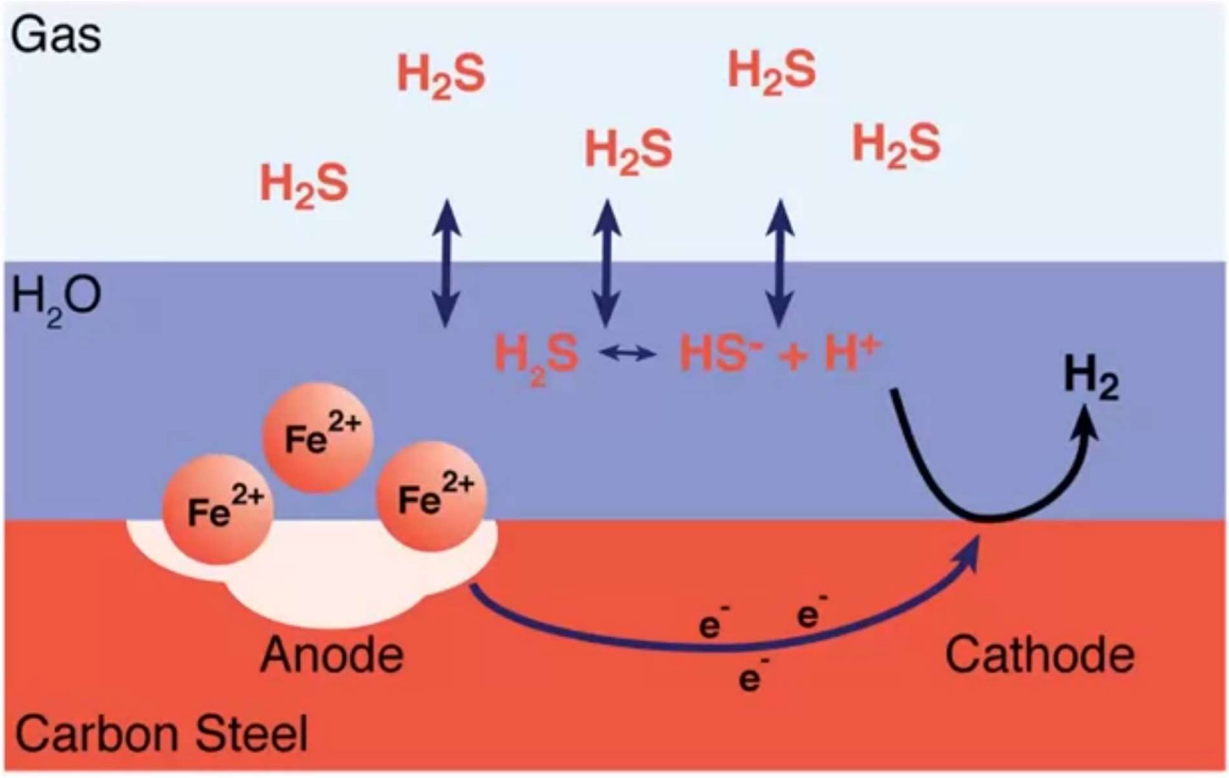

Figure 2. H_2S (Sour) corrosion mechanism
Source: "Protecting the World: Oilfield corrosion and control - Sour corrosion", The University of Manchester lecture course on Coursera [4].

The sour corrosion mechanism represented in Figure 2 is remarkably close to the CO_2-inflicted one, which was explained in detail in the previous section. The H^+ atoms left after hydrogen sulfide are dissolved in the water and entering the Cathodic reaction on the pipeline's wall, thus inflicting corrosion on it.

The list of parameters affecting the corrosion reaction rate consists of the following **[4]**:

- H_2S partial pressure;
- Fluid chemistry / pH / flow;
- Steel chemistry and microstructure;
- Temperature and the presence of microscales;
- Applied and/or residual stress in the material.

Although the sour corrosion reaction looks extremely close to the sweet one, some dependencies of its reaction rate parameters differ quite drastically. In particular, the formation of protective scales does not directly improve with an increase in stream temperature: the protective layer degradation starts around 100ºC, almost nullifying its effect for the higher temperature cases.

The sour corrosion results in severe metal defects, most of which are represented by pitting and cracking. The cracking inflicted by this reaction has three main types, which are known as:

- Sulfide Stress Cracking (SSC)
- Step Wise Cracking or Hydrogen-Induced Cracking (SWC / HIC)
- Stress Oriented Hydrogen-Induced Cracking (SOHIC)

4.2. Multiphase flow

Multiphase flow is a flow of more than one fluid (phase). The examples of multiphase flow regimes are represented in Figure 3 below.

Although the definition leaves a significant variety of options, there are only three main types of multiphase flow cases in the midstream sector of the hydrocarbon industry:

1) “Gas & liquid phase” – the most common case; the liquid phase is represented by water, condensate, oil, or their mixture/emulsion;

2) “Liquid phase 1 & liquid phase 2” – where the phases are represented by water and liquid hydrocarbons, which are immiscible in each other (thus, either having a distinct phase boundary or forming an emulsion in case of being severely mixed);

3) ”Gas & liquid phase 1 & liquid phase 2” – an extremely rare case in its pure form; appears only under severely low velocities, where the system has a distinctly stratified flow due to the density differences of the fluids.

Additionally, it is worth mentioning that the presence of solid particles in a stream provides an additional phase, which inflicts the problem of pipeline erosion. However, this issue significantly differs from other multiphase-flow-inflicted constraints, and, simultaneously, has almost no effect on the flow regime, if the number of solid particles remains at an adequate level for the safe operation of the system. Note that the problem of pipeline erosion will be considered in a separate section.

As a rule, any multiphase flow system should be operated while taking into account the possibility of pressure surges, also known as water hammers. Although the effect is commonly associated with liquid streams, it is also presented in “gas & water” and purely gas flows; however, posing a much lesser potential threat to a pipeline in the last case, due to the lesser inertia of a gas stream in comparison with a liquid stream of a same velocity. The threat dictates the rapidity of stopping the flow within the system and might lead to leaks or even a pipe rupture, and, thus, must always be taken into account.

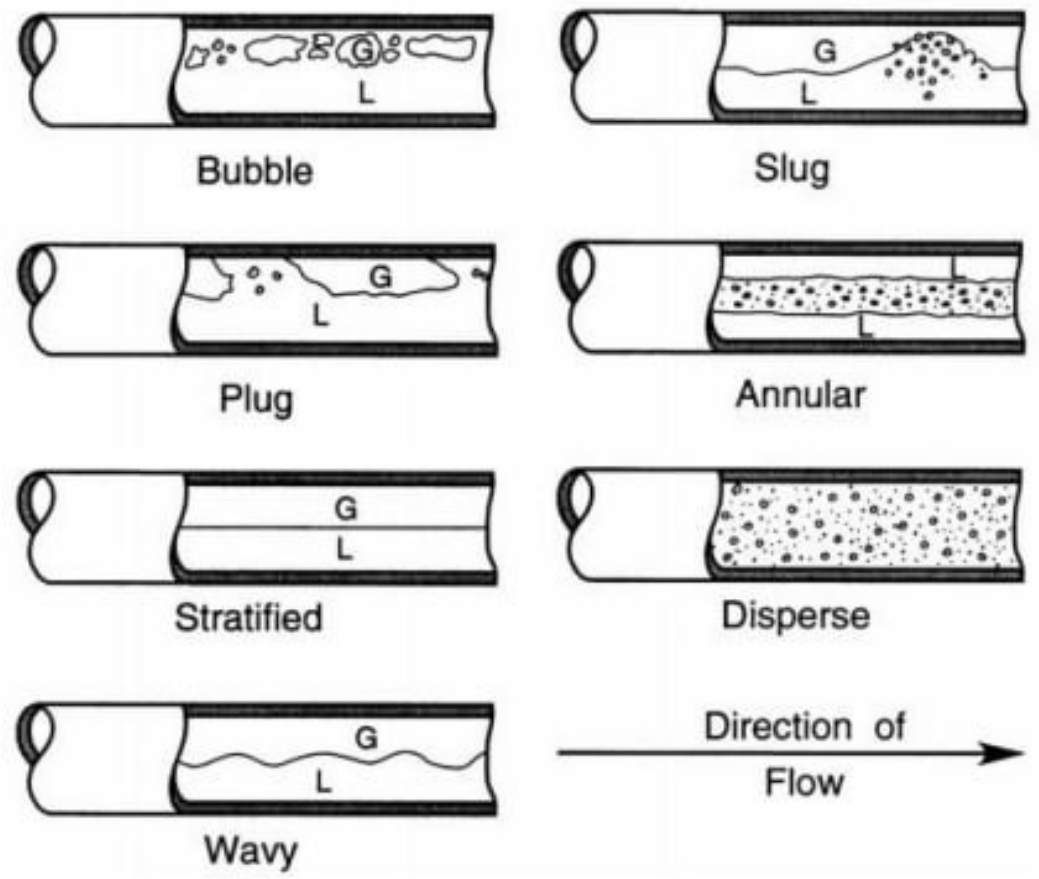

Figure 3. Two-phase flow regimes: L – liquid, G - gas
Source: "Handbook of Fluids in Motion" by Weisman, J. [5].

Especially the problem of pressure surges aggravates in the "gas & liquid" multiphase pipelines. There are two main reasons for that:

- Hydrodynamic slugs;
- Terrain-induced slugs;

Whereas hydrodynamic slugs can irregularly appear at certain flowrates causing stochastic loads onto the system, terrain-induced slugs are formed due to the differences in the altitude along a pipeline. Terrain-induced slugs are significantly more predictable in their appearance. The slug problems are fought by a combination of the three following practices:

1) Reduction in the liquid phase content of a stream (if possible and economically feasible);

2) Maintaining the stream's velocity at the level, which prevents liquid (water and/or condensate) accumulation in the terrain-lowered pipeline's areas;

3) Regular removal of the accumulated liquid via physical intervention by pigging operations.

Finally, a flow-related issue experienced by any multiphase pipeline is the inner-flow-induced vibrations. The vibrations can appear due to both the high velocity of the flow (turbulent flow regimes) and due to the two-phase plug flow. The problem imposes equipment to an increased fatigue rate, which could lead to a faster equipment failure; thus, flow-induced vibrations must be mitigated. The mitigation is commonly conducted by real-time operation mode adjustments since its appearance can hardly be forecasted.

4.3. Erosion

Pipeline erosion is a gradual loss of a pipeline's inner wall material; commonly expressed as metal loss, mm/year **[6]**. The process occurs through three main mechanisms:

1) Erosion by solid particles – the most common and frequently considered type; rate of erosion, in this case, correlates with flow velocity, solid particle's size and hardness, and the number of solid particles present in the stream.

2) Erosion by droplets of liquid – relevant for the "gas & liquid" multiphase flow systems with high flow velocities; the erosion rate correlates with the size and number of droplets in the stream and the stream's velocity.

3) Erosion by cavitation – the phenomenon is caused by severe pressure fluctuations in a stream, e.g., when hydraulic hammering is occurring. In a low-pressure period of the cycle, the pressure might drop so low that it will cause partial evaporation of the fluid in the stream, which will lead to the formation of vapor-filled bubbles. When the bubbles are experiencing high pressure again, they collapse producing an implosion. When it takes place near the pipeline's wall, its erosion is caused.

The list of erosion mitigation practices includes downhole screens and infield separation units, as well as the selection of optimal flow regimes for each pipeline's case based on the results of the dynamic modeling conducted.

4.4. Wax accumulation

Wax accumulation poses a severe threat to any element of the system on its way from the reservoir up to the very refinery plant. When deposited, wax accumulations can consist of a range of substances such as normal and branched paraffins, incorporated oil, etc.; however, the primary role in the wax accumulation is played by paraffins of $C7^{+}$.

The primary threat of the wax accumulation is considered to be its sedimentation on the pipeline's walls, which, if uncontrolled, will continue its gradual increase and will start limiting the maximum flow capacity of the pipeline. If the problem is not solved timely, a complete obstruction of the pipeline's segment can occur, which will result in a stop of continuous production and/or transportation until the flow obstruction will be removed. Additionally, the wax formation can not only pose a threat to the continuity of the production and/or transportation process while their active stage, but also will cause difficulties to restart flow within the system due to the wax solids appearance. The wax solids when are formed within the oil causing it to turn into "gel" under temperatures below WAT even while a relatively-short shut-in period.

The abbreviation of WAT stands for "Wax Appearance Temperature", and is also known as "Cloud point" as the formation of paraffins under the temperatures below it obstructs the light penetration through oil liquid, thus making it "cloudy" and untransparent. The second point characterizing the wax properties of the oil is called a "Pour point" and refers to the temperature at which an oil loses its ability to flow under the system's conditions. The two points named are used to provide a general understanding of system conditions when the wax formation and oil gelling will pose a threat to the system.

To conduct a full-scale wax deposition prediction for each particular case, highly precise data on the chemical composition of the fluid has to be accessible – to obtain it, gas chromatography is used. The chemical composition data is used to conduct thermodynamic modeling, which will allow to build a wax formation chart as a function of pressure/temperature relationship, and forecast in which segments

of the pipeline the wax deposition will occur as well as how high the accumulation rate will be. Having the answers to these questions will allow industry flow assurance engineers to plan the wax management and remediation methods to be applied.

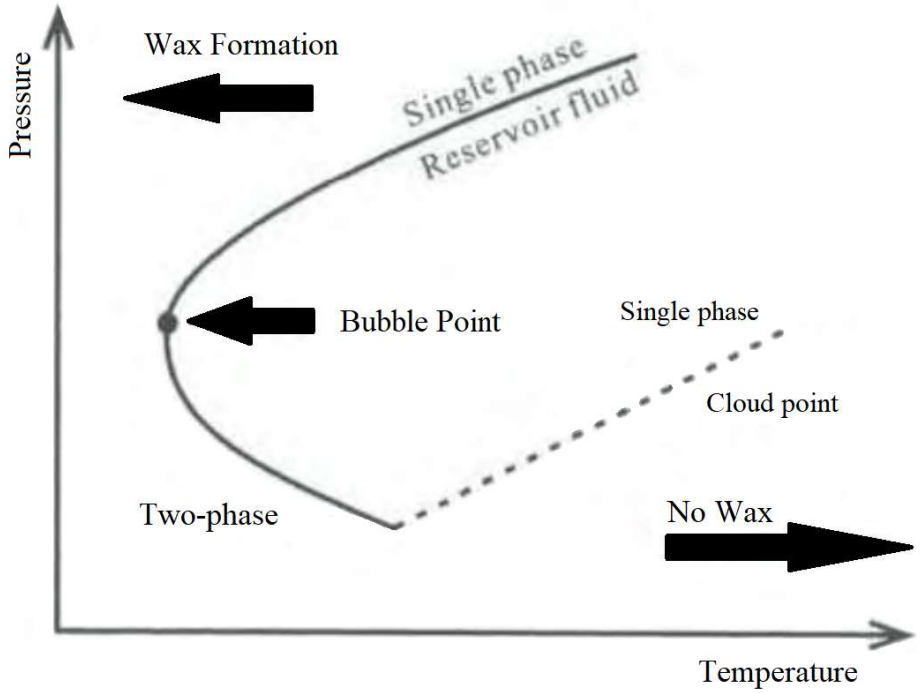

Figure 4. Wax formation as a function of pressure/temperature relationship
Source: "Subsea Pipelines and Risers" by Yong Bai & Qiang Bai [7].

There are three main methods that are forming the core of wax management: thermal insulation (including pipeline heating), inhibitor injection, and pigging.

In some cases, soundly designed and applied thermal insulation can completely eliminate the problem of wax deposition in the system by keeping the temperature above the WAT along an entire pipeline.

The injection of inhibitors can almost never fully prevent wax deposition – its main purpose is to significantly reduce the deposition rate, thus allowing to reduce the required frequency of mechanical intervention operations for the wax removal.

Pigging is the most-commonly applied way of mechanical intervention for wax control. It has to be applied frequently, to prevent an excessive wax buildup since in the case of a thick wax layer the maximum allowable pressure applied might be insufficient to push the pig through the line with all the wax accumulated in front of it. The design process of the pigging schedule is conducted via specialized

dynamic modeling software (e.g., OLGA by Schlumberger), and has to be planned in a way such that pig runs will neither be too frequent to be uneconomical, nor too rare to bear risk for the pig-sticking in a flowline throughout its run.

As for the additional wax remediation methods: heating, injection of wax solvents and dispersants, etc. might be used. However, these practices are rarely used as a main tool for wax removal and are mostly used in coherence with pigging instead of replacing it completely.

4.5. Asphaltene accumulation

Asphaltenes are high-molecular-weight components, which originate from the complex molecules of living organisms both plants and animals. Being not fully broken down over geologic time by high pressure and temperature conditions, they are composed of polyaromatic and heterocyclic aromatic rings along with oxygen, nitrogen, and sulfur. They are insoluble by common petroleum solvents such as n-heptane, but can be solved by aromatic solvents, e.g., toluene.

Although asphaltenes are present in some quantities in all oils, they do not pose any problem while being stable. The stability of asphaltenes directly correlates with asphaltenes' ratio to stabilizing components such as aromatics and resins, as well as pressure and temperature conditions.

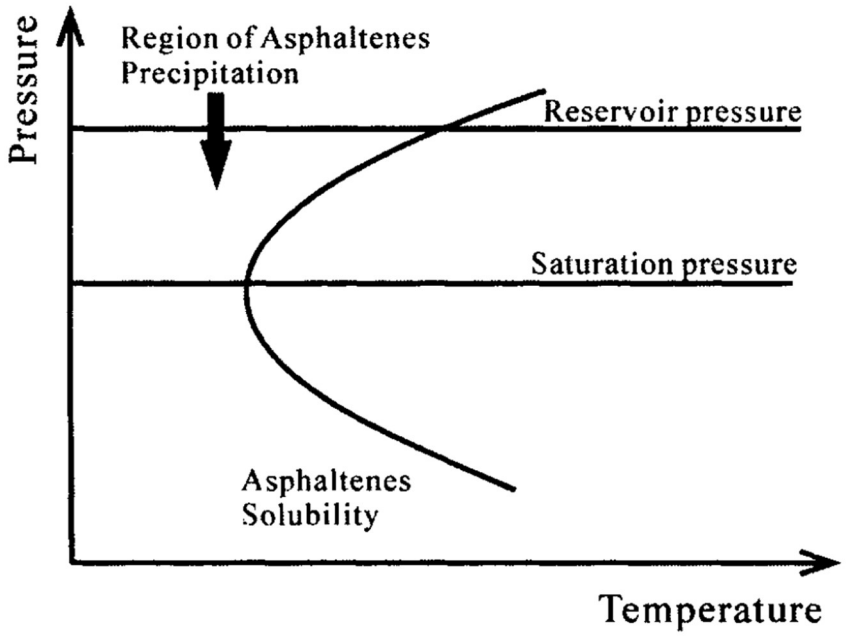

Figure 5. Asphaltene formation as a function of pressure/temperature relationship
Source: "Subsea Pipelines and Risers" by Yong Bai & Qiang Bai [7].

Precipitation of asphaltenes has similar consequences as from waxes, thus these two problems are always considered simultaneously. It poses a threat to limit the flow capabilities of a pipeline, and can even obstruct the cross-section completely. As an addition to that, asphaltene solids have a severe effect on the stabilization of the oil-water emulsions in the pipeline.

There are several means to assess the asphaltene-precipitation-capabilities of oil, e.g., P-value test, PVT analysis, and SARA screening test. The SARA test mechanism is based on determining the relation between pairs of primary crude components such as saturating to aromatics and asphaltenes to resins, which are used to determine the asphaltenes' stability in it.

As can be seen from the asphaltene formation chart in Figure 5, maintaining the pressure-temperature conditions within the system above the asphaltene precipitation level is considered to be the main tool against the problem. If it is impossible to completely avoid asphaltene precipitation, asphaltene dispersants, and precipitation inhibitors can be injected. These actions will not completely eliminate asphaltene precipitation but will significantly reduce its speed, thus, reducing the frequency of mechanical intervention, such as pigging, for the regular removal of the asphaltenes deposited.

4.6. Hydrate accumulation

Gas hydrates, also known as clathrates, are crystalline cage-like structures, which skeleton is formed by water molecules, and can entrap small-molecule gasses such as methane, ethane, propane, butane, carbon dioxide, nitrogen, and hydrogen sulfide.

For gas hydrates to form, a very specific set of conditions has to be presented, namely: access to the small-molecule gasses, access to free water, high-enough pressure, and low-enough temperature. Knowing the chemical composition of the fluid in the system, the hydrate equilibrium curve can be constructed to define the domain of conditions allowing the hydrates to form for each particular case. A schematic example of a hydrate equilibrium curve is represented in Figure 6.

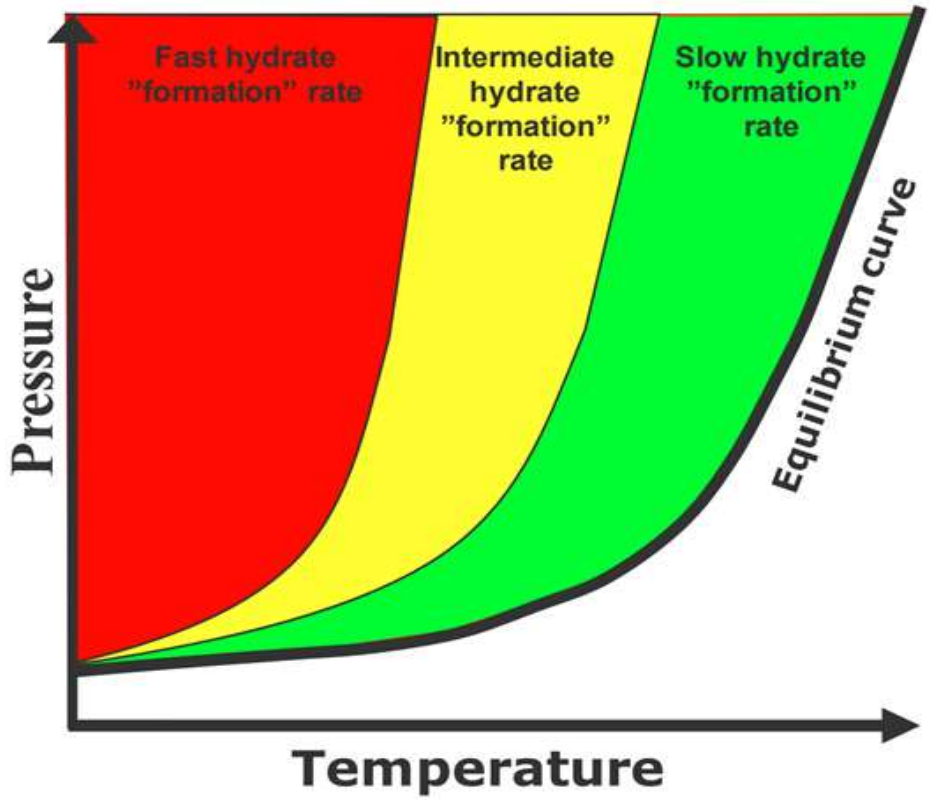

Figure 6. Schematic hydrate equilibrium curve on a pressure/temperature diagram *Source: "Introduction to Flow Assurance" by* Sigurd Næss, Equinor *[8].*

Since the formation process of hydrates does not require any specific components except for small-molecule gasses and water, which are presented in all of the production wells' and pipelines' streams, hydrate formation is a universal problem for both upstream and midstream sectors of the petroleum industry.

The consequences of hydrate formation within a pipeline include a partial flow restriction which will cause an increase in pressure drop along the pipeline, and, if not spotted and treated timely, will result in a complete blockage. Pipeline blockage will inflict operational downtime and additional costs to solve the problem, as well as will jeopardize the pipeline's integrity.

There are several hydrate-control methods, which can be divided into four main groups: process-based methods, thermal methods, hydraulic methods, and chemical methods.

1) Process-based methods are represented by gas dehydration and water cut reduction, which are both aimed to reduce the water content within the stream. Their logic is simple: the lesser material there is to form hydrates – the lesser effort engineers need to apply to keep the problem under control.

2) Thermal methods are based on the idea of maintaining the temperature along the system at such a level that the temperature level in every system's point will be higher than needed for the hydrates to form. The thermal methods might be passive, such as an application of thermal insulation, or active, e.g., direct electric heating. The active methods can be used not only as preventative measures but also as reactional ones when hydrates have already been formed.

3) Hydraulic methods are founded on the same idea as thermal ones – to keep the pressure along the system at such a level that with the given temperature the system will be out of the hydrate-formation domain at every point. Both compression and depressurization might be used in this case – the choice will depend on the required system's pressure/temperature conditions to be obtained.

4) Chemical methods are utilizing ethanol, methanol, mono-, di-, and tri-ethylene glycols, etc., to affect the equilibrium curve for the hydrate formation. They can be used as both preventative and reactive measures against the hydrates. An illustrative example can be seen in Figure 7 below:

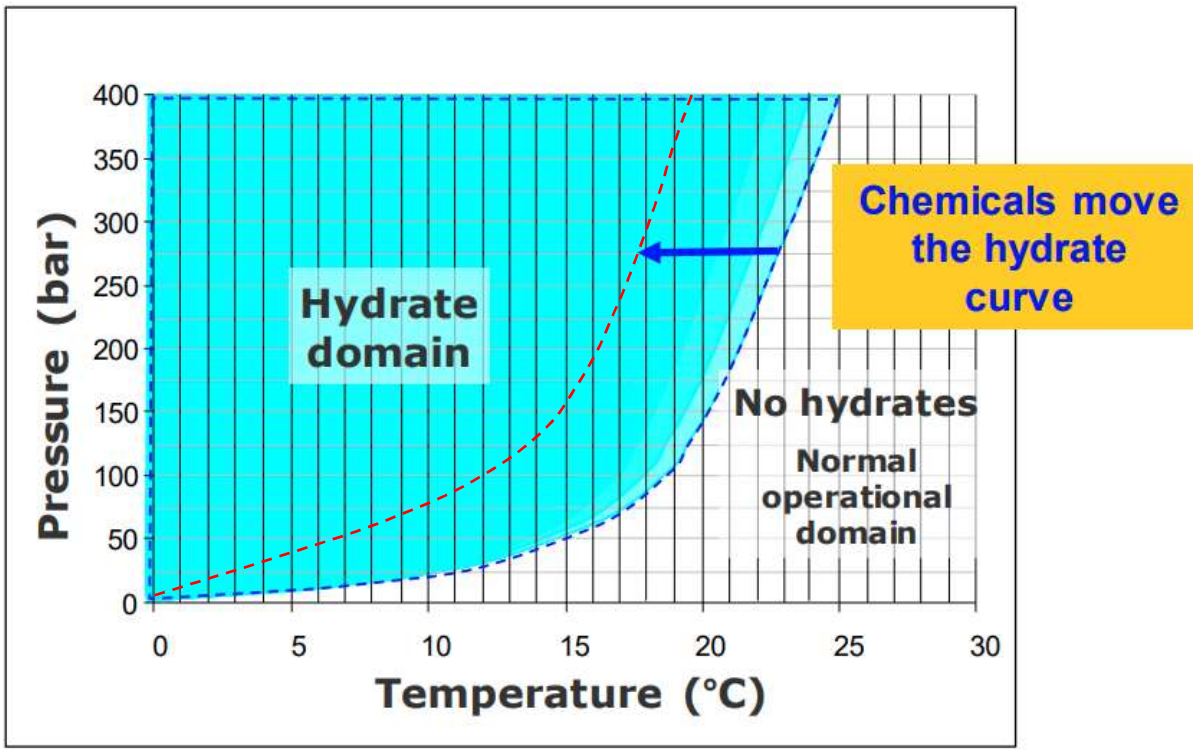

Figure 7. Schematic effect on the hydrate equilibrium curve achieved by the injection of a hydrate inhibitor in a stream
Source: "Introduction to Flow Assurance" by Sigurd Næss, Equinor *[8].*

It is important to mention that all of the hydrate-inhibiting chemicals are having colligative properties. Colligative properties are the properties of chemical solutions that are dependent on the number of molecules in the solvent and are regardless of the molecules' nature. This property implies the fact that to achieve an equal effect with different inhibitors, the molar injection rate for all these inhibitors should be the same, whereas the mass and volume rates are differing and determined by the density and molecular weight.

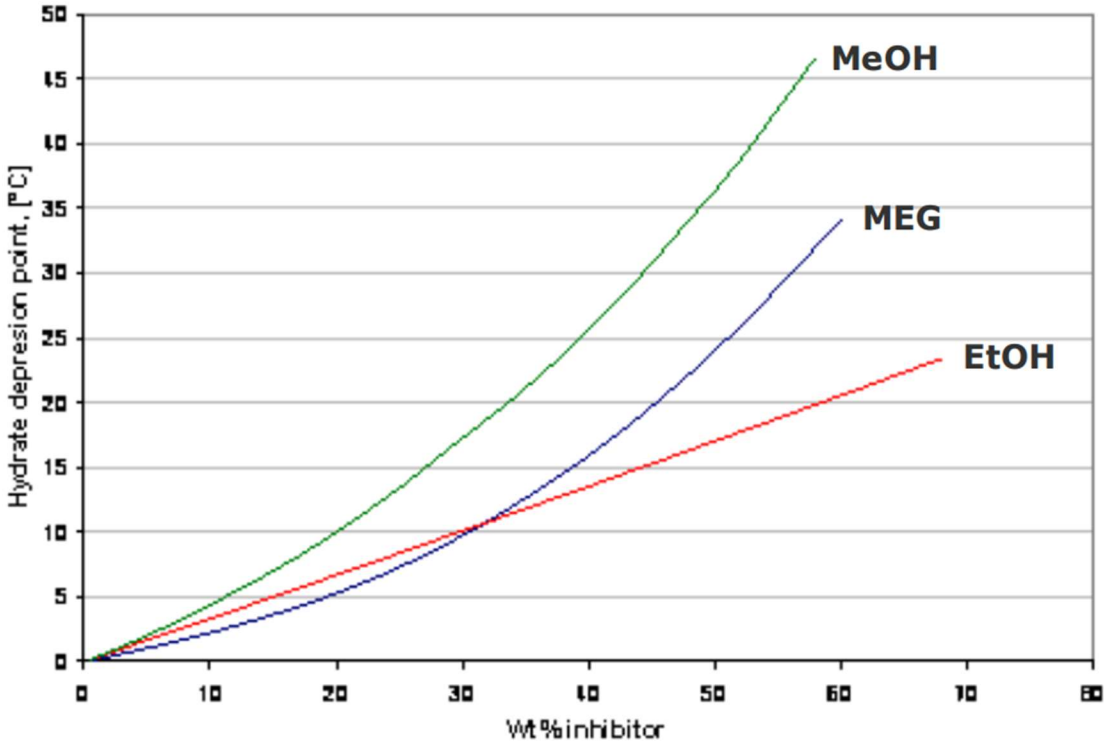

Figure 8. Hydrate depression point as a function of an injected inhibitor's percentage by weight

Source: "Introduction to Flow Assurance" by Sigurd Næss, Equinor *[8].*

In the past, pipelines had to be operated strictly out of the hydrate formation domain, however, after decades of practice, the present-day hydrate control approach has evolved. Now the operational pressure-temperature conditions partially laying within the hydrate formation domain at some system's segments has become a common practice along the industry's pipelines. However, it is worth mentioning that this approach is mostly applied to the onshore pipelines, where the project budgets and costs are significantly lower than in the subsea part of the industry, thus the relation between possible cost reduction on the inhibitors' usage to the economical risk is significantly more acceptable.

4.7. Pigging operations as a core part of the flow assurance

Plainly speaking, pigging is an action of propelling a device (called a “pig”) of a cylindrical (or, in some cases, spherical) form through a pipeline.

Pigs are always selected in a way that their outer diameter is slightly exceeding the inner diameter of the pipeline being pigged. This small difference in diameters creates an “interference” which allows the pig to successfully seal the pipeline’s cross-section while moving along its way. The force of a moving pig unit can be estimated as the pipeline’s cross-section multiplied by the force applied to the back of the pig being propelled.

At present, it is considered that the “PIG” abbreviation stands for Pipeline Inspection Gauge. However, this “official” deciphering of the abbreviation has developed sometime after the names “pig” and “pigging” became widely used in the industry. Initially, the names were universally picked by the industry specialists, which were observing the pigging operations, because of the squealing sound produced by the pig moving through a pipe.

The pig is inserted into a pipeline via a special pig launching unit which can be an onshore / platform placement or subsea installation. The onshore / platform launching units commonly can also serve as the receiving units for pigs, thus, reducing the number of structures added to the pipeline system. However, a subsea pig launching chamber can never be an endpoint for a pig run (or, at least, has never been so far in the industry) due to the fact that it has to have the capacity to receive not only the pig itself but also to safely dispose of the liquids removed by the pig run, along with waxes, asphaltenes, and other solid debris. An example of a subsea pig launching unit can be seen in Figure 9 below.

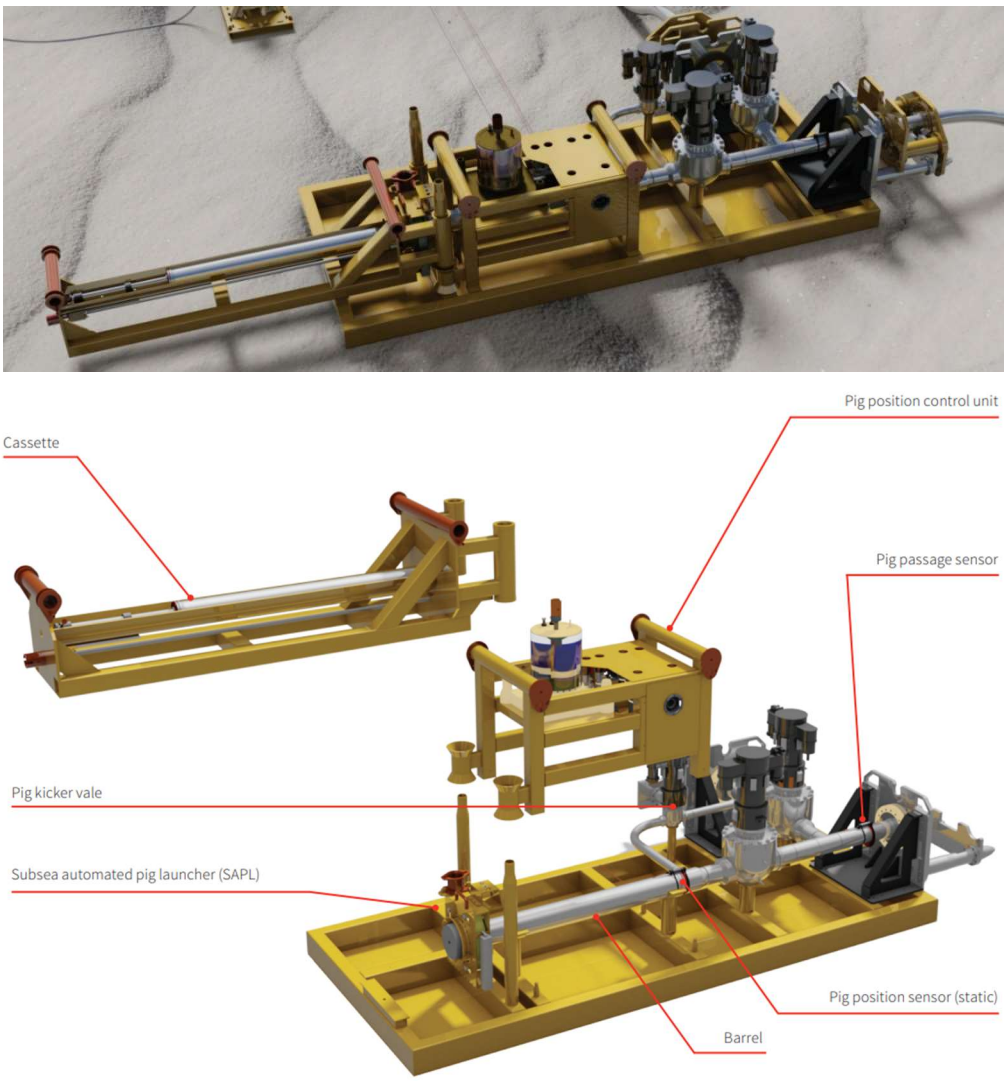

Figure 9. Schematic drawings of an automatic subsea pig launching unit
Source: "Subsea automatic pig launcher (SAPL)" flyer by NOV Completion & Production Solutions [9].

Overall, pigging is a well-known and widely-explored practice in the industry. There are several applications of this technique that make it an essential practice for the flow assurance engineers worldwide:

4.7.1. Sequential transport of hydrocarbon products

In some cases, different hydrocarbon products have to be transported sequentially via the same pipeline. The pigs used for this operation have no other purpose than to serve as a seal in between of two transported fluids and have no electronics. Such pigs are called utility pigs and have cylindrical shapes due to the better sealing capacity. Several examples of utility pigs can be seen below, in Figure 10.

Previously, industry specialists have thought that it is essential to use pigs to separate transported fluids from each other. However, at present, the techniques of transporting different hydrocarbon fluids “back-to-back”, without the sealing pigs, are widely explored and applied in most cases.

Figure 10. Examples of the cylindrical (mandrel) utility pigs
Source: “Girard Mandrel-Pigs” by Girard Industries *[10].*

4.7.2. Removal of water and liquid hydrocarbons accumulated in a pipeline

The problem is extremely relevant to the pipelines of gas and gas-condensate fields. An extensive accumulation of liquid within a pipeline can lead to a severe increase in its corrosion by the water itself, as well as by additional stream components reacting with it such as carbon dioxide and hydrogen sulfide. Additionally, to the corrosion processes, the presence of water will result in an increased pressure drop along the pipeline, a change of the flow regime to the slug and/or plug flow, and serve as an enabling environment for gas hydrates formation. Due to all of the problems named, timely removal of accumulated liquids is a crucial part flow assurance.

In most cases, liquid removal is conducted via the application of cylindrical utility pigs, which were represented in Figure 10. However, on some gas / gas-

condensate fields, pipelines are having such an extreme level of water produced and/or low flow rates that water removal operations are needed to be conducted several times per day. For those cases of extremely frequent water removal operations, the spherically shaped pigs are used.

The main benefit of spherical pigs in comparison with cylindrical ones is that a number of them (10-12 at a time) can be loaded into the launching unit. In this remotely-controlled unit, spherical pigs will be launched one by one according to a pre-programmed schedule or "manually" – via the remote controlling action of a flow assurance engineer **[11]**.

Figure 11. Spherical pigs and their launching unit on one of Tulsa's fields
Source: "The re-emergence of spherical pigs" by Larry Payne *[11].*

4.7.3. Removal of wax, asphaltenes, and solid debris from a pipeline

Each of the substances named is always presented in a pipeline network before the full-scale treatment facilities. Whereas on a high-viscosity oil field with a high content of waxes and asphaltenes or on an almost purely gas field with an unconsolidated reservoir – the problem of solids removal from a pipeline always has to be solved, as it never can be fully avoided.

For the purposes named, the cylindrical-shaped pigs are used due to their rigid bodies and the ability to get equipped with additional brushes, magnets, and other features to further enhance their cleaning ability. Multiple examples of cylindrical pigs enhanced for the improved removal of solids can be seen in Figure 12.

Figure 12. Cylindrical (mandrel) utility pigs for an enhanced solid-removal
Source: "Girard Mandrel-Pigs" by Girard Industries *[10].*

4.7.4. Need for the regular collection of data along a pipeline

For some onshore pipelines, where the access to the outer wall is not obstructed, data can be collected via multiple inspection practices, several of which are investigating the pipeline's wall's state from the side of its outer surface. However, in the present day, for the subsea pipelines, there is only one technologically-proven and economically-feasible solution that is applied worldwide: the data is collected via smart pigging, which sometimes is also referred to as in-line inspection (ILI) or intelligent pigging.

The essence of the technology is in running a "smart" pig that is equipped with sensor(s) of different physical principles (the most important and widely spread will be discussed in the following sub-chapters). The sensor(s) will continuously conduct measurements while the pig's movement along the pipeline, which will be stored in the pig's memory and will be retrieved and analyzed by the engineers after the end of the pig run.

Smart pigging has an essential role in the flow assurance and pipeline integrity management allowing the engineers to locate, identify and address the potential issues proactively. The types of data collected via smart pigging include the following:

1. Geometry and strain data:

Collected geometrical parameters of a pipeline include such as ovality, dents, buckles, wrinkles, and even geographical coordinates. The last ones are important, since in some cases pipelines can change their geometry due to the tectonic activity in the region (both onshore and offshore), as well as suffer movements if being not properly fixed (by concrete blankets or trenching) in the areas of sea currents.

Strain data is directly correlated with the stress level experienced by the pipeline and is essential for assessing its structural integrity margin and the potential risks associated with it.

2. Wall thickness data and metal loss defects:

Overall, this type of data is related to the metal loss due to corrosion, erosion, and other forms of metal degradation throughout the life cycle of a pipeline. However, different smart pigging technologies have different strengths in this area of expertise, and up to the present day not a single one of them can singlehandedly cover all of the defects in this category. Further information on different technologies' strengths and weaknesses in regard to metal loss defects will be provided in the following sub-chapters dedicated to the several most widely-used detecting principles in smart pigging.

3. Data on the pipeline’s coating condition:

Modern smart pigs are capable of collecting data on the current state of the pipeline’s coatings such as fusion-bonded epoxy (FBE) and polyethylene (PE). **[12]**

4. Operational conditions’ data:

Smart pigs can be equipped with additional pressure, temperature and etc., sensors. The data collected by them, in most cases, is not of crucial importance. However, it contributes to the full picture of the pipeline's operational conditions, thus, helping the flow assurance and structural engineers to perform their decisions.

The following sub-chapters 4.7.4.1 to 4.7.4.5 are dedicated to the four main methods of non-destructive in-line testing in the Petroleum Industry such as Magnetic Flux Leakage (MFL), Ultrasonic Testing (UT), Electromagnetic Acoustic Transducer (EMAT), and Inspection Eddy Current (IEC), as well as their comparative analysis. A comparative analysis is based on the present-day capabilities of the technologies and does not take the potential for future improvements into the scope of consideration.

4.7.4.1. Magnetic Flux Leakage (MFL)

Magnetic Flux Leakage (further, MFL) is probably the oldest of all the in-line diagnostic technologies used. Its first appearance in the industry took place in the late 1960s, and, after some years, the technology became industry-wide acknowledged in the 1970s -1980s. At present, MFL is the most common technology used during ILI operations. **[13]**

The physical principle behind the technology bears the same name as the technology itself and can be seen in Figure 13 below. Magnets mounted on the smart pig are generating a permanent magnetic field, which can be well-conducted via the pipeline wall, due to the fact that the wall's steel is a ferromagnetic material. If any abnormalities of the steel media are encountered by the magnetic field going through it, the field will be disrupted from its natural path. This field disruption is registered by the hall sensor in-between the magnetic field emitters, which is represented by a sensor coil. The method allows engineers to determine both the anomaly's location and orientation in the pipeline's wall.

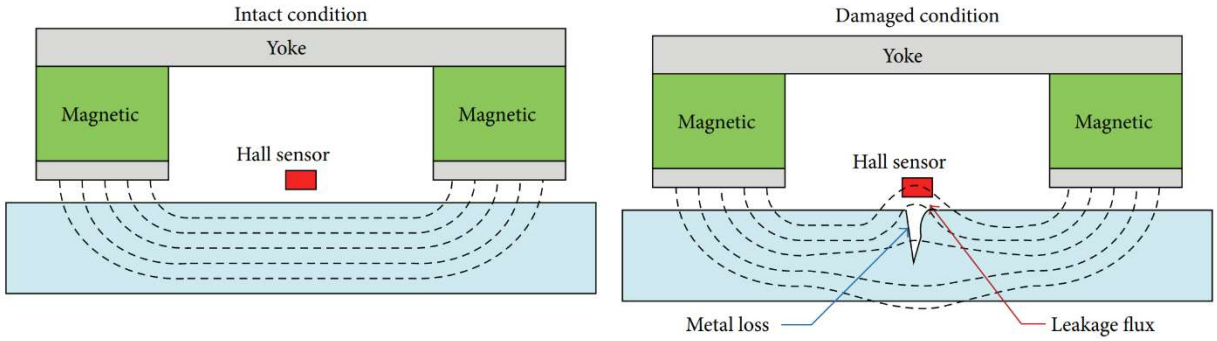

Figure 13. MFL inspection working principle:
Intact condition – left, damaged condition – right
Source: "In-line inspection with magnetic flux leakage" by EPCM Holdings [14].

Depending on the magnets' orientation, the MFL non-destructive testing has two modifications:

1) MFL with longitudinal magnetization – is capable of locating and measuring the severity of internal and external metal losses due to corrosion and erosion, as well as ring weld and factory anomalies.

2) MFL with transverse magnetization – makes it possible to detect and measure even the narrowest longitudinally-oriented anomalies such as scoring, streaky corrosion, and crack-like anomalies.

Regarding the technology limitations, MFL is relatively fitted for almost all conditions and fluid media. The measurements can be done in the pig velocity range starting from 0,5 m/s and up to above 5 m/s. The maximum value varies on the tools' manufacturing company and can reach 10 m/s for the cutting-edge models. It is also worth mentioning that MFL in-line diagnostics is possible only in ferromagnetic material pipes due to the physical nature of the measurement principle.

4.7.4.2. Ultrasonic Test (UT)

The first ideas for the implementation of ultrasonic testing for welds are documented around the 1950s. After two decades of constant improvement in sensors and the development of smart inspection tools, the level of technology exceeded the critical threshold allowing it to be used for the in-line testing. **[15]**

The testing is performed via high-frequency sound waves. In the perfect case, the waves emitted by the transducer are penetrating through the pipeline wall's material with a constant speed, and are reflected by the back of the wall back to the transducer again, which simultaneously acts as the receiver. When the parameters of the emitted wave and the pipeline wall's material are known, the distance traveled by the wave, i.e., the pipeline wall's thickness in place of the measurement can be simply calculated from the wave traveling time.

If an anomaly is encountered along the wave's route in the wall's media, the wave will be partially reflected back, and this reflected wave will be registered by the receiver, as well as the wave reflection from the back of the wall. The amount of energy carried by the initially emitted wave will be "split" between the reflected

ones, thus making the peak areas on the graph for them smaller. The type of anomaly encountered in this case can be determined by the peak's parameters (i.e., height and width), and the anomaly's positioning depth – by the time gaps before and after the anomaly-reflected wave until the expected wall reflection.

The illustrations for both cases can be seen on the left and right in Figure 14 below, respectively.

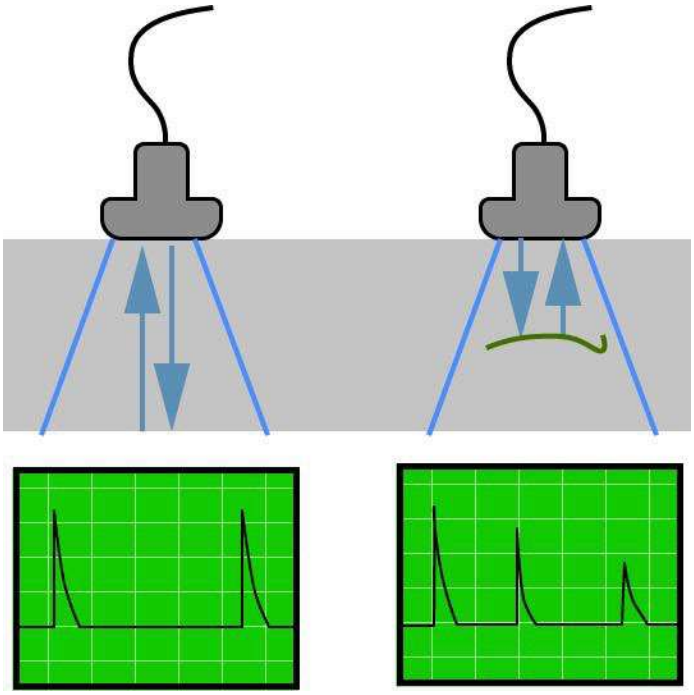

Figure 14. UT inspection working principle:
Intact condition – left, damaged condition – right
Source: "Ultrasonic Testing (UT)" by G. Cotter Enterprises [16].

Ultrasonic Testing can be used for the high-accuracy measurements of the residual pipeline's wall thickness. It also enables the detection of internal and external metal losses, inclusions, scratches, dents, scoring, and delamination zones, as well as their combinations.

The greatest weakness of the technology is defined by its physics principle – Ultrasonic Testing ILI can be successfully conducted only in the pipelines with liquid media but not in gas pipelines.

Regarding the pig's traveling speed: depending on the tool parameters, the measurements can be performed on the velocities exceeding 5 m/s, however, for the greater mass of the UL in-line inspection tools on the market, 5 m/s is the maximum limit allowing them to operate without a reduction in the measurement quality.

4.7.4.3. Electromagnetic Acoustic Transducer (EMAT)

In 1969 the first patent for the Electromagnetic Acoustic Transducer was granted. This event marked the start of the transition period for non-destructive testing from piezoelectric transducers to the EMATs. The first commercial application for EMAT's non-destructive testing was funded by the American Gas Association in the early 1970s. The technology was used to inspect buried gas pipelines **[17]**. A photo of the first experimental EMAT pig can be seen in Figure 15 below.

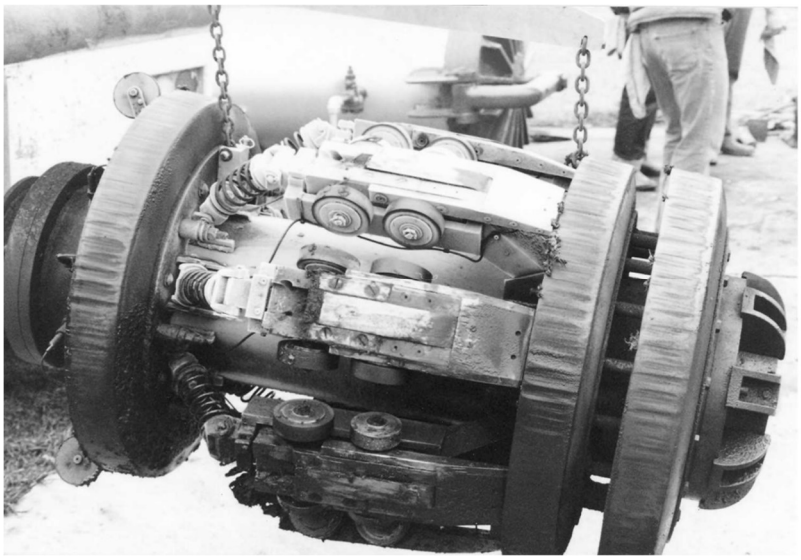

Figure 15. World-first EMAT-based smart pig
Source: "A history of EMATs" by George Alers [17].

Electromagnetic Acoustic Transducers utilize ultrasonic waves for their testing. The waves are induced by the interaction of two magnetic fields. The first one, a high-frequency field is generated by the EMAT coil circuit due to the alternating electric current flowing through it. The second, static magnetic field is generated by the magnet. When these two magnetic fields interact, the Lorentz force is induced, which generates the ultrasonic wave within the material media without any direct contact with it from the EMAT side.

Similar to the UT testing principle which was discussed previously, the generated ultrasonic waves propagate through the wall's material media. When these waves encounter an internal anomaly and/or the back of the wall, they are reflected back to the receiver coil (emitting coil also plays the receiving role). The

registration is performed via the same physical principle where the alternating magnetic field affects the receiving coil, thus, inducing in it an electric current whose value is stored in the test log. A schematic representation of the EMAT sensor working principle can be seen below in Figure 16.

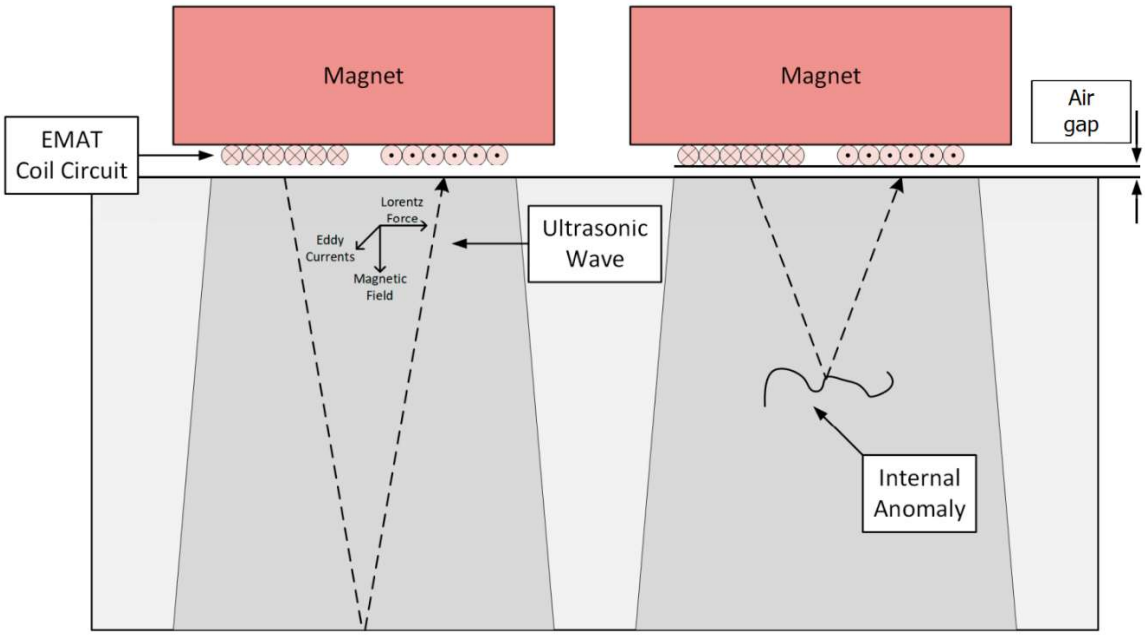

Figure 16. EMAT inspection working principle:
Intact condition – left, damaged condition – right
Source: "A Comprehensive Analysis of In-Line Inspection Tools and Technologies for Steel Oil and Gas Pipelines" by Berke O.P. and Huseyin A.Y. [18].

Non-destructive testing based on the EMAT technology allows the detection of the damage to the insulation coating and their dimensions and identifies and sizes cracks with a high degree of accuracy. A significant strength of the technology (especially in comparison with the standard UT) is the fact that it does not depend on the pipeline media – it is capable of operating with the same degree of accuracy in gas, liquid, and gas-liquid mixtures of all types.

It is also worth mentioning that EMAT unlike MFL can be used in both ferromagnetic and non-ferromagnetic pipes. However, the ultrasonic waves generated by the EMAT principle have limited penetration depth which makes the technology dependent on the surface condition of the pipe expected as well as the material of the pipeline being tested. Its sensitivity is also affected by the orientation of the magnetic field and wave propagation, which, in some cases, can reduce its detecting ability the defects inspected.

4.7.4.4. Inspection Eddy Current (IEC)

The discovery of Eddy Currents is dated 1851 and attributed to French Physicist Leon Foucault. The physical principle was adapted for industrial use in terms of non-destructive testing only 8 decades later, in 1933, by Professor Friedrich Förster. Later he established his own testing company based on IEC testing in 1948. However, the first appearance of the testing principle for in-line diagnostics is not plainly documented in any of the available information sources **[19]**.

The physical principle of Inspection Eddy Current (also known as ECT – Eddy Current Testing) is represented in Figure 17 below:

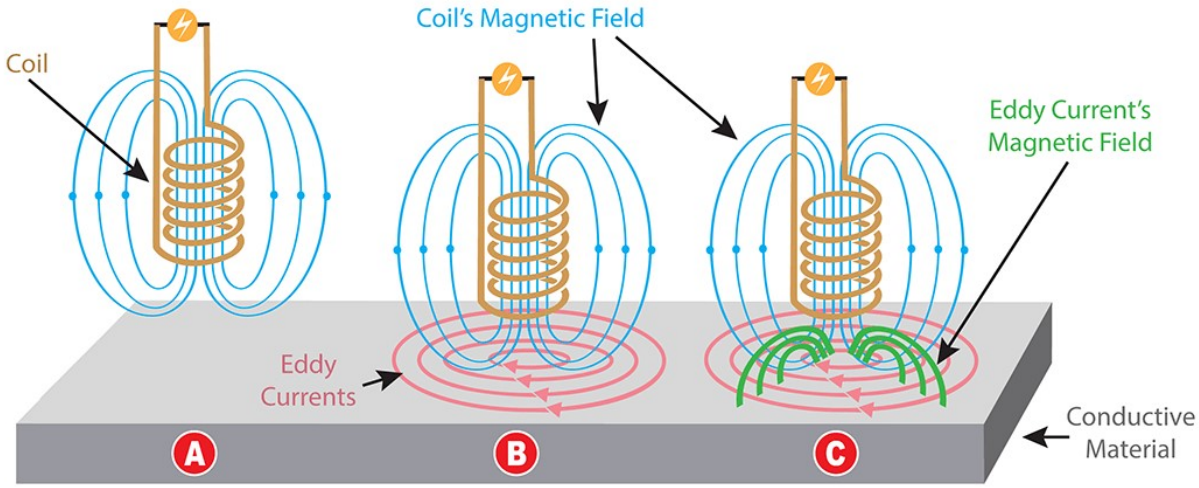

Figure 17. IEC inspection working principle
Source: "Eddy Current Testing 101" by The Severn Group [20].

Step A: An alternating magnetic field is generated by the coil under the influence of alternating current flowing through it.

Step B: Eddy Current is induced in the ferromagnetic material plate below the coil, which represents a pipeline's wall.

Step C: Eddy Currents in the ferromagnetic material are inducing their own magnetic field (represented by the green curved in Figure 17), which in the intact case are forming a magnetic coupling with the field induced by the coil. If Eddy currents are interrupted by an encountered anomaly in the material, the equilibrium in the system will be disturbed and the anomaly causing is defined by the coil impedance variation **[20]**.

The IEC testing can be used to locate, define and estimate material anomalies in the upper layer of pipeline's wall such as cracks and carrion detection. It is also frequently used for the coating thickness testing **[21]**.

The technology does not depend on the pipeline's media due to its physical principle. However, due to the same reason, it has a very shallow depth of testing and can be used only in pipelines made of ferromagnetic materials.

4.7.4.5. Comparison analysis of ILI technologies

Table 4.1 below provides a comparison analysis of the ILI technologies discussed in chapters 4.7.4.1 to 4.7.4.4, and is based on **[22]**, **[23]**, and **[24]**.

Table 4.1 – Comparison analysis of ILI (In-Line Inspection) technologies

Metal loss defects	ILI technology				
	MFL Longitudinal Magnetization	MFL Transverse Magnetization	UT	EMAT	IEC
Extensive corrosion	IV	IV	III	III	III (Shallow)
Ulcerative corrosion	III	II	II	II	II
Longitudinal groove / slit	II	III	II	I	I
Transverse groove / slit	III	I	III	II	II
Narrow longitudinal corrosion	I	III	II	I	I
Ring seam anomaly	III	0	II	0	0
Longitudinal seam defect	I	III	I	0	0
Dents with metal loss	III	III	II	II	II
Metal objects in the vicinity	III	II	0	0	0
Defects in the pipe body (Delaminations etc.)	II	II	IV	I	0
Defect analysis					
Defect detection	III	III	III	II	II
Sizing determination	III	III	III	III	II
Depth determination	II	II	III	II	I
Operating media					
Gas	IV	IV	0	III	III
Liquid	IV	IV	IV	III	III
Multiphase flow	IV	IV	IV	III	III
ILI pig recommended velocity					
Pig velocity more than 5 m/s	III	III	II	I	II

Notation system:
0 – application is not possible; I – ineffective solution; II – poor solution efficiency; III – effective solution; IV – best solution.

5. Pipeline modeling

Overall, pipeline modeling is the process of creating a mathematical computational model of a pipeline. It allows the simulation of pipelines' behavior under a set of various conditions and is used for the analysis and optimization of pipelines' design, operational conditions, and maintenance.

The understanding of the term "pipeline modeling" drastically differs depending on the specialist's thinking of it. It can be related to pipeline stress analysis, simple hydraulic modeling, modeling of the heat exchange with outer media, etc. In the context of flow assurance in particular, it is usually a question of dynamic multiphase flow modeling and all the problems associated with this phenomenon.

5.1. Historical overview

An interesting and not at all obvious fact is that, for the first time, dynamic two-phase flow modeling has been applied not in the oil and gas industry: the two-phase "water-steam" dynamic models were initially implemented to describe the flow within the core of nuclear reactors!

However, the models used in the nuclear industry have been sharpened to the fast pressure transients rather than the transient mass transport modeling, needed for the petroleum industry pipelines. This mismatch between "demand" and "supply" has caused the development of the OLGA dynamic modeling simulator.

The project was initiated by Statoil and carried out in coherent joint research with SINTEF and the Institute for Energy Technology (IFE). The development of OLGA at this stage was also supported by Conoco Norway, Esso Norge, Mobil Exploration Norway, Norsk Hydro A/S, Petro Canada, Saga Petroleum, and Texaco Exploration Norway.

As a result, the first version of OLGA has seen the light in 1983. Initially, it was a dynamic simulator for the two-phase-flow systems. It was aimed to solve the challenges of various production rates, pipeline start-up and shut-in operations, terrain slugging, and pigging operations. **[25]**

5.2. OLGA modeling software at the present

Over the years of its existence, OLGA has significantly evolved. At present, OLGA is positioned as a dynamic multiphase flow simulator and has collected the world's largest database of laboratory and field data, and is capable of the following flow simulation applications **[26]**:

- Liquid handling;
- Sizing separators and slug catchers;
- Managing solids;
- Simulating key operational procedures including start-up, shut-down, and pigging;
- Modeling for contingency planning;
- Assessing environmental risk in complex deepwater drilling environments.

5.3. PVTSim simulation tool

PVTSim (also known as PVTSim Nova) is a fluid characterization software tool developed by Calsep company. The first version was released in 1990 and even since has been constantly improved by its developing company.

PVTSim list of capabilities includes **[27]**:

- Simple fluid characterization (e.g., density, viscosity, phase behavior, interfacial tension, etc.);
- Equation of state modelling (e.g., Peng-Robinson, Cubic Equations of State, etc.);
- Phase behavior analysis (e.g., phase envelopes calculation for mixes);
- PVT Data Regression analysis (needed to enable the construction of reliable reservoir fluid models for the simulation purposes).

As well as OLGA, the program is industry-wide and known as one of the main and most reliable tools for fluid simulation purposes in terms of fluid compositions and their properties.

6. Practical flow assurance modelling in OLGA

6.1. Research question

This research aims to solve several flow assurance concerns commonly presented in a subsea pipeline's operational cycle. In particular, the two following problems are addressed in this work:

1. Modelling of the hydrate formation condition zones within a pipeline and their diagnostics and mitigation via continuous inhibitor injection;
2. Estimation of the required slug-catcher unit's capacity for liquid collection and water disposal.

6.2. Initial data

The modeling in this work is conducted for the hypothetical subsea pipeline which is based on the example of a production gathering subsea pipeline implemented on the Kirinskoye gas-condensate field (further, GCF).

The pipeline connects subsea manifold which gathers production from all the wells producing on Kirinskoye GCF and brings it to an onshore treatment facility. Chemical composition of the pipeline stream is represented in Table 6.1 below:

Table 6.1 – Initial stream's chemical composition

Component	Mol	Mol %
CH_4	913,88	87,881
C_2H_6	35,10	3,375
C_3H_8	15,25	1,466
i-C_4H_{10}	3,49	0,336
n-C_4H_{10}	5,26	0,506
i-C_5H_{12}	2,54	0,244
n-C_5H_{12}	2,19	0,211
C_6H_{14}	6,02	0,579
C_7H_{16}	5,80	0,558
C_8H_{18}	3,98	0,383
C_9H_{20}+	7,24	0,696
N_2	1,53	0,147
CO_2	28,75	2,765
H_2O	8,88	0,854
∑	1039,91	100,000

The water content of 0,854 Mol% requires an additional clarification:

Water content in a production feed of gas and/or gas condensate fields is based on the initial content of water stored in the gaseous phase within the productive formation. The value for the water content might slightly vary across the entire formation, so the maximum value is assumed for the simulation due to safety reasons.

For Kirisnkoye GCF and this work in particular, the content of water equal to 0,854 Mol% is considered as a maximum value. This value will not change throughout the production cycle of the field until the moment when a waterfront breakthrough will take place on at least one of the producing wells.

Several industry practices can be implemented in this case. However, quite frequently an event of the waterfront breaking through to a production well serves to ask a key factor to cut off the production of the well or even of the entire field due to economic reasons. Due to this fact, the constant maximum water content within the production feed is assumed for the following modeling within the work.

Pig launching point:

The first section of the pipeline getting out of the subsea manifold is considered to be a pig launching point for this work. The specification of the pig launching unit itself would not have a major effect on the simulation results.

Slugcatcher unit:

At the endpoint of the pipeline, a pig-receiving unit and slugcatcher are installed. Slugcatchers have several purposes for their installation, probably the most important of which is receiving and disposal of liquid slugs.

A slugcatcher from the Ormen Lange gas field of 1500 m^3 capacity is taken as a reference for this work due to the similarities between these two fields. Both fields have two parallel lines in their production gathering system of identical diameter, every one of which is equipped with the named slugcatcher, making it 3000 m^3 of receiving liquid capacity in total **[28]**.

Pipeline parameters and materials:

The pipeline is divided into two sections along its way. The first section starts from the subsea manifold and lasts for the next 22 km. This pipeline section is lying on the seabed, covered by thermal insulation and concrete coating.

The second section starts from the 22nd kilometer and lasts until the receiving end of the pipe, at the slugcatcher. This section has a slightly reduced inner diameter in comparison with the 1st one (while the outer diameter remains the same for both pipe and its coatings) and is trenched into the soil for 3,5 m.

The complete list of pipeline dimensions, materials properties, and environmental parameters used can be viewed in Tables 6.2, 6.3, and 6.4, respectively.

Table 6.2 – Pipeline dimensions

Pipeline segment	Internal diameter, mm	Wall thickness, mm	Insulation coating thickness, mm	Concrete coating thickness, mm
Segment № 1 (On-bottom)	463,6	22,2	2,7	80
Segment № 2 (Trenched)	460,4	23,8	2,7	80

Table 6.3 – Pipeline material properties

Material	Heat capacity, J/(kg·K)	Heat conductivity, Wt/(m·K)	Density, kg/m^3
Steel	270	45	7850
Concrete	880	2,7	3100
Insulation	2200	0,4	900

Table 6.4 – Environmental parameters

Media	Temperature, ^oC	Heat conductivity coefficient for a pipeline segment, Wt/(m^2·K)
Sea water	-1,8	8
Sea bottom	-0,5	4

Pipeline profile:

As it was mentioned earlier, the pipeline profile for this work is based on the subsea production gathering pipeline from the Kirinskoye GCF. The seabed topography in the area of the Kirinskoye gas condensate field is characterized by depths ranging from 0,0 m onshore to 85 ÷ 90 m in the field development area.

The representation of pipeline profile geometrical data can be seen below in Figure 18:

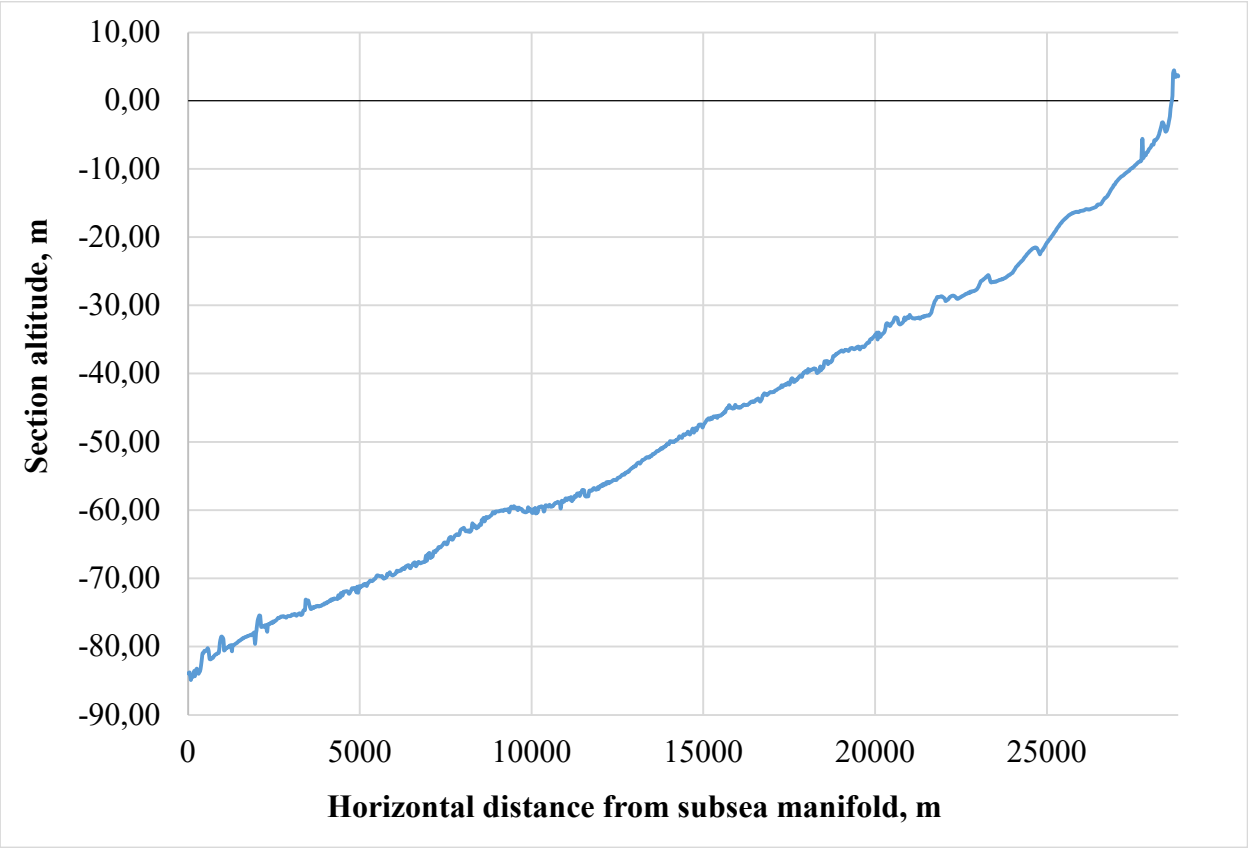

Figure 18. Subsea pipeline profile

The distance between the start- and end-points of the pipeline is 28825 m and is divided into sections of 25 m each. The full dataset of segments' coordinates used to build the model is provided in Appendix A.

6.3. Hydrate formation modelling

While modeling in OLGA, the fluid composition cannot be defined in the program itself – it has to be fed to the model in the .tab file format. For this purpose, PVTSim software was used.

After feeding the initial fluid composition data, which was presented in Table 6.1, to the PVTSim – the following phase envelope and hydrate curve were received:

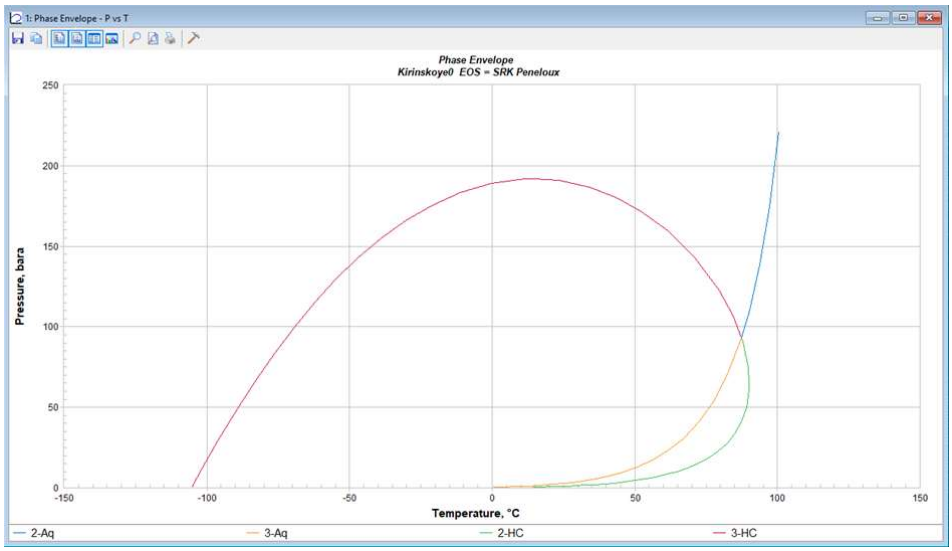

Figure 19. Phase envelope for the initial fluid composition with 0,854 mol% water and no hydrate inhibitors added

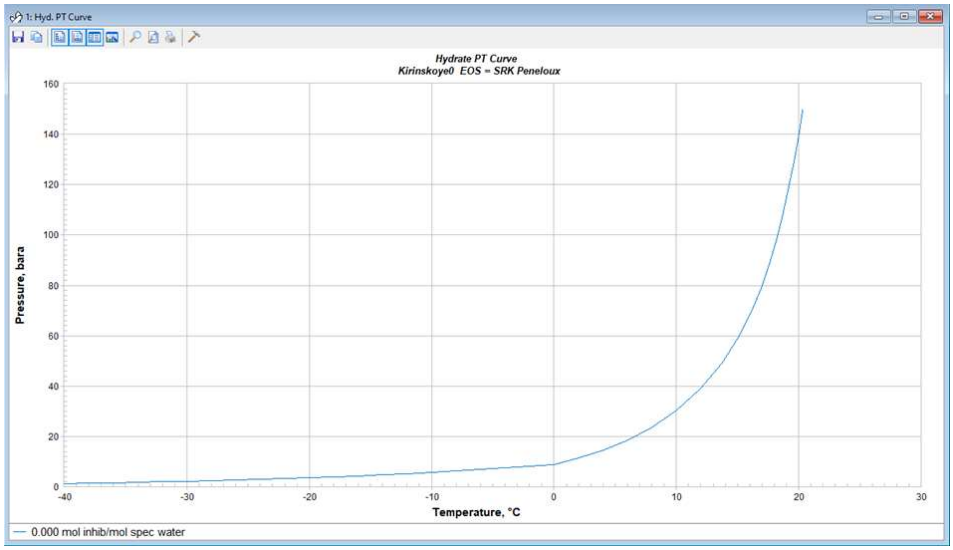

Figure 20. Hydrate curve for the initial fluid composition with 0,854 mol% water and no hydrate inhibitors added

From this moment forward, starting from Figure 19, all of the graphs provided in this work are duplicated in Appendix B with higher resolution and in such an order that Figure B.1 is linked to Figure 19, Figure B.2 to Figure 20, etc.

The .tab file received as a result of fluid simulation in PVTSim was fed to OLGA and the simulation was run for 2.64 million m^3/day flow. As the boundary conditions were taken pressure and temperature for the start point as of 119 bar and 95 °C, for the start point, respectively, and 112 bar for the receiving end. The flow and boundary condition values were selected according to the project values of the pipeline implemented on the Kirinskoye GCF.

The dynamic model has simulated 15 hours of the pipeline's operation since the start-up – to let the system reach its operation mode and get stabilized. Figure 21 below represents the pressure, fluid temperature, and liquid volume fraction holdup distribution along the pipeline at the moment of 12 hours since the beginning of the simulation when the system gets fully stabilized.

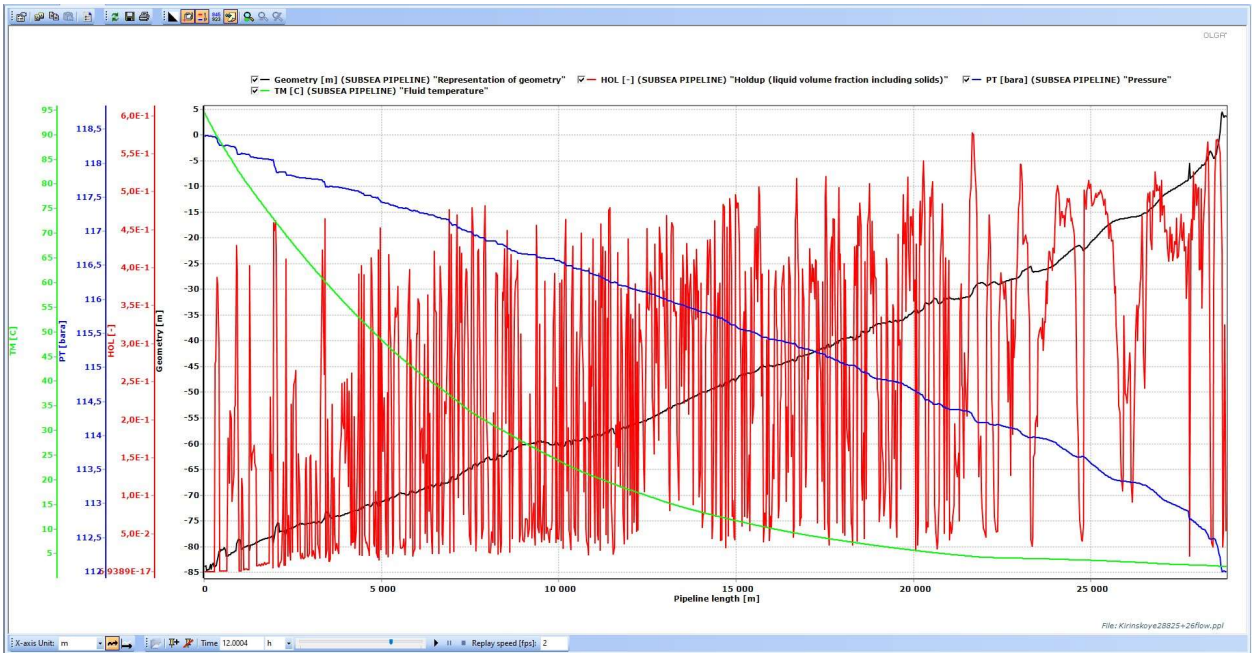

Figure 21. Pressure, temperature, and liquid volume fraction holdup distribution along the pipeline in the stable operational mode (12 hours since the start-up)

As can be seen from Figure 21, fluid temperature along the pipeline significantly drops with the distance, almost reaching 0 °C at the end-point regardless of the thermal insulation measures implemented against it.

Figure 22 below utilizes OLGA's DTHYD function, which calculated the temperature difference between the actual temperature within the pipe and the temperature of hydrate formation under the given pressure within the pipe segment.

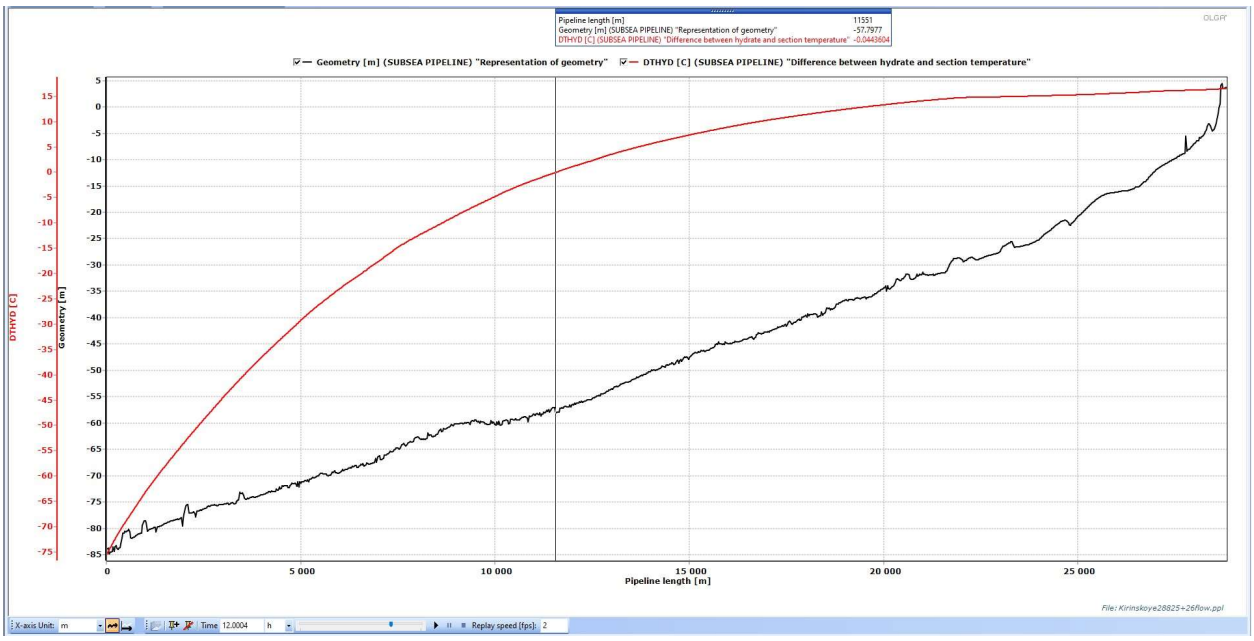

Figure 22. DTHYD value distribution along the pipeline in its operational mode and without any hydrate inhibitor injection in the pipeline system

DTHYD function shows a negative value when the operating conditions in the calculation point are out of the hydrate domain. It means that approximately 11600 m from the pipeline start-point, where DTHYD becomes positive, pressure-temperature conditions within the pipeline are entering the domain of hydrate formation. Taking into account the liquid volume fraction holdup value (the HOL curve in Figure 21, represents the fraction of the pipeline cross-section filled with a liquid fraction), it is clear that this pipeline zone will suffer severe hydrate formation even in its operation mode, and this problem has to be eliminated.

According to the Kirinskoye GCF project data, the field system was designed to use Mono-Ethylene Glycol (further, MEG) as the hydrate formation inhibitor, with its concentrations in the liquid phase up to 80%. However, from the economic perspective, it is always beneficial to calculate and utilize the minimum required concentration of the inhibitors used – to minimize the field's operational cost.

Lastly, with the size of the hydrate formation zone, as was modeled above, the only economically effective scheme of hydrate problem mitigation would be the inhibitor injection in the pipeline in the regime of continuous injection. This fact additionally highlights the importance of defining the minimum required inhibitor volumes to be used.

The pipeline pressure-temperature operational domain in terms of hydrates is defined by the minimum achievable pressure and minimum achievable temperature. Since the pipeline in this work has no Joule-Thompson effect zones, the minimum achievable pressure for the system lies in the pipeline end-point and for this case equals 112 bar. Regarding the minimum achievable temperature – it will be defined by the ambient media temperature and for the case equal to -1.8 °C. The minimum achievable temperature is not presented in the pipeline in the case of its operational mode with 2,64 million m3/day, however, it will be achieved if the temporary shut-down of pipeline operation will take place. Thus, it must be taken into account.

To initially find the minimum required concentration of MEG in the liquid phase within the pipeline, PVTSim was used. As an addition to the initial hydrate formation curve without MEG added to the stream, 4 more curves were constructed – for the 10, 20, 30, and 40% of MEG solution, respectively. All 5 of the hydrate formation curves are represented in Figure 23 below. The blue-shaded area represents the zone of pipeline operational pressure-temperature conditions.

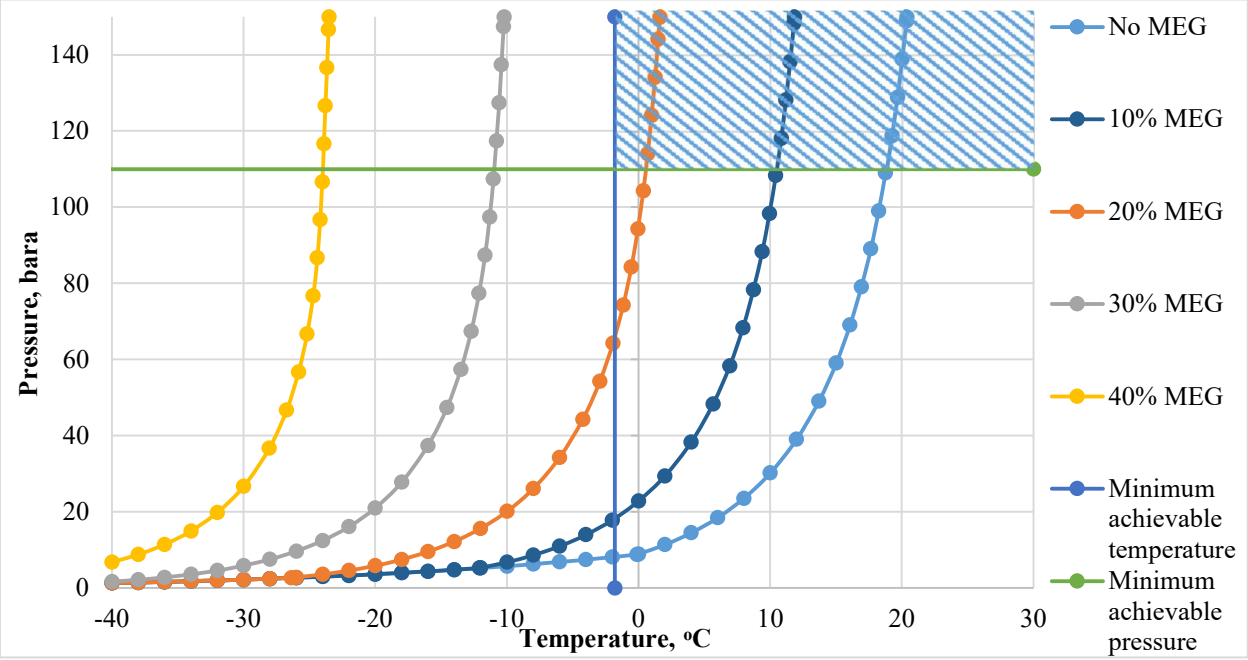

Figure 23. The first iteration of the hydrate formation curves plotting to find the optimum MEG content: 0, 10, 20, 30, and 40% concentrations are plotted

As can be seen from Figure 23, the 20% MEG concentration turns out to be insufficient to fully eliminate the problem of hydrate formation for the given pipeline system whereas 30% gives an excessive safety margin, which will further increase

the operational cost of the pipeline operation. Due to these conclusions, the second iteration of finding the optimal MEG injection concentration for the system was conducted – for the 25% MEG concentration case. The hydrate formation curve received as the result is plotted in Figure 24 below.

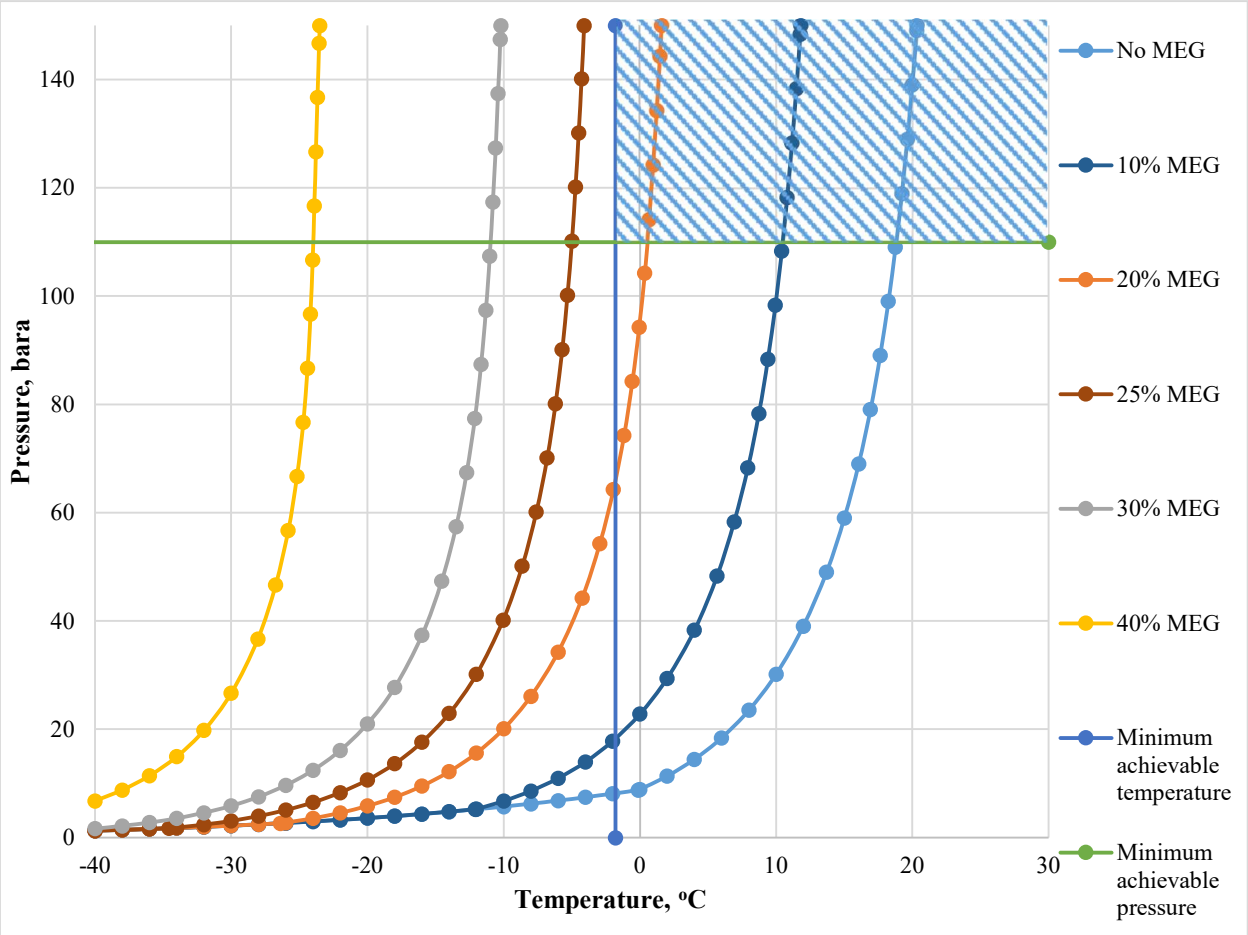

Figure 24. The second iteration of the hydrate formation curves plotting to find the optimum MEG content: 25% concentration is added to the plot

According to the hydrate formation's condition modeling provided in Figure 24, the 25% concentration of MEG solution in the system's liquid phase is considered to be the optimal solution due to the following facts:

1) This hydrate inhibitor concentration in the case of its continuous injection into the pipeline system allows it to fully escape the hydrate formation conditions within it;

2) While providing a moderate safety margin between the hydrate formation dominion and operational conditions within the system, the solution turns out to be the optimal balance between the safety of operations and their economic efficiency.

Due to all of the above, the concentration of 25% MEG as a hydrate inhibitor was selected as an optimum one for the operational needs. The updated system fluid composition is provided below in Table 6.5 and is used in all of the simulations performed in the work from now on.

Table 6.5 – Updated stream's chemical composition

Component	Mol	Mol %
CH_4	913,88	87,631
C_2H_6	35,10	3,366
C_3H_8	15,25	1,462
i-C_4H_{10}	3,49	0,335
n-C_4H_{10}	5,26	0,504
i-C_5H_{12}	2,54	0,244
n-C_5H_{12}	2,19	0,210
C_6H_{14}	6,02	0,577
C_7H_{16}	5,80	0,556
C_8H_{18}	3,98	0,382
C_9H_{20}+	7,24	0,694
N_2	1,53	0,147
CO_2	28,75	2,757
H_2O	8,88	0,851
MEG	2,96	0,284
∑	1042,87	100,000

The fluid composition was updated according to Table 6.5 data in the OLGA simulation model, and the following DTHYD function graph was received for the system (see Figure 25 on the next page). As can be seen from Figure 25, DTHYD values are all negative along the pipeline system, which indicates that the entire system operates out of the hydrate formation domain of pressure-temperature values.

The hydrate-free operational mode is achieved regardless of the liquid being holdup within the system with the considered fluid composition. An approximate amount of liquid can be seen in Figure 26 of the OLGA simulation (on the next page as well). The problem of liquid removal from the pipeline system is being solved in the next chapter of this work – Chapter 6.4.

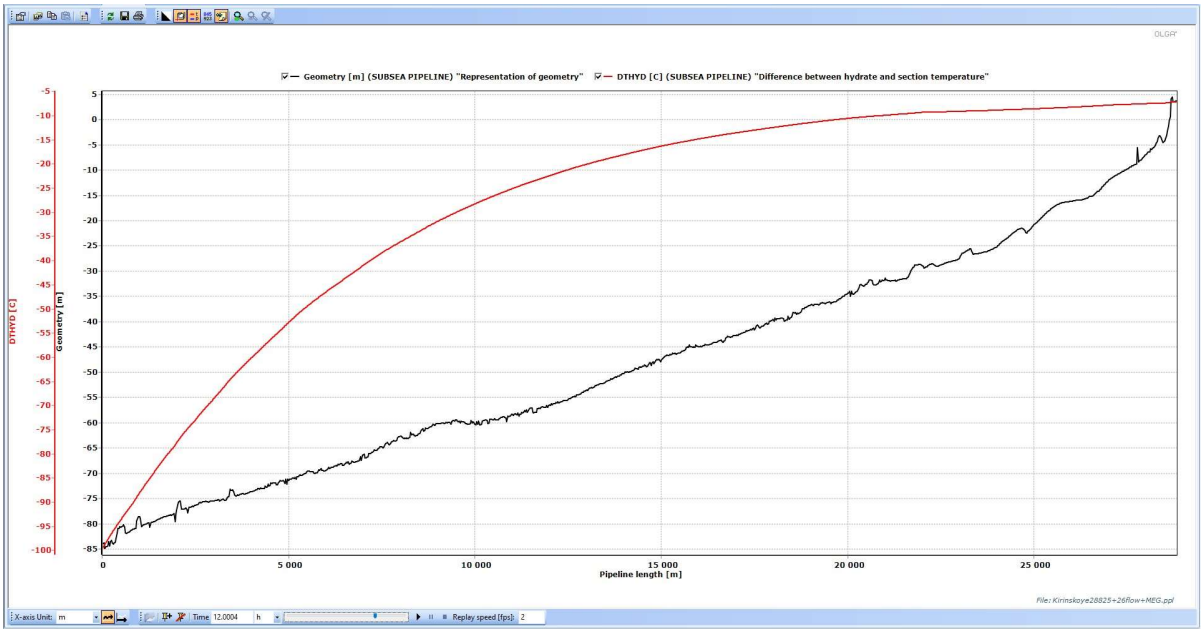

Figure 25. DTHYD value distribution along the pipeline in its operational mode with continuous injection of hydrate inhibitor (25% MEG solution in the system)

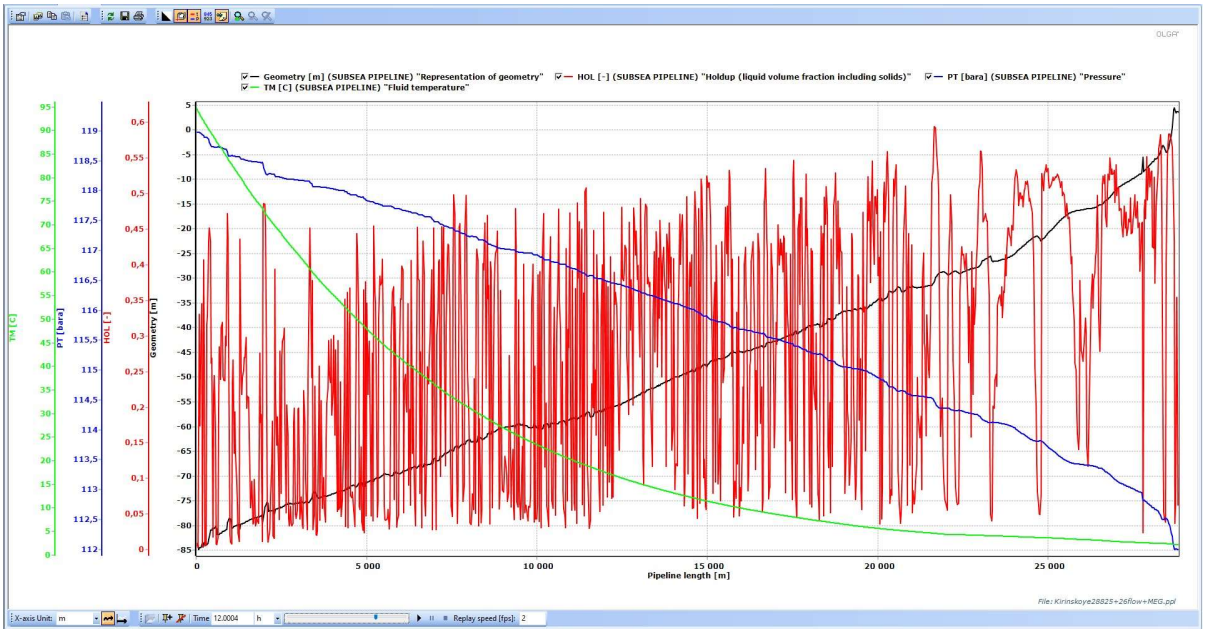

Figure 26. Pressure, temperature, and liquid volume fraction holdup distribution along the pipeline in the stable and hydrate-free operational mode (12 hours since the start-up, continuous injection of hydrate inhibitor: 25% MEG)

Lastly, it is important to highlight that the selected hydrate formation remediation plan of continuous MEG injection allows the elimination of the hydrate formation problem not only while the operational mode but also in the case of the pipeline's shut-down. The result is achieved due to the fact that the pipeline hydrate formation conditions zone does not overlap with the presented pressure-temperature conditions.

6.4. Water surge modelling

6.4.1. Standard operating mode

Although the problem of hydrate formation within the pipeline was solved in the previous section, the following Figure 27 shows us a significant volume of liquid being holdup within the system:

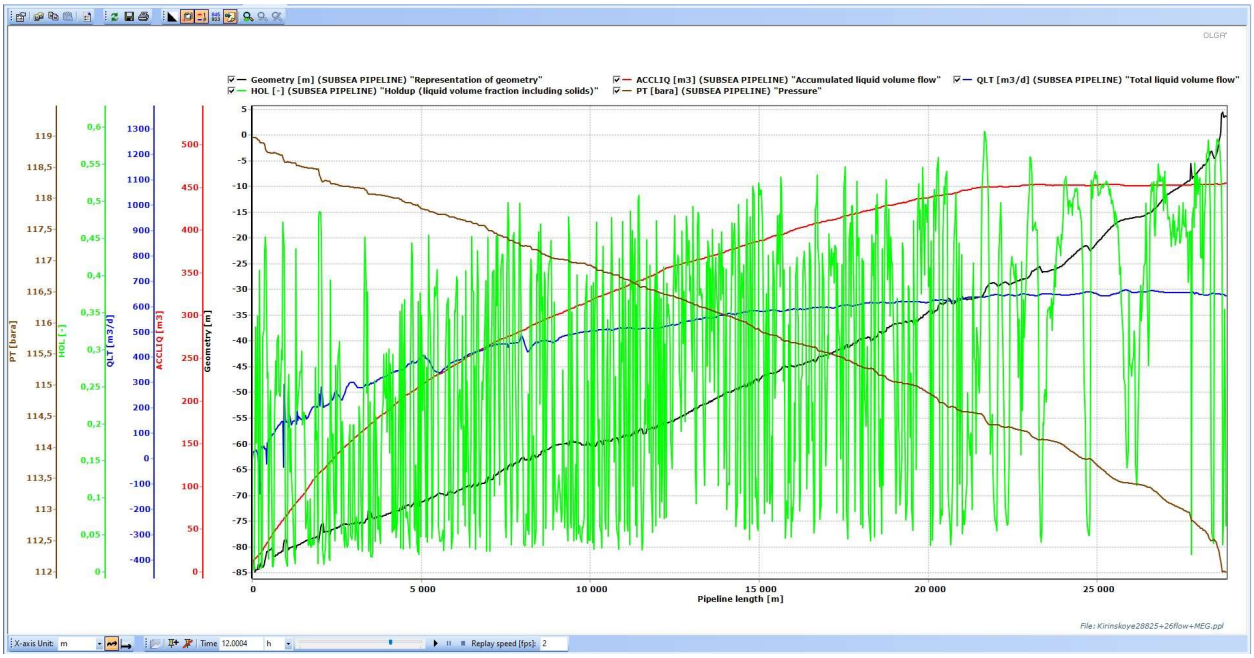

Figure 27. Pressure and holdup liquid volume fraction distribution along the pipeline & accumulated liquid volume / volume flow parameters for the pipeline (12 hours since the start-up, continuous injection of hydrate inhibitor: 25% MEG)

To estimate the actual picture at the receiving end of the pipeline a trend plot for the last pipeline segment (segment № 1153) was plotted. A trend plot for the named segment can be seen in Figure 28 (see the next page). The fully-stabilized operational conditions are considered to start approximately 12 hours (43200 seconds) since the start-up for the given model.

An approximate value of the surge liquid volume can be taken from this chart, its value is at the level of ~45 m^3. However, OLGA has a special interface for the precise estimation of liquid surge volume and maximum surge rate. The screenshot of this interface being applied for the case is represented in Figure 29 (see the next page). According to the calculations made by OLGA, the maximum surge volume for the 15 hours of the simulation was equal to 46,84 m^3 of liquid with a maximum surge rate of 860,9 m^3/day. Comparing those values to the slug catcher's capacity

installed at the end of the pipeline (which was discussed in Section 6.2: "Initial data"), it can be concluded that with the given system's parameters, the pipeline operates significantly below the liquid receiving capacity of its slugcatcher unit.

However, the maximum slugcatcher's liquid receiving capacity is rarely exceeded in a normal operational mode. The real challenge is faced while the pigging operations: when the intelligent and/or maintenance pig delivers a gigantic water slug, which is made of all the liquid being held up in the pipeline before its run. The critical case named is modelled in the further sub-section of this work.

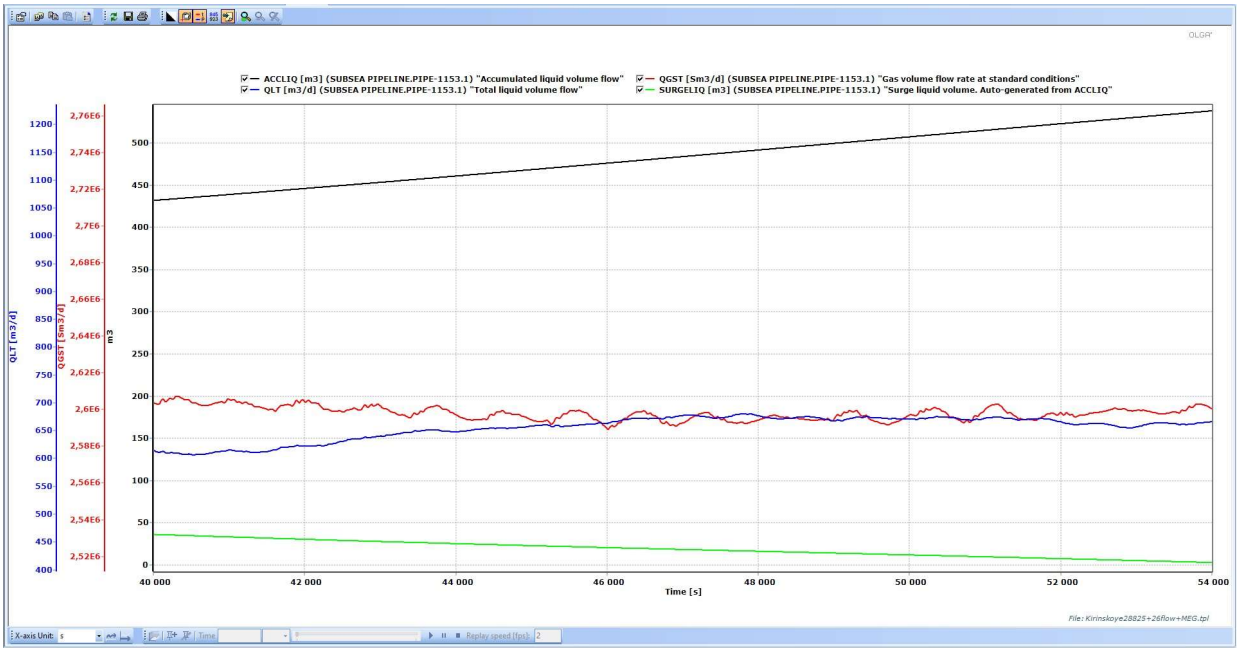

Figure 28. Trend plot for the last segment at the receiving end of the pipeline in the stabilized operational mode (12 hours / 43200 seconds since the start-up)

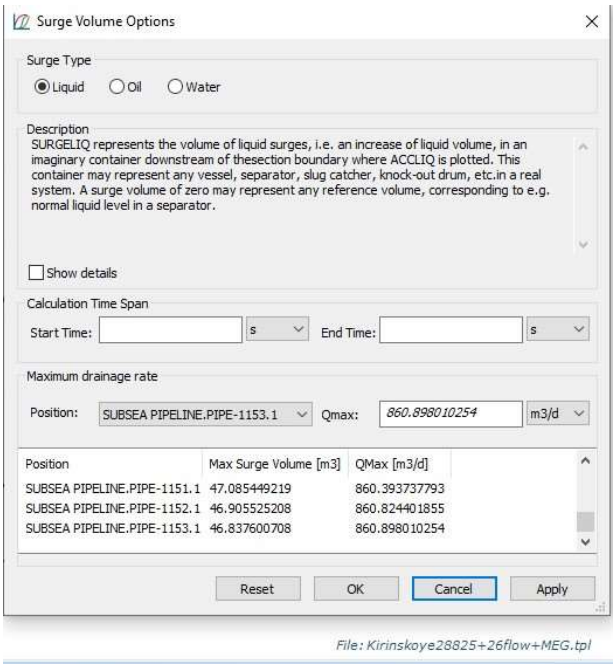

Figure 29. Precise maximum liquid surge volume and maximum liquid surge rate calculated by OLGA's Surge Volume interface (steady operational conditions; 2,64 million m^3/day flow)

6.4.2. Pig run: 2,64 million m^3/day flow

The only two differences between the OLGA model in this and the previous sub-section are in a pig being run through the pipeline during the simulation and the changed simulation period length, which was increased up to 21 hours, so as to let pig travel through the entire pipeline. Pig insertion and receiving points were discussed in sub-section 6.2 and are located in the start- and end-points of the pipeline, respectively. The pig insertion time takes as 12 hours from the start-up when the system fully stabilizes in its operational mode. The pre-run stabilized conditions within the system can be seen in Figure 30 below:

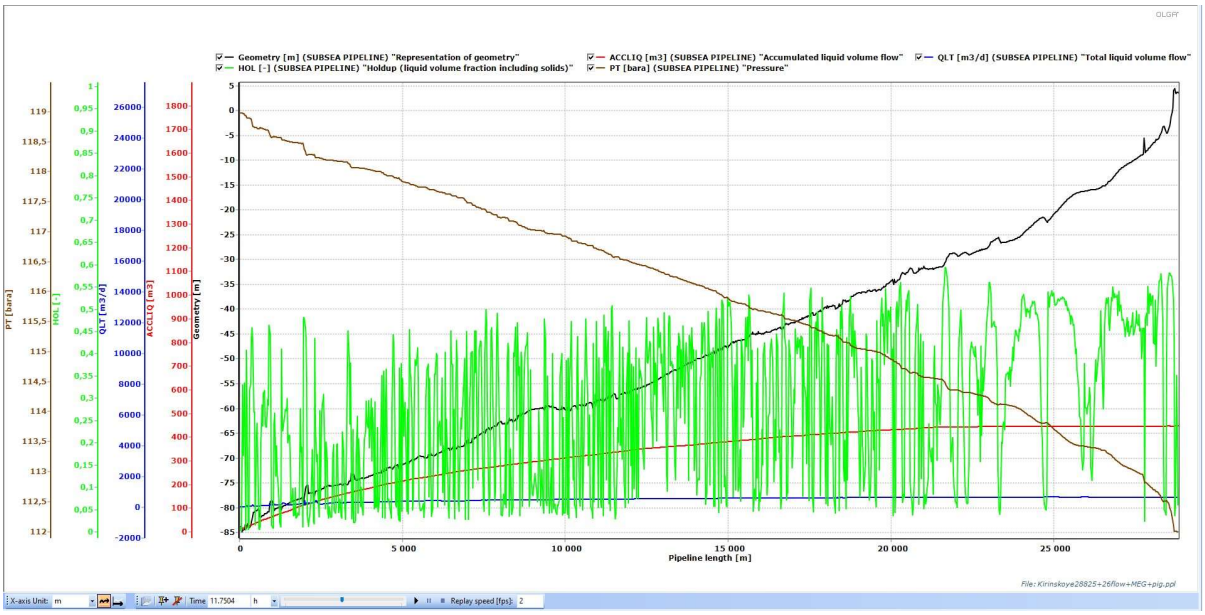

Figure 30. Distribution of pressure and holdup liquid within the system in its stabilized state & liquid flow data (11,75 hours since the start-up; $2{,}64 \cdot 10^6$ m^3/day)

As can be seen from the chart, minimum and maximum values for the holdup liquid along the pipeline are varying from 2 and 45% at the start, and up to 10 and 60% of its cross-section, respectively. Combining this with an extremely low QLT value, which stands for the total liquid volume flow, it is clear, that a tremendous volume of liquid is stored within the pipeline while it is in a normal operation mode.

Dynamic simulation before an actual pig run in this case is mandatory to ensure the safety of the operation planned. It is crucial to prove the fact that the slugcatcher will be capable to receive all the liquid removed by the pig without exceeding its capacity.

As the heading of the sub-section implies, the pig run is conducted for the flow of 2.64 million m^3/day, which means that the flow value is not reduced for the pig run in comparison with the stabilized operational conditions shown before.

The following Figures 31, 32, and 33 show the system parameters change along the pipeline during the pig run; Figure 34 represents the system's after-run conditions, where liquid flow out of the pipe is significantly reduced. It happens due to the fact that all the holdup liquid was removed by the pig, and now the pipeline system is gradually coming to its "stabilized state", which was seen in Figure 30.

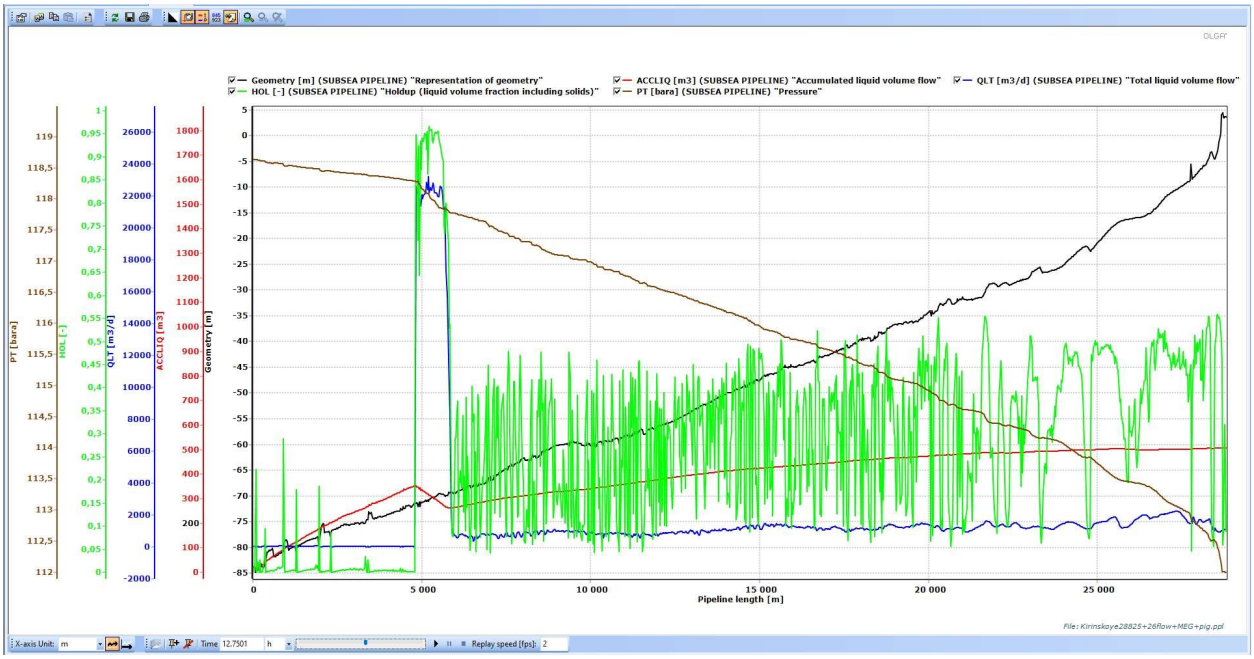

Figure 31. Pig run, part 1 of 3 (0,75 hour since the pig launch; $2{,}64 \cdot 10^6$ m^3/day)

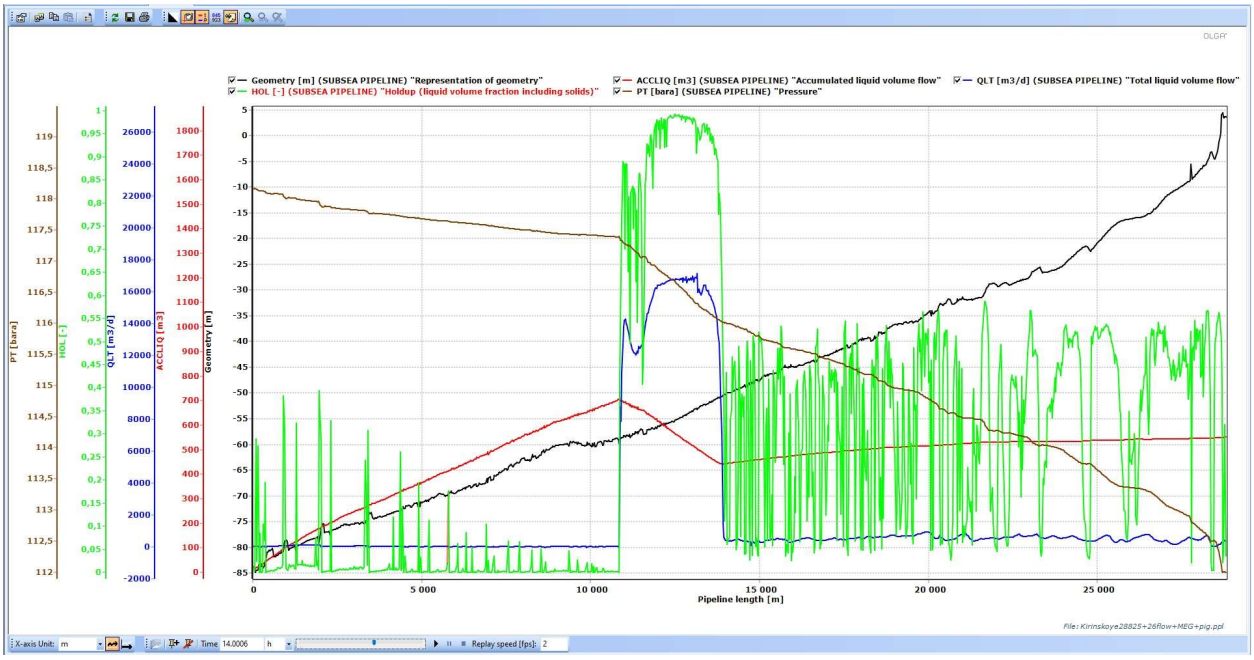

Figure 32. Pig run, part 2 of 3 (2,00 hours since the pig launch; $2{,}64 \cdot 10^6$ m^3/day)

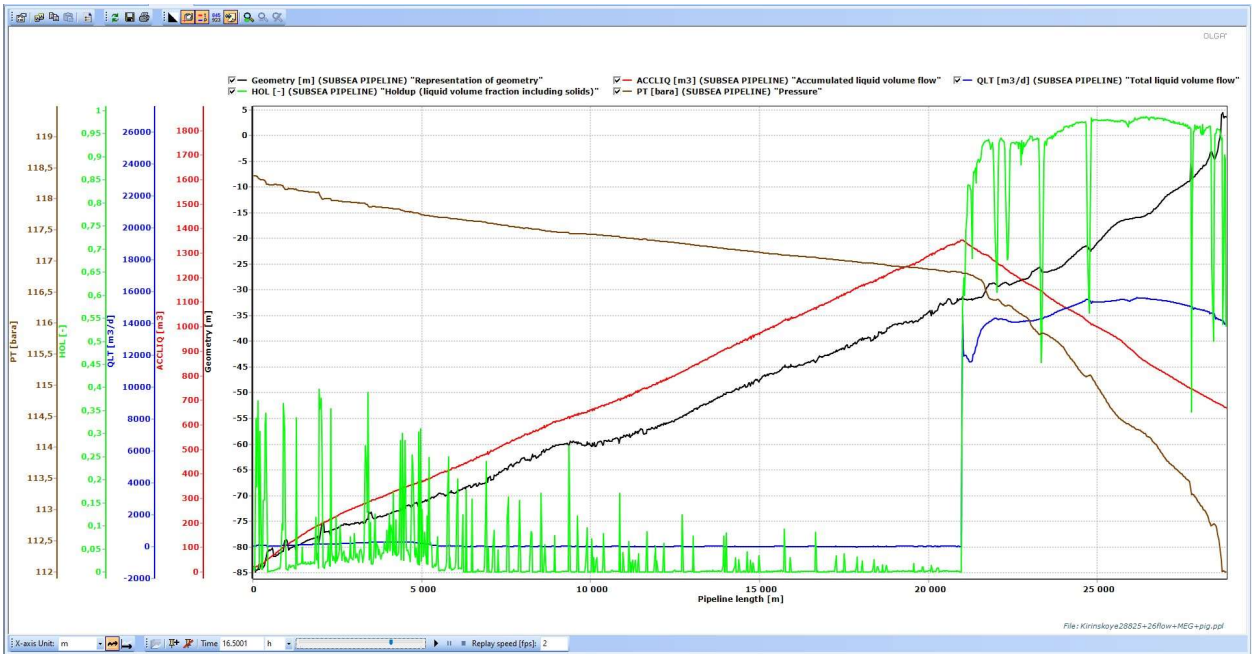

Figure 33. Pig run, part 3 of 3 (4,50 hours since the pig launch; $2{,}64 \cdot 10^6$ m^3/day)

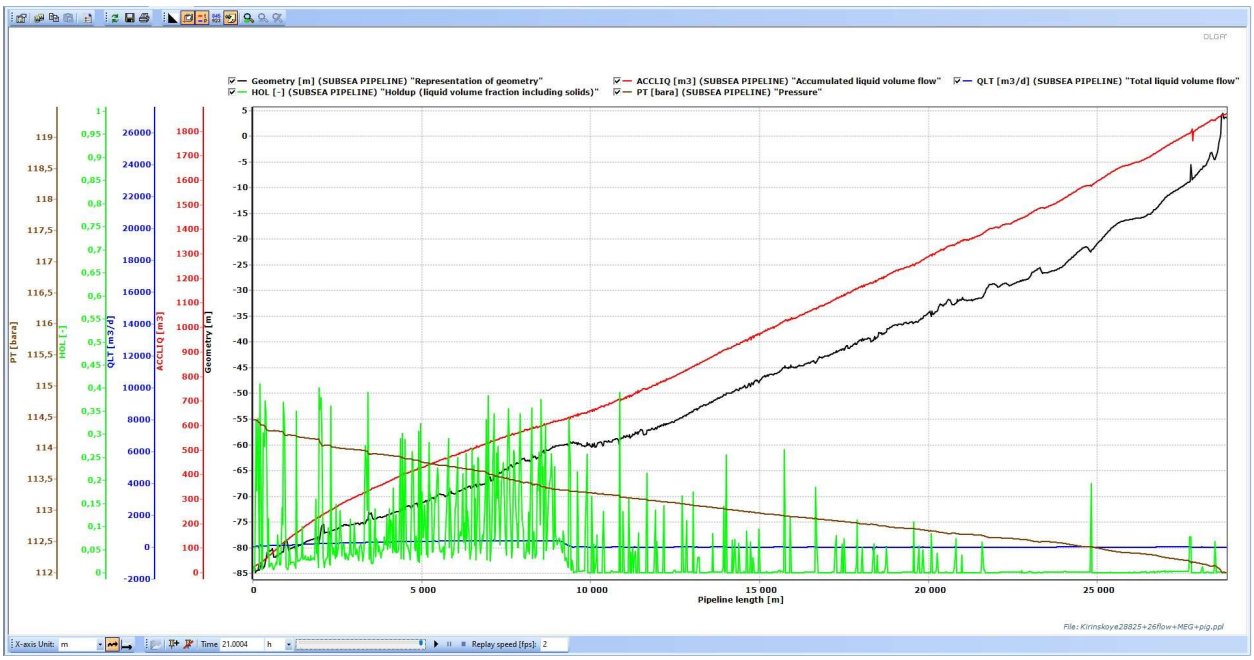

Figure 34. After-run distribution of pressure and holdup liquid in the system & changes in the accumulated and current liquid volume flow ($2{,}64 \cdot 10^6$ m^3/day)

To better trace the changes in total liquid volume flow out of the pipeline during the simulation time, a trend chart for the last pipeline' segment is plotted in Figure 35 on the next page. As it was discussed above, after the pig run and receiving of pig-collected water slug, liquid flow out of the pipe drops to zero, which can be easily seen on the chart. For the precise calculation of surge liquid volume and maximum rate, OLGA's surge volume interface was used, which can be seen in Figure 36 as well:

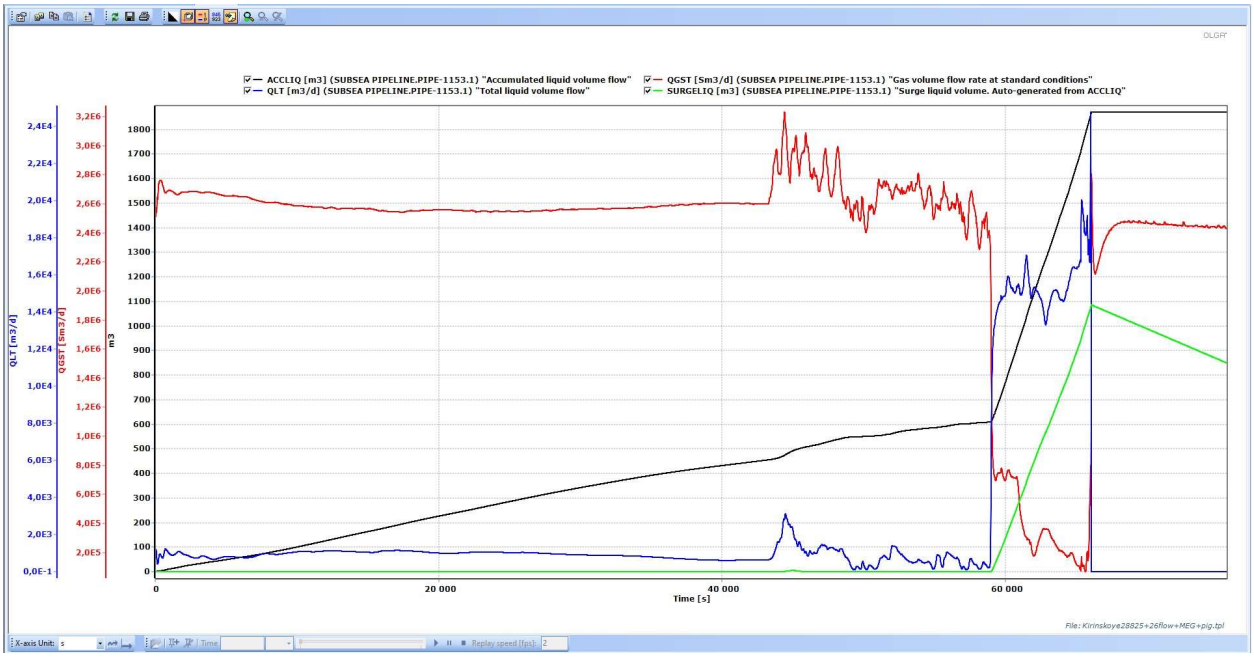

Figure 35. Liquid trend plot in the end-point for the entire simulation timespan ($2{,}64 \cdot 10^6$ m^3/day)

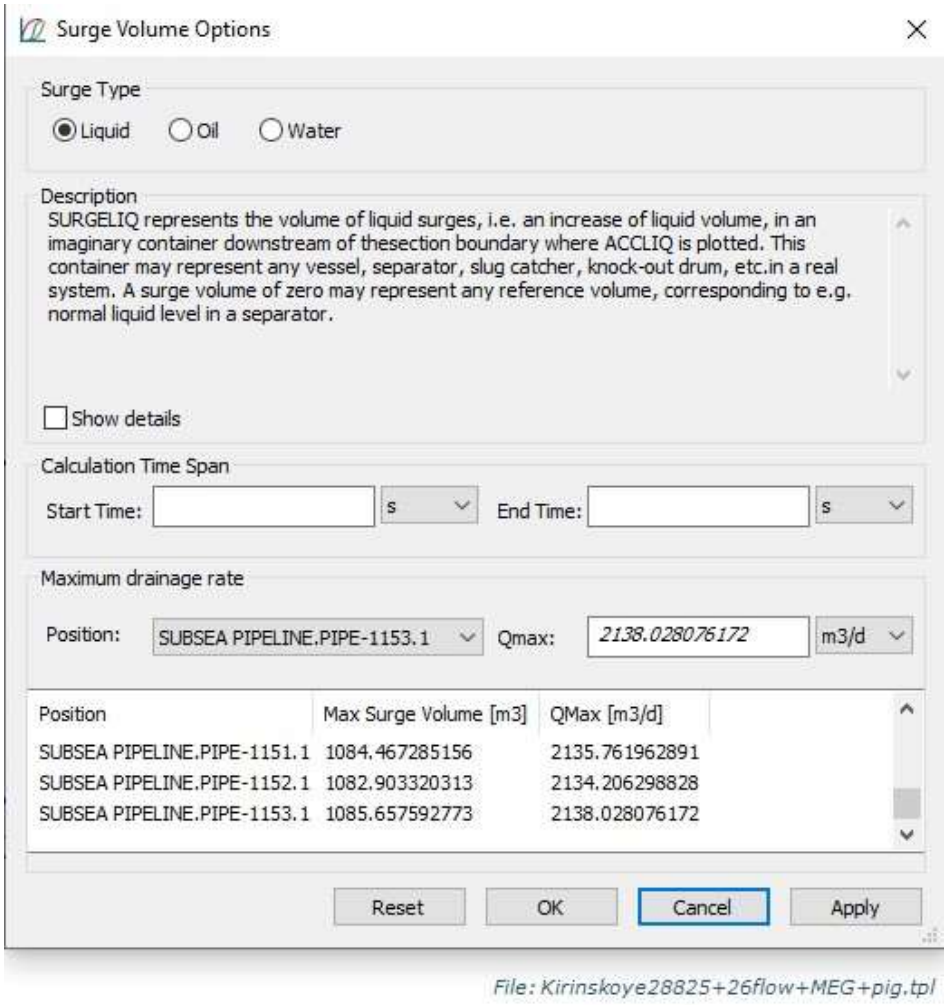

Figure 36. Precise maximum liquid surge volume and maximum liquid surge rate calculated by OLGA's Surge Volume interface (pig run simulation for the $2{,}64 \cdot 10^6$ m^3/day)

According to the surge volume calculations done by OLGA, the maximum liquid volume received by the slugcatcher as a result of the pig run will be at the level of 1085.66 m^3 of liquid. This value is quite high but still significantly lower than the slugcatchers liquid receiving capacity of 1500 m^3. This fact says that an actual pig run for the system under the given condition can be conducted safely regarding the possibility of exceeding the slugcatcher's liquid receiving limit.

The maximum liquid surge rate parameter is also worth mentioning. It represents the maximum flow into the slugcatcher per unit time of throughout the simulation (which, in this case, is definitely will take place at the moment of receiving the water slug being brought by the pig). Since the total volume of liquid received does not exceed the maximum slugcatcher's capacity, this parameter is safe as long as it does not exceed the maximum receiving rate per unit time for the slugcatcher.

However, if the total surge volume should exceed the capacity of a slugcatcher, this parameter should be compared to the maximum daily rate for the liquid treating capacity of the slugcatcher unit. It must be done to ensure the fact that all the volume of liquid received can be safely treated by the slugcatcher, while it is fully filled and operates close to its maximum treatment rate for some period of time.

6.4.3. Pig run: 3,5 million m^3/day flow

An actual project for Kirinskoye GCF was modeled for two flow values: 2,64 and 3,5 million m3/day, respectively. After conducting the pig run the simulation with the 2,64 million m3/day flow, it was decided to simulate the 3,5 million m3/day flow on the same operational scenario – to both prove its safety for the system and to conduct a comparative analysis for the result received.

Similarly to the previous sub-section of the work, the next Figures 37, 38, 39, 40, and 41 will represent the system's conditions in a stabilized operational mode before the pig run as well as throughout and after it.

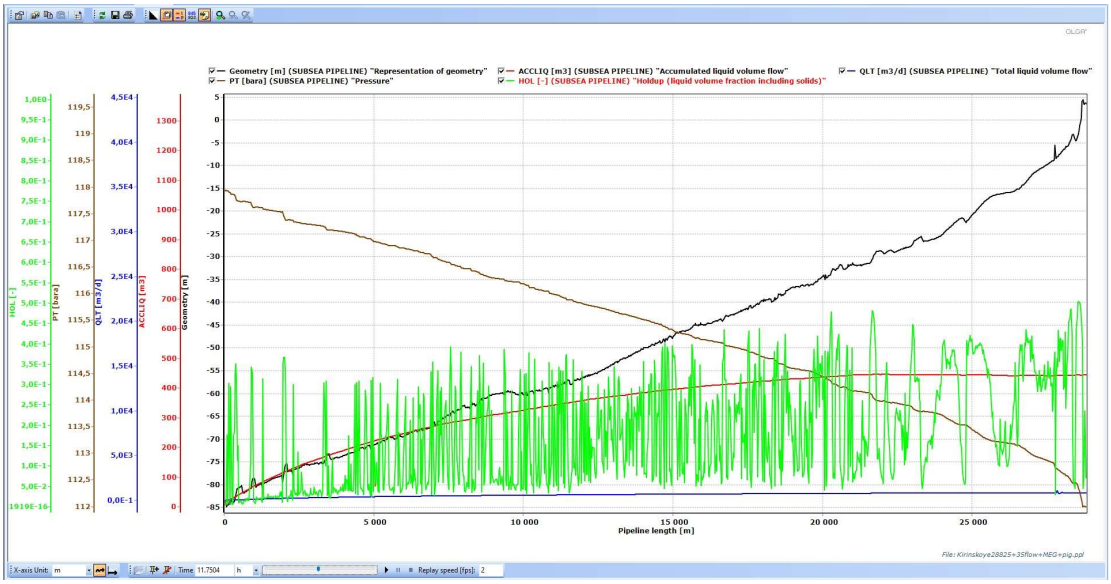

Figure 37. Pressure & holdup liquid distribution within the system in the stabilized state & liquid flow data (11,75 hours since the start-up; $3{,}5 \cdot 10^6$ m^3/day)

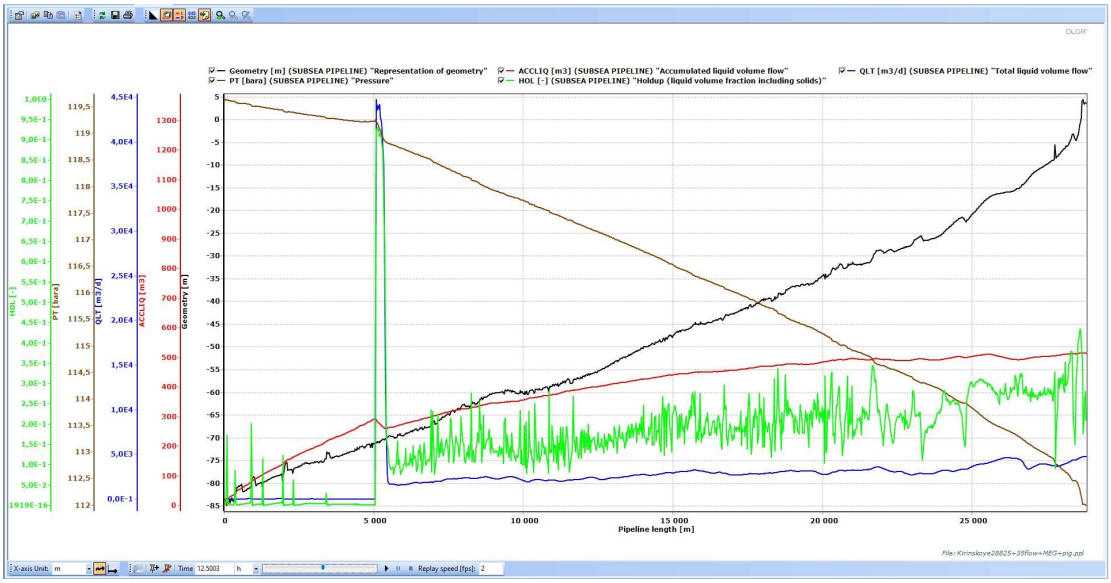

Figure 38. Pig run, part 1 of 3 (0,5 hours since the pig launch; $3{,}5 \cdot 10^6$ m^3/day)

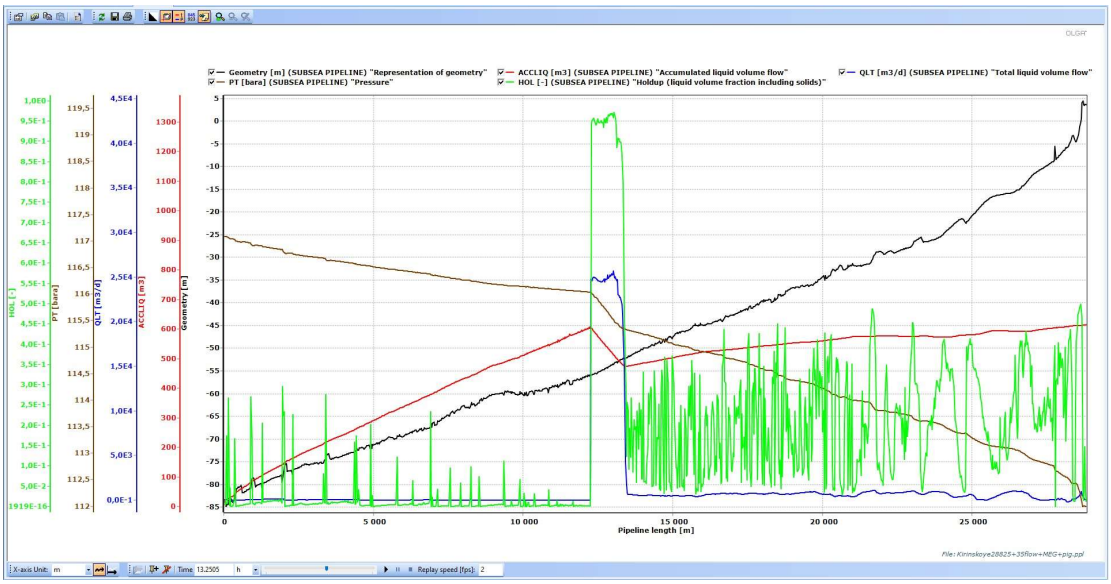

Figure 39. Pig run, part 2 of 3 (1,25 hours since the pig launch; $3{,}5 \cdot 10^6$ m^3/day)

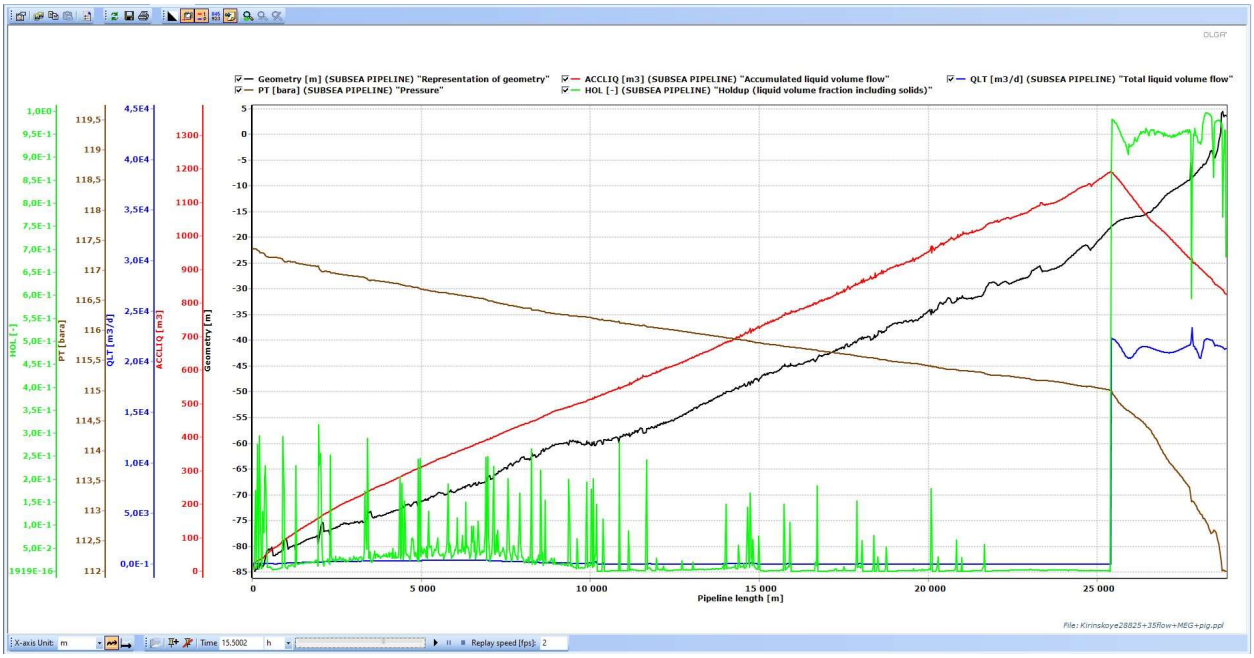

Figure 40. Pig run, part 3 of 3 (2,5 hours since the pig launch; $3{,}5 \cdot 10^6$ m^3/day)

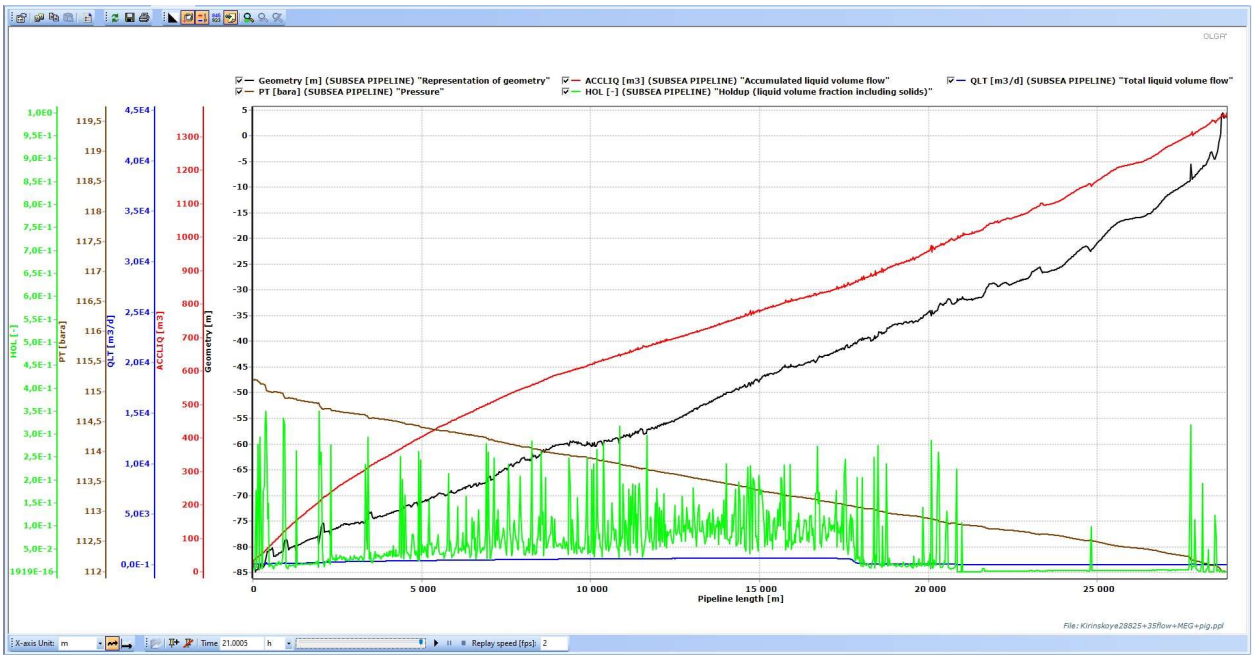

Figure 41. After-run distribution of pressure and holdup liquid in the system & changes in the accumulated and current liquid volume flow ($3{,}5 \cdot 10^6$ m^3/day)

Figures 37 ÷ 41 have a lot of similarities with the identical charts for the $2{,}64 \cdot 106$ m^3/day flow case, however, they have one significant difference that has to be highlighted. The distribution of the holdup liquid fraction function along the pipeline has a similar spike pattern due to the identical geometry data but the values are steadily lower by, approximately, 35%. In other words: a much lesser volume of liquid phase if being held up within the pipeline. This behavior was expected due to the higher flow velocity in this case.

As can be seen from Figures 42 and 43 below, to find the precise volume of surge liquid received by the slugcatcher a trend graph for the end-point of the pipeline was built and the Surge Volume interface in OLGA was used:

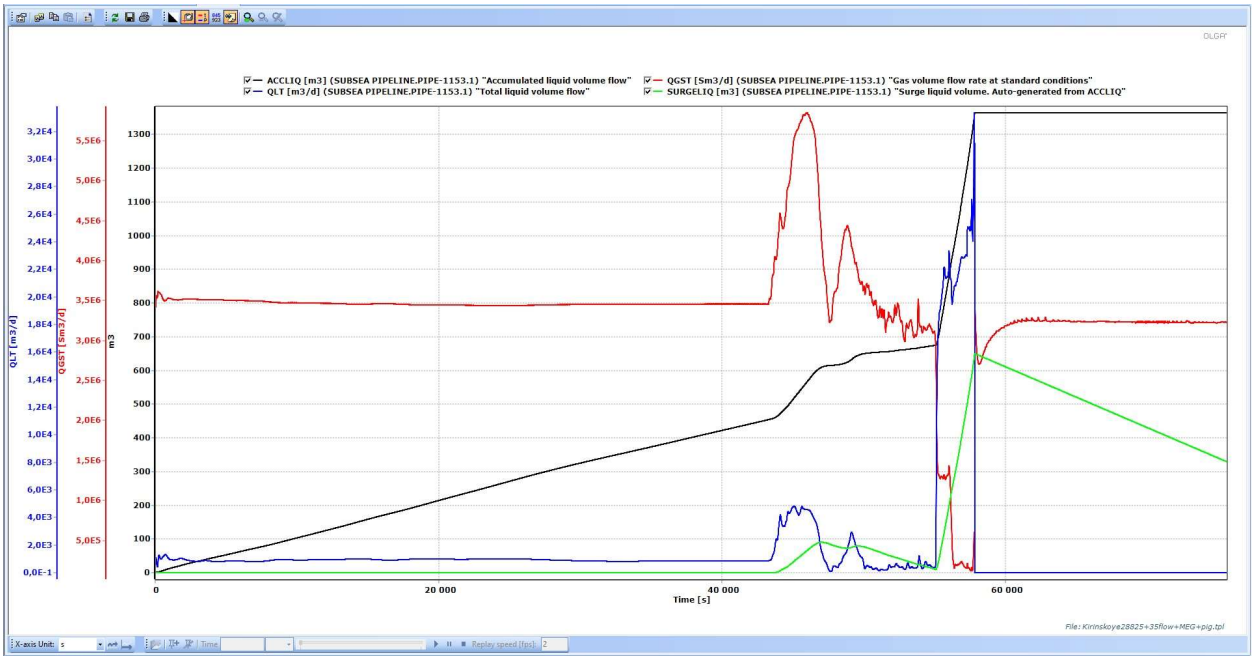

Figure 42. Liquid trend plot in the end-point for the entire simulation timespan ($3{,}5 \cdot 10^6$ m^3/day)

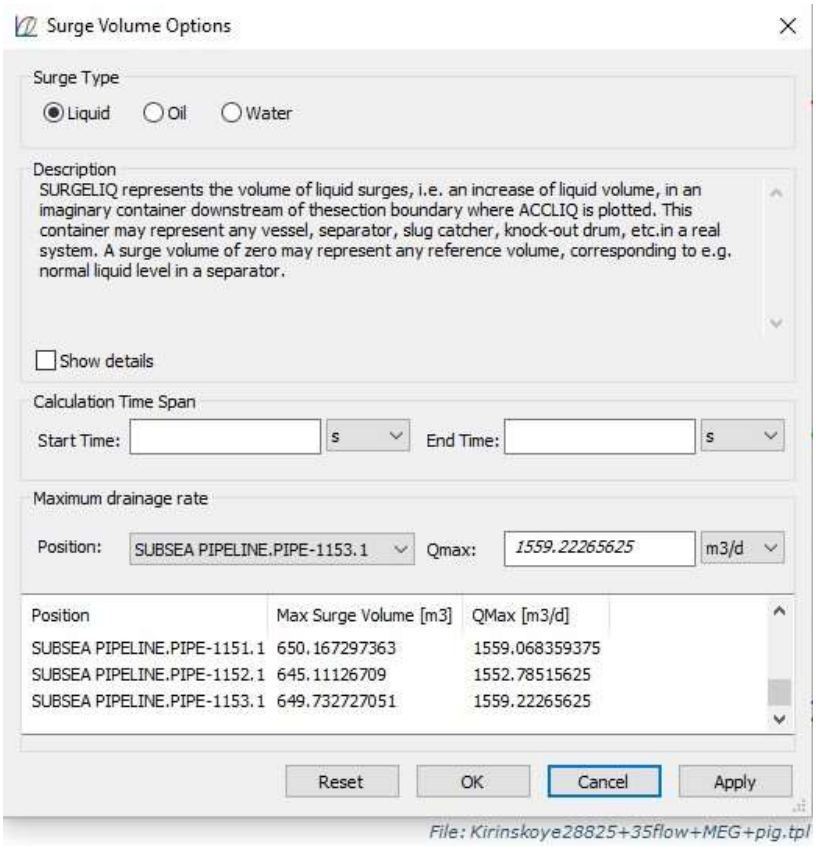

Figure 43. Precise maximum liquid surge volume and maximum liquid surge rate calculated by OLGA's Surge Volume interface (pig run simulation for the $3{,}5 \cdot 10^6$ m^3/day)

According to the surge volume calculations done by OLGA, the maximum liquid volume received by the slugcatcher as a result of the pig run for the system with $3{,}5 \cdot 10^6$ m^3/day flow will be at the level of 649,74 m^3 of liquid. Comparing this value to the surge volume of 1085,66 m^3 for the $2{,}64 \cdot 10^6$ m^3/day case, a reduction of 40% in the surge liquid volume received by the slugcatcher is observed. Hence, the case of a pig run with $3{,}5 \cdot 10^6$ m^3/day flow level is proved to be safe for implementation in the actual operations in regards to the slugcatcher's liquid receiving capacity.

This observation highlights the importance of selecting an optimal operational parameters setup for pipeline systems in the industry. Whereas both operational modes are safe to be implemented, the second case with an increased flow value allows a lesser volume of liquid to be held up within the pipeline during its stabilized operational mode and, thus, reducing the water corrosion level in the system, as well as the total volume of hydrate inhibitor needed for maintaining a constant concentration of 25% MEG solution within the system.

6.4.4. Pig run: pig velocity evaluation

Both modeled cases of pig runs turned out to be safe for their implementation in the actual operations according to the modeling result. However, as was mentioned in the sub-sections of the theoretical basis, the velocity of pig movement directly correlated with the quality of inspection data received. For some intelligent pigging measuring principles exceeding the velocity of 5 m/s would be critical and it will not be possible to effectively implement them. Due to this fact, the pig velocity in the simulations made has to be estimated.

When industry specialists perform simulations similar to the ones that have been conducted in this work, they commonly have access to all of the OLGA capabilities and can simply track the pig velocity parameter directly in the software. However, this work was made by me as a university student, and the only available version of OLGA in the University laboratories included just the standard license, which does not allow to track the pig velocity parameter directly.

Luckily, OLGA provides both pig's launch and removal time in the command prompt window during the simulation process. The screenshots for both flow cases of $2{,}64 \cdot 10^6$ m^3/day and $3{,}5 \cdot 10^6$ m^3/day are represented in Figures 44 and 45, respectively:

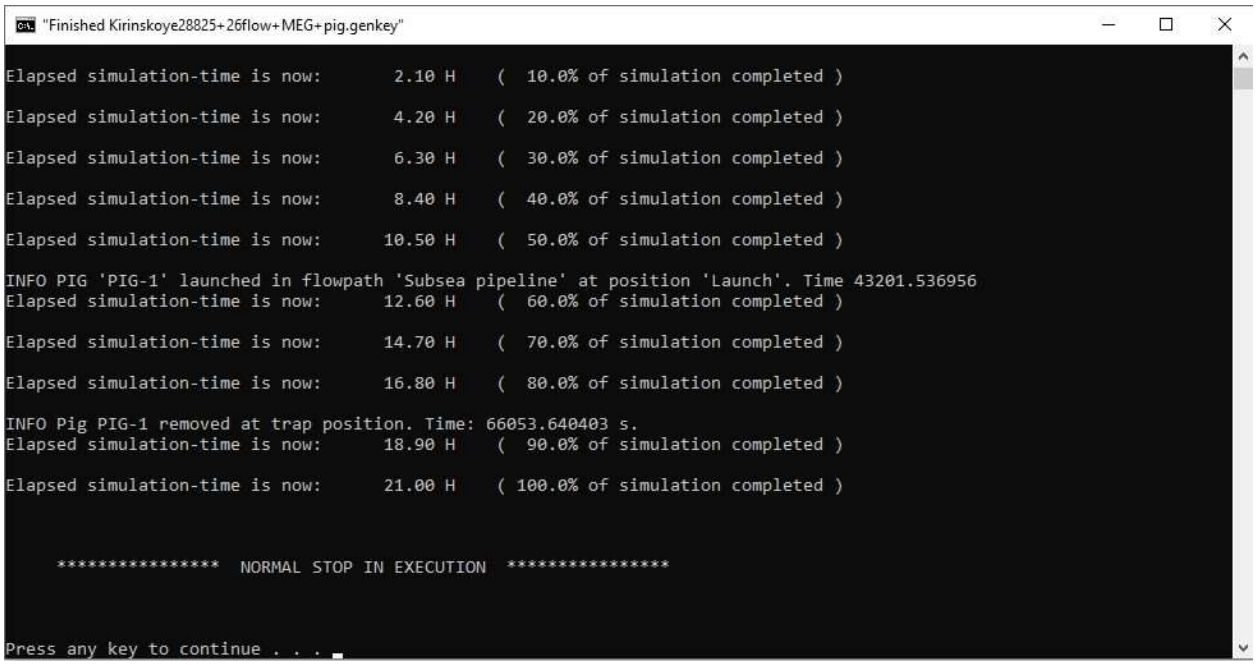

Figure 44. Pig launch and removal time, simulation for the $2{,}64 \cdot 10^6$ m^3/day flow

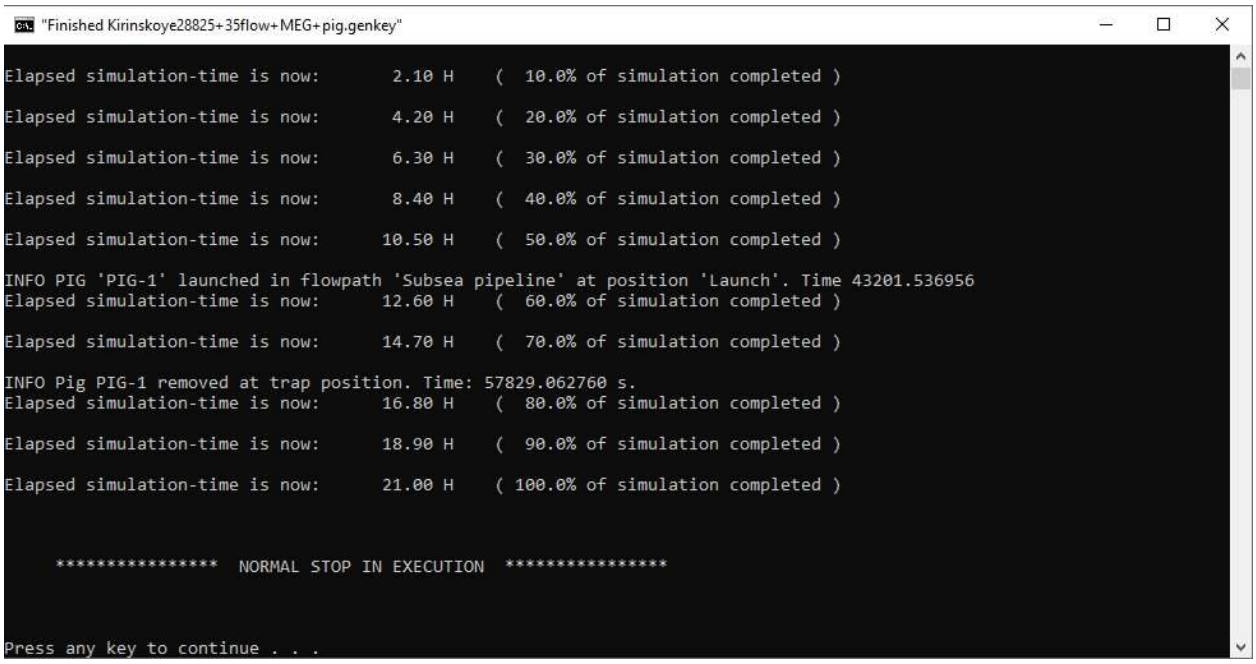

Figure 45. Pig launch and removal time, simulation for the $3{,}5 \cdot 10^6$ m^3/day flow

Having these time values and knowing the exact length of pig's route being equal to 28825 m, average pig velocities and pig travel time values can be simply calculated for both of the modelling cases.

Table 6.6 – Pig travel time and average velocity calculation

Pig №	Launch time, s	Removal time, s	Distance travelled, m	Travel time, h	Average velocity, m/s
Pig 1	43202	66054	28825	6,35	1,26
Pig 2	43202	57829	28825	4,06	1,97

According to the results of the pigs' average velocity calculation for the modeled cases, the following conclusion can be done: during both modeled cases, smart-pigging technologies of any type considered in the theoretical basis before in this work can be implemented without damaging the quality of measurements being received.

6.5. Observations made

A) Hydrate formation modelling:

According to the results of OLGA modeling for the initial chemical composition, the pipeline pressure-temperature conditions in a stabilized operational state are entering the hydrate formation domain starting at 11600 m from the start point, if none of the known hydrate formation inhibitors is injected.

According to the industry practices, the most economically effective measure in such a severe hydrate formation case would be the continuous injection of hydrate inhibitor into the pipeline system.

Monoethylene glycol (MEG) was selected as the hydrate formation inhibitor to be implemented due to the pipeline's systems being designed for its use. The systems were designed to inject up to 80% concentration of MEG according to the initial data.

The actual optimal concentration of hydrate inhibitor injection was modeled with the use of OLGA and PVTSim software. According to the results of modeling, 25% MEG concentration (in "MEG + water" solution) was selected as optimal for the given case.

The concentration selected fully eliminates the problem of hydrate formation along the entire pipeline in both stabilized operational and shut-down conditions due

to the absence of overlap between the hydrate formation pressure-temperature domain and possible operational conditions of the pipeline (see Figure 24 / B.6).

It is also important to mention that during the continuous injection of hydrate inhibitor into the system, it is regained back with the liquid phase on the slugcatcher unit, regenerated up to the required concentration, and injected back into the system. Such an approach is a standard industry practice and allows for a significant reduction of the volume of hydrate inhibitor spent (hence, the operational expenditures for the pipeline are also reduced).

Last but not least, the water received from the system during the continuous hydrate inhibitor injection is thoroughly purified up to the required PPM value in it, before being disposed out of the system. Thus, the environmental impact of the operations is minimized.

B) Water surge modelling:

The first water surge modelling was conducted for the stabilized operational case with the flow value of $2{,}64 \cdot 10^6$ m^3/day; the second and third modelling cases included the pig run during the simulation time and were simulated for the $2{,}64 \cdot 10^6$ m^3/day and $3{,}5 \cdot 10^6$ m^3/day flow cases, respectively.

According to the results of OLGA's Surge Volume calculation interface, surge volume in all three cases was calculated and amounted to 46,84 m^3, 1085,66 m^3, and 649,74 m^3, respectively. The surge volumes were proved to lie within the liquid receiving capacity limit of the slugcatcher installed and, thus, all three simulated cases can be safely implemented in real operations for the system of given parameters.

However, if the surge volumes would have exceeded the liquid receiving capacity of the slugcatcher, the maximum surge rate values would have played a decisive role. The calculated maximum surge rate values have amounted to 860,89 m^3, 2138,03 m^3, and 1559,22 m^3, respectively to the order of simulations conducted. In case of a critical surge volume obtained as a result of simulation, these maximum surge rate values should have been smaller than the slugcatcher's ability to treat and safely dispose of liquid per unit time, to ensure the safety of operations.

Lastly, even though both $2{,}64 \cdot 10^6$ m^3/day and $3{,}5 \cdot 10^6$ m^3/day flow values are safe for being implemented in the considered pipeline system, it is highly recommended to use the higher value of flowrate. This recommendation is based on the fact that the higher flowrate value reduces the volume of liquid being held up along the pipeline, which was additionally proved by the OLGA simulation results. The reduction in the holdup liquid volume will lead to lesser pressure losses and reduced water corrosion along the pipeline, as well as will minimize the volume of required hydrate inhibitor to be presented in the system to maintain the selected optimal concertation of it in relation to water.

C) Pig velocity evaluation:

For both $2{,}64 \cdot 10^6$ m^3/day and $3{,}5 \cdot 10^6$ m^3/day flowrate cases, all types of intelligent pigging measurement principles can be effectively implemented without any concerns regarding the loss of measurement quality. This conclusion is made on the fact that the calculated pig velocities in these two cases amounted to 1,26 m/s and 1,97 m/s, respectively. These velocity values can be classified as moderate and lying within the limits of allowable pig velocities for even the most sensitive measurement methods on the ones being considered for in this work (EMAT in particular).

7. Conclusions

Regardless of being the most widespread method of hydrocarbon transportation, pipelines bear significant challenges in their operation and maintenance. The challenges become particularly acute when it comes to subsea pipeline transportation, where the access to the pipeline's outer wall is significantly obstructed due to its placement on the seabed or even beneath it in case of trenching protection.

At present, for extreme conditions like that in-line inspection tools and dynamic modeling software turn out to be the most accessible and reliable source of information about the pipeline system's operational state and capabilities.

In this thesis, OLGA and PVTSim software packages were utilized to model a hypothetical subsea pipeline, which was based on the Kirinskoye GCF subsea pipeline dataset. The modeling was conducted for the two following flow assurance concerns presented in the system:

1) Severe hydrate formation zone within the pipeline (around 17 km length in the initial case, when no hydrate inhibitor is added);

2) Liquid surge volume in the stabilized operational regime and while a pig run.

Concluding the hydrate simulations and their analysis conducted, it is recommended to implement a continuous injection of MEG as a hydrate inhibitor for the considered subsea pipeline. The injection should be performed at such a rate that the 25% concentration of MEG in water-MEG solutions is being maintained inside the system.

The solution selected will have a positive effect on the pipeline’s operational and possible maintenance costs due to the fact that the concentration of MEG is being kept as close to the hydrate-free minimum concentration level for the system as reasonably possible (thus, minimizing the operational costs for the inhibitor used), whereas maintaining a zero probability for the hydrate formation even in a case of pipeline’s shutdown (hence, the absence of hydrate formation risk minimizes the possible maintenance cost due to the hydrate problem up to zero as well).

The costs of this method implementation are additionally minimized by the application of a hydrate inhibitor regeneration system, which separates liquid received by the slugcatcher unit into hydrate inhibitor of a selected concentration (80% according to the hydrate inhibitor system' specification in the considered case), liquid hydrocarbons fraction and purified water. The last one is purified up to the standardized ppm level of other chemicals' presence and can afterward be safely discarded with a minimized environmental effect.

Regarding the surge liquid volume modeling results, it can be concluded that both of the considered flow regimes of $2{,}64 \cdot 10^6$ m^3/day and $3{,}5 \cdot 10^6$ m^3/day can be safely implemented for the system. However, it is recommended to operate the system with a higher value of the flow rate. This recommendation is based on the fact that higher flow velocity allows the lesser liquid volume to stay held up inside the pipeline, thus, minimizing the pressure losses and water-driven corrosion along the pipeline. Furthermore, the reduction of total liquid volume within the system will result in the reduced volume of the hydrate inhibitor required to be distributed along the system to maintain the hydrate-free operational mode as well.

Lastly, according to the calculated pig velocities, in both cases, the pig run can be conducted with any type of intelligent pig measuring principle without any loss on the measurement quality (which can be significantly reduced in cases of smart pig speed exceeding the 5 m/s threshold) if it would be needed for the in-line inspection purposes.

References

1. Mansurov M.N.: “Offshore pipelines in the Arctic. Geotechnical monitoring problems”, Neftegaz journal, May 2019.
   Link: https://magazine.neftegaz.ru/articles/transportirovka/473739-morskie-truboprovody-v-arktike-problemy-geotekhnicheskogo-monitoringa/
2. DNVGL: Recommended failure rates for pipelines – Report for Statoil Petroleum AS, DNV GL, Report № 2017-0547, Rev-2; Document № 114ORRJD-17.
3. Lindsay, R: “Protecting the World: Introducing Corrosion Science and Engineering”, lecture “Oilfield corrosion and control – Sweet corrosion”, The University of Manchester, accessed via Coursera, 2023.
   Link: https://www.coursera.org/lecture/corrosion/sweet-and-sour-corrosion-AUorp
4. Lindsay, R: “Protecting the World: Introducing Corrosion Science and Engineering”, lecture “Oilfield corrosion and control - Sour corrosion”, The University of Manchester, accessed via Coursera, 2023.
   Link: https://www.coursera.org/lecture/corrosion/sour-corrosion-RrEmS
5. Cheremisinoff, N.P., Gupta, R.: “Handbook of Fluids in Motion”. Ann Arbor Science Publishers: Ann Arbor, Michigan, USA, 1983.
6. Mokhatab S, Poe W.A., Speight J.G.: "Handbook of Natural Gas Transmission and Processing", Elsevier, 2006.
7. Bai Y., Bai Q.: “Subsea Pipelines and Risers”, Elsevier, UK, 2005.
8. Næss S.: “Introduction to Flow Assurance”, Equinor’s specialist presentation as a part of the course OFF550 “Subsea technologies”, UiS, 2022.
9. NOV Completion & Production Solutions: “Subsea automatic pig launcher (SAPL)” flyer, Asker, Norway, 2023.
10. Girard Industries Inc.: “Mandrel-pigs Brochure”, Houston, Texas, 2023. Link: https://girardindustries.com/mandrel-pigs.php
11. Payne L.: “The re-emergence of spherical pigs”, Pipeline & Gas Journal, p. 44-45, January 2018.

12. Brockhaus S., Ginten M., Klein S., Teckert M., Stawicki O., Oevermann D., Meyer S., and Storey D.: “In-line inspection (ILI) methods for detecting corrosion in underground pipelines”, ROSEN Group, Germany, December 2014; DOI: http://dx.doi.org/10.1533/9780857099266.2.255
13. Shi Y., Zhang C., Li R., Cai M., and Jia G.: “Theory and application of Magnetic Flux Leakage pipeline detection”, PetroChina Pipeline Company, China, December 2015; DOI: 10.3390/s151229845.
14. EPCM Holdings: “In-line inspection with Magnetic Flux Leakage” article Link: https://epcmholdings.com/magnetic-flux-leakage-inline-inspection/
15. Dijkstra F., De Raad J.: “The history of Automated Ultrasonic Testing”, Rotterdam, Netherlands, 2006.
Link: https://www.ndt.net/search/docs.php3?id=3774
16. G. Cotter Enterprises: “Our Ultrasonic Testing (UT) Service” article
Link: https://gcotter.com/ultrasonic-testing
17. Alers G.: “A History of EMATs”, EMAT Consulting, San Luis Obispo, California, 2008; DOI: https://doi.org/10.1063/1.2902745
18. Berke O.P., Huseyin A.Y.: “A Comprehensive Analysis of In-Line Inspection Tools and Technologies for Steel Oil and Gas Pipelines”, Department of Mechatronics Engineering, Yildiz Technical University, Istanbul, Turkey, February 2023; DOI: https://doi.org/10.3390/su15032783
19. Olympus InSight blog: “History of Eddy Current Testing”, 2023; Link: https://www.olympus-ims.com/en/ndt-tutorials/eca-tutorial/intro/history/
20. The Severn Group: “Eddy Current Testing 101”, February 2018.
Link: https://www.theseverngroup.com/eddy-current-testing-101/
21. Onestop NDT: “Applications of Eddy Current Testing – All You Need To Know”, January 2023.
Link: https://www.onestopndt.com/ndt-articles/applications-of-eddy-current-testing-all-you-need-to-know

22. GOST R (Russian National Standard) № 54382-2021: “Petroleum and natural gas industry. Subsea pipeline systems. General technical requirements”, Moscow, Russia, May 2021.
23. GOST R (Russian National Standard) № 55999-2014: “In-line inspection of gas pipelines. General requirements”, Moscow, Russia, October 2019.
24. ND № 2-090601-007: “Guidelines for the design, construction and operation of the offshore subsea pipelines”, Russian Maritime Register of Shipping, Saint Peterburg, Russia, January 2020.
25. Bendiksen K. H., Maines D., Moe R., etc.: ”The Dynamic Two-Fluid Model OLGA: Theory and Application”, SPE Production Engineering, May, 1991. Link: https://doi.org/10.2118/19451-PA
26. SLB Product Solutions: “OLGA Core and Modules - Overview”, 2022. Link: https://www.software.slb.com/products/olga
27. Calsep: “PVTsim Technical Overview”, Houston, Texas, 2020. Link: https://www.calsep.com/pvtsim-nova/
28. Karam T.: “Slug Catchers in Natural Gas Production”, Trondheim, Norway, December 2012. Link: https://www.yumpu.com/en/document/read/23496504/slug-catchers-in-natural-gas-production-ntnu

Appendix A – Pipeline profile dataset

Horizontal distance, m	Altitude, m
0	-83,88
25	-83,88
50	-83,76
75	-84,86
100	-84,43
125	-84,43
150	-84,32
175	-83,53
200	-84,32
225	-83,54
250	-83,22
275	-83,70
300	-83,97
325	-83,72
350	-83,59
375	-82,84
400	-81,71
425	-80,94
450	-80,88
475	-80,57
500	-80,66
525	-80,55
550	-80,39
575	-80,21
600	-80,63
625	-81,78
650	-81,85
675	-81,79
700	-81,62
725	-81,59
750	-81,43
775	-81,23
800	-81,15
825	-81,06
850	-81,01
875	-80,86
900	-80,86
925	-79,45
950	-78,76
975	-78,51
1000	-78,61
1025	-78,90
1050	-80,53
1075	-80,41
1100	-80,22
1125	-80,22
1150	-80,10
1175	-80,00
1200	-79,90
1225	-79,80
1250	-79,81
1275	-80,68
1300	-79,77
1325	-79,73
1350	-79,67
1375	-79,59
1400	-79,51
1425	-79,41
1450	-79,33
1475	-79,15
1500	-79,11
1525	-79,03
1550	-78,92
1575	-78,80
1600	-78,76
1625	-78,71
1650	-78,60
1675	-78,56
1700	-78,55
1725	-78,43
1750	-78,42
1775	-78,37
1800	-78,30
1825	-78,25
1850	-78,32
1875	-78,13
1900	-78,09
1925	-77,90
1950	-79,57
1975	-78,01
2000	-77,31
2025	-76,22
2050	-75,71
2075	-75,41
2100	-75,46
2125	-77,08
2150	-77,07
2175	-77,07
2200	-77,03
2225	-77,01
2250	-76,83
2275	-77,15
2300	-77,80
2325	-76,75
2350	-76,68
2375	-76,66
2400	-76,54
2425	-76,45
2450	-76,55
2475	-76,30
2500	-76,35
2525	-76,25
2550	-76,16
2575	-76,07
2600	-75,88
2625	-75,76
2650	-75,80
2675	-75,69
2700	-75,56
2725	-75,55
2750	-75,62
2775	-75,53
2800	-75,57
2825	-75,63
2850	-75,72
2875	-75,65
2900	-75,49
2925	-75,50
2950	-75,50
2975	-75,53
3000	-75,45
3025	-75,29
3050	-75,33
3075	-75,29
3100	-75,20
3125	-75,27

3150	-75,44
3175	-75,32
3200	-75,22
3225	-75,14
3250	-75,10
3275	-75,34
3300	-75,33
3325	-75,19
3350	-74,82
3375	-74,60
3400	-74,62
3425	-73,13
3450	-73,38
3475	-73,42
3500	-73,20
3525	-73,76
3550	-74,24
3575	-74,46
3600	-74,43
3625	-74,21
3650	-74,34
3675	-74,21
3700	-74,12
3725	-74,13
3750	-74,04
3775	-74,00
3800	-74,11
3825	-74,07
3850	-74,02
3875	-74,00
3900	-73,88
3925	-73,82
3950	-73,80
3975	-73,65
4000	-73,64
4025	-73,63
4050	-73,45
4075	-73,47
4100	-73,33
4125	-73,19
4150	-73,30
4175	-73,04
4200	-73,06
4225	-73,11
4250	-72,91

4275	-72,98
4300	-72,98
4325	-72,98
4350	-72,99
4375	-72,47
4400	-72,77
4425	-72,77
4450	-72,13
4475	-72,52
4500	-72,43
4525	-71,94
4550	-71,95
4575	-71,92
4600	-71,86
4625	-71,87
4650	-71,90
4675	-72,21
4700	-72,20
4725	-71,92
4750	-71,68
4775	-71,44
4800	-71,47
4825	-71,51
4850	-71,38
4875	-71,52
4900	-72,02
4925	-71,20
4950	-72,08
4975	-71,15
5000	-71,37
5025	-71,15
5050	-71,15
5075	-71,09
5100	-70,92
5125	-70,84
5150	-71,01
5175	-70,77
5200	-71,09
5225	-70,69
5250	-70,61
5275	-70,47
5300	-70,29
5325	-70,35
5350	-70,41
5375	-70,32

5400	-70,18
5425	-70,08
5450	-69,99
5475	-69,79
5500	-69,55
5525	-69,56
5550	-69,60
5575	-69,64
5600	-69,67
5625	-69,69
5650	-69,64
5675	-69,95
5700	-70,02
5725	-69,95
5750	-69,88
5775	-69,78
5800	-69,33
5825	-69,44
5850	-69,24
5875	-69,09
5900	-69,40
5925	-69,44
5950	-69,54
5975	-69,51
6000	-69,40
6025	-69,34
6050	-69,20
6075	-68,86
6100	-69,01
6125	-68,94
6150	-68,86
6175	-68,81
6200	-68,83
6225	-68,56
6250	-68,60
6275	-68,46
6300	-68,61
6325	-68,24
6350	-68,28
6375	-68,14
6400	-68,06
6425	-68,08
6450	-68,43
6475	-68,47
6500	-68,16

6525	-68,08
6550	-67,79
6575	-67,88
6600	-67,65
6625	-68,18
6650	-68,10
6675	-67,89
6700	-67,59
6725	-67,63
6750	-67,75
6775	-67,75
6800	-67,67
6825	-67,65
6850	-67,60
6875	-67,58
6900	-67,50
6925	-66,66
6950	-67,38
6975	-66,51
7000	-66,39
7025	-66,26
7050	-66,98
7075	-66,89
7100	-66,85
7125	-66,72
7150	-66,05
7175	-66,11
7200	-66,13
7225	-65,84
7250	-65,84
7275	-65,54
7300	-65,40
7325	-65,46
7350	-65,42
7375	-65,29
7400	-65,15
7425	-64,96
7450	-64,78
7475	-64,73
7500	-64,77
7525	-65,01
7550	-64,89
7575	-64,40
7600	-64,10
7625	-63,97
7650	-63,91
7675	-64,23
7700	-64,31
7725	-64,06
7750	-63,85
7775	-63,70
7800	-63,60
7825	-63,51
7850	-63,55
7875	-63,65
7900	-63,44
7925	-62,99
7950	-62,79
7975	-62,74
8000	-62,67
8025	-62,57
8050	-62,81
8075	-63,05
8100	-63,07
8125	-63,01
8150	-63,12
8175	-62,94
8200	-63,17
8225	-63,04
8250	-62,90
8275	-61,93
8300	-62,42
8325	-62,29
8350	-62,25
8375	-62,53
8400	-62,67
8425	-62,50
8450	-62,45
8475	-62,20
8500	-62,07
8525	-62,13
8550	-61,45
8575	-61,42
8600	-61,13
8625	-61,64
8650	-61,46
8675	-60,97
8700	-61,11
8725	-61,13
8750	-61,04
8775	-60,94
8800	-60,83
8825	-60,73
8850	-60,52
8875	-60,29
8900	-60,39
8925	-60,47
8950	-60,20
8975	-60,18
9000	-60,17
9025	-60,17
9050	-60,15
9075	-60,10
9100	-60,06
9125	-60,01
9150	-60,05
9175	-60,11
9200	-60,00
9225	-59,88
9250	-59,98
9275	-59,95
9300	-59,86
9325	-59,94
9350	-60,30
9375	-59,81
9400	-59,48
9425	-59,55
9450	-59,71
9475	-59,44
9500	-59,45
9525	-59,70
9550	-59,72
9575	-59,61
9600	-59,98
9625	-59,61
9650	-59,77
9675	-59,79
9700	-59,81
9725	-59,96
9750	-60,19
9775	-60,18
9800	-60,23
9825	-60,33
9850	-60,23
9875	-60,17

9900	-59,56
9925	-60,01
9950	-59,81
9975	-60,08
10000	-60,25
10025	-60,39
10050	-59,83
10075	-60,31
10100	-59,66
10125	-60,45
10150	-60,38
10175	-60,30
10200	-59,63
10225	-59,50
10250	-59,53
10275	-59,40
10300	-59,47
10325	-59,54
10350	-60,18
10375	-60,08
10400	-59,31
10425	-59,26
10450	-59,31
10475	-59,47
10500	-59,42
10525	-59,18
10550	-59,45
10575	-59,45
10600	-59,43
10625	-59,39
10650	-59,11
10675	-59,05
10700	-58,91
10725	-58,94
10750	-58,78
10775	-58,80
10800	-58,88
10825	-59,02
10850	-59,77
10875	-58,62
10900	-58,80
10925	-58,70
10950	-58,73
10975	-58,34
11000	-58,26

11025	-58,53
11050	-58,29
11075	-58,19
11100	-58,26
11125	-58,47
11150	-58,07
11175	-58,68
11200	-58,32
11225	-58,32
11250	-57,93
11275	-58,05
11300	-57,94
11325	-57,55
11350	-57,78
11375	-57,49
11400	-57,90
11425	-57,57
11450	-57,29
11475	-57,04
11500	-57,02
11525	-57,09
11550	-57,80
11575	-57,99
11600	-57,98
11625	-57,91
11650	-57,97
11675	-57,15
11700	-57,17
11725	-57,07
11750	-57,14
11775	-56,97
11800	-56,80
11825	-56,77
11850	-56,96
11875	-56,97
11900	-56,93
11925	-56,63
11950	-56,90
11975	-56,55
12000	-56,44
12025	-56,51
12050	-56,23
12075	-56,41
12100	-56,14
12125	-56,18

12150	-56,25
12175	-55,91
12200	-56,08
12225	-55,87
12250	-56,05
12275	-55,90
12300	-55,86
12325	-55,78
12350	-55,70
12375	-55,59
12400	-55,55
12425	-55,57
12450	-55,59
12475	-55,55
12500	-55,30
12525	-55,24
12550	-55,18
12575	-55,12
12600	-55,01
12625	-54,83
12650	-54,79
12675	-54,73
12700	-54,80
12725	-54,52
12750	-54,53
12775	-54,43
12800	-54,29
12825	-54,37
12850	-54,14
12875	-53,99
12900	-53,94
12925	-53,78
12950	-53,74
12975	-53,63
13000	-53,53
13025	-53,58
13050	-53,29
13075	-53,13
13100	-53,05
13125	-53,02
13150	-53,17
13175	-53,01
13200	-52,85
13225	-52,64
13250	-52,61

13275	-52,53
13300	-52,47
13325	-52,31
13350	-52,26
13375	-52,22
13400	-52,29
13425	-52,26
13450	-52,07
13475	-52,11
13500	-51,95
13525	-51,76
13550	-51,80
13575	-51,64
13600	-51,66
13625	-51,46
13650	-51,31
13675	-51,35
13700	-51,26
13725	-51,14
13750	-51,06
13775	-50,87
13800	-51,00
13825	-50,82
13850	-50,71
13875	-50,71
13900	-50,52
13925	-50,50
13950	-50,25
13975	-50,27
14000	-50,33
14025	-49,89
14050	-49,96
14075	-49,94
14100	-49,92
14125	-49,99
14150	-49,92
14175	-49,92
14200	-49,72
14225	-49,70
14250	-49,60
14275	-49,44
14300	-49,13
14325	-49,30
14350	-49,33
14375	-49,40

14400	-49,09
14425	-48,87
14450	-49,00
14475	-48,91
14500	-48,81
14525	-48,78
14550	-48,48
14575	-48,67
14600	-48,92
14625	-48,76
14650	-48,54
14675	-48,13
14700	-48,06
14725	-48,63
14750	-48,15
14775	-47,97
14800	-48,29
14825	-47,94
14850	-47,71
14875	-47,45
14900	-47,50
14925	-47,44
14950	-47,57
14975	-47,88
15000	-47,51
15025	-47,35
15050	-47,16
15075	-46,94
15100	-46,78
15125	-46,68
15150	-46,55
15175	-46,72
15200	-46,66
15225	-46,43
15250	-46,60
15275	-46,39
15300	-46,24
15325	-46,29
15350	-46,31
15375	-46,21
15400	-46,46
15425	-46,28
15450	-46,13
15475	-46,13
15500	-46,16

15525	-46,07
15550	-45,88
15575	-45,87
15600	-45,65
15625	-45,67
15650	-45,40
15675	-45,13
15700	-44,99
15725	-45,03
15750	-44,59
15775	-44,95
15800	-44,99
15825	-44,96
15850	-45,13
15875	-44,93
15900	-45,05
15925	-44,55
15950	-44,89
15975	-44,85
16000	-44,94
16025	-44,97
16050	-44,88
16075	-44,96
16100	-44,86
16125	-44,73
16150	-44,68
16175	-44,49
16200	-44,57
16225	-44,62
16250	-44,57
16275	-44,59
16300	-44,50
16325	-44,42
16350	-44,30
16375	-44,19
16400	-44,07
16425	-44,14
16450	-44,04
16475	-44,13
16500	-43,99
16525	-43,85
16550	-43,76
16575	-43,77
16600	-43,64
16625	-43,90

16650	-44,10
16675	-43,87
16700	-43,74
16725	-43,20
16750	-43,13
16775	-42,86
16800	-42,99
16825	-43,00
16850	-43,15
16875	-42,99
16900	-42,92
16925	-42,77
16950	-42,70
16975	-42,71
17000	-42,74
17025	-42,66
17050	-42,69
17075	-42,53
17100	-42,44
17125	-42,40
17150	-42,29
17175	-42,23
17200	-42,12
17225	-42,10
17250	-41,99
17275	-41,69
17300	-41,92
17325	-41,74
17350	-41,69
17375	-41,64
17400	-41,52
17425	-41,61
17450	-41,37
17475	-41,30
17500	-41,59
17525	-41,29
17550	-40,90
17575	-40,68
17600	-40,75
17625	-41,16
17650	-41,20
17675	-41,06
17700	-40,86
17725	-40,89
17750	-40,70

17775	-40,49
17800	-40,42
17825	-40,25
17850	-40,45
17875	-40,43
17900	-39,94
17925	-39,91
17950	-39,71
17975	-39,61
18000	-39,58
18025	-39,87
18050	-39,32
18075	-39,68
18100	-39,44
18125	-39,43
18150	-39,39
18175	-39,41
18200	-39,30
18225	-39,22
18250	-39,30
18275	-39,36
18300	-39,89
18325	-39,82
18350	-39,67
18375	-39,65
18400	-38,93
18425	-39,50
18450	-39,23
18475	-39,18
18500	-38,97
18525	-38,20
18550	-38,21
18575	-38,25
18600	-38,13
18625	-38,58
18650	-38,24
18675	-38,37
18700	-38,34
18725	-38,19
18750	-38,06
18775	-37,45
18800	-37,42
18825	-37,39
18850	-37,14
18875	-37,16

18900	-37,02
18925	-36,95
18950	-36,83
18975	-36,76
19000	-36,72
19025	-36,60
19050	-36,71
19075	-36,77
19100	-36,59
19125	-36,57
19150	-36,51
19175	-36,56
19200	-36,58
19225	-36,66
19250	-36,51
19275	-36,30
19300	-36,27
19325	-36,21
19350	-36,33
19375	-36,36
19400	-36,42
19425	-36,32
19450	-36,15
19475	-36,18
19500	-36,04
19525	-36,10
19550	-36,46
19575	-36,18
19600	-36,17
19625	-36,01
19650	-36,07
19675	-36,10
19700	-35,97
19725	-35,72
19750	-35,66
19775	-35,45
19800	-35,46
19825	-35,38
19850	-35,02
19875	-34,93
19900	-34,93
19925	-34,76
19950	-34,61
19975	-34,53
20000	-34,29

20025	-34,28
20050	-33,99
20075	-34,98
20100	-33,97
20125	-34,49
20150	-34,63
20175	-34,40
20200	-34,19
20225	-34,14
20250	-34,01
20275	-33,77
20300	-33,22
20325	-32,68
20350	-32,61
20375	-32,78
20400	-32,79
20425	-33,00
20450	-32,87
20475	-32,65
20500	-32,55
20525	-32,34
20550	-32,06
20575	-31,75
20600	-31,77
20625	-31,79
20650	-31,91
20675	-32,54
20700	-32,71
20725	-32,77
20750	-32,70
20775	-32,62
20800	-32,51
20825	-32,30
20850	-31,76
20875	-32,11
20900	-32,01
20925	-31,72
20950	-31,83
20975	-31,83
21000	-31,37
21025	-31,71
21050	-31,70
21075	-31,83
21100	-31,90
21125	-31,91
21150	-31,95
21175	-31,88
21200	-31,85
21225	-31,83
21250	-31,83
21275	-31,75
21300	-31,94
21325	-31,86
21350	-31,71
21375	-31,69
21400	-31,59
21425	-31,65
21450	-31,57
21475	-31,51
21500	-31,48
21525	-31,49
21550	-31,49
21575	-31,45
21600	-31,28
21625	-31,11
21650	-30,77
21675	-30,31
21700	-29,88
21725	-29,54
21750	-29,28
21775	-29,09
21800	-28,81
21825	-28,76
21850	-28,77
21875	-28,76
21900	-28,69
21925	-28,68
21950	-28,69
21975	-28,79
22000	-28,89
22025	-29,01
22050	-29,34
22075	-29,27
22100	-29,18
22125	-29,11
22150	-28,92
22175	-28,77
22200	-28,69
22225	-28,63
22250	-28,57
22275	-28,55
22300	-28,60
22325	-28,72
22350	-28,85
22375	-28,99
22400	-29,03
22425	-28,97
22450	-28,90
22475	-28,81
22500	-28,74
22525	-28,66
22550	-28,59
22575	-28,54
22600	-28,45
22625	-28,36
22650	-28,28
22675	-28,29
22700	-28,19
22725	-28,11
22750	-28,20
22775	-27,97
22800	-28,02
22825	-27,92
22850	-27,91
22875	-27,89
22900	-27,83
22925	-27,76
22950	-27,66
22975	-27,51
23000	-27,36
23025	-27,04
23050	-26,72
23075	-26,47
23100	-26,40
23125	-26,30
23150	-26,19
23175	-26,07
23200	-25,97
23225	-25,83
23250	-25,75
23275	-25,59
23300	-25,56
23325	-25,93
23350	-26,45
23375	-26,64

23400	-26,58
23425	-26,58
23450	-26,55
23475	-26,51
23500	-26,53
23525	-26,48
23550	-26,43
23575	-26,38
23600	-26,32
23625	-26,29
23650	-26,21
23675	-26,20
23700	-26,14
23725	-26,12
23750	-26,02
23775	-25,99
23800	-25,92
23825	-25,82
23850	-25,72
23875	-25,63
23900	-25,54
23925	-25,48
23950	-25,37
23975	-25,30
24000	-25,19
24025	-25,00
24050	-24,81
24075	-24,59
24100	-24,40
24125	-24,23
24150	-24,13
24175	-23,98
24200	-23,83
24225	-23,70
24250	-23,55
24275	-23,45
24300	-23,29
24325	-23,14
24350	-22,96
24375	-22,80
24400	-22,62
24425	-22,45
24450	-22,33
24475	-22,19
24500	-22,06

24525	-21,94
24550	-21,79
24575	-21,70
24600	-21,62
24625	-21,57
24650	-21,51
24675	-21,51
24700	-21,58
24725	-21,74
24750	-22,02
24775	-22,31
24800	-22,51
24825	-22,16
24850	-22,00
24875	-21,87
24900	-21,67
24925	-21,46
24950	-21,22
24975	-21,03
25000	-20,80
25025	-20,63
25050	-20,48
25075	-20,32
25100	-20,16
25125	-19,98
25150	-19,79
25175	-19,62
25200	-19,44
25225	-19,25
25250	-19,07
25275	-18,87
25300	-18,68
25325	-18,49
25350	-18,32
25375	-18,17
25400	-17,98
25425	-17,85
25450	-17,70
25475	-17,55
25500	-17,42
25525	-17,33
25550	-17,19
25575	-17,07
25600	-16,97
25625	-16,85

25650	-16,74
25675	-16,69
25700	-16,59
25725	-16,53
25750	-16,48
25775	-16,41
25800	-16,38
25825	-16,32
25850	-16,29
25875	-16,27
25900	-16,28
25925	-16,34
25950	-16,20
25975	-16,18
26000	-16,14
26025	-16,12
26050	-16,09
26075	-16,07
26100	-16,01
26125	-15,89
26150	-15,89
26175	-15,92
26200	-15,93
26225	-15,94
26250	-15,92
26275	-15,88
26300	-15,79
26325	-15,78
26350	-15,72
26375	-15,67
26400	-15,60
26425	-15,58
26450	-15,37
26475	-15,24
26500	-15,19
26525	-15,19
26550	-15,20
26575	-15,09
26600	-14,91
26625	-14,71
26650	-14,56
26675	-14,32
26700	-14,23
26725	-14,17
26750	-14,02

26775	-13,81
26800	-13,66
26825	-13,36
26850	-13,19
26875	-12,97
26900	-12,78
26925	-12,59
26950	-12,35
26975	-12,28
27000	-11,99
27025	-11,88
27050	-11,72
27075	-11,54
27100	-11,44
27125	-11,32
27150	-11,19
27175	-11,09
27200	-11,02
27225	-10,93
27250	-10,78
27275	-10,71
27300	-10,57
27325	-10,50
27350	-10,41
27375	-10,30
27400	-10,22
27425	-10,04
27450	-9,97

27475	-9,89
27500	-9,79
27525	-9,69
27550	-9,52
27575	-9,42
27600	-9,33
27625	-9,17
27650	-9,09
27675	-8,95
27700	-8,92
27725	-8,87
27750	-8,75
27775	-5,57
27800	-8,40
27825	-8,17
27850	-8,02
27875	-7,99
27900	-7,62
27925	-7,55
27950	-7,31
27975	-7,08
28000	-6,95
28025	-6,74
28050	-6,46
28075	-6,42
28100	-6,41
28125	-5,84
28150	-5,86

28175	-5,73
28200	-5,60
28225	-5,41
28250	-5,07
28275	-4,74
28300	-4,26
28325	-3,75
28350	-3,23
28375	-3,19
28400	-3,51
28425	-3,88
28450	-4,53
28475	-4,47
28500	-4,15
28525	-3,78
28550	-3,02
28575	-2,29
28600	-1,17
28625	-0,26
28650	0,69
28675	4,03
28700	4,46
28725	3,64
28750	3,48
28775	3,65
28800	3,74
28825	3,58

Appendix B – OLGA and PVTSim charts in high resolution

Table B.1 – List of Figures in Appendix B & their links to Figures in Chapter 6

Figure B.1 ≡ Figure 19	Phase envelope for the initial fluid composition with 0,854 mol% water and no hydrate inhibitors added
Figure B.2 ≡ Figure 20	Hydrate curve for the initial fluid composition with 0,854 mol% water and no hydrate inhibitors added
Figure B.3 ≡ Figure 21	Pressure, temperature, and liquid volume fraction holdup distribution along the pipeline in the stable operational mode (12 hours since the start-up)
Figure B.4 ≡ Figure 22	DTHYD value distribution along the pipeline in its operational mode and without any hydrate inhibitor injection in the pipeline system
Figure B.5 ≡ Figure 23	The first iteration of the hydrate formation curves plotting to find the optimum MEG content: 0, 10, 20, 30, and 40% concentrations are plotted
Figure B.6 ≡ Figure 24	The second iteration of the hydrate formation curves plotting to find the optimum MEG content: 25% concentration is added to the plot
Figure B.7 ≡ Figure 25	DTHYD value distribution along the pipeline in its operational mode with continuous injection of hydrate inhibitor (25% MEG solution in the system)
Figure B.8 ≡ Figure 26	Pressure, temperature, and liquid volume fraction holdup distribution along the pipeline in the stable and hydrate-free operational mode (12 hours since the start-up, continuous injection of hydrate inhibitor: 25% MEG)

Figure B.9 ≡ Figure 27	Pressure and holdup liquid volume fraction distribution along the pipeline & accumulated liquid volume / volume flow parameters for the pipeline (12 hours since the start-up, continuous injection of hydrate inhibitor: 25% MEG)
Figure B.10 ≡ Figure 28	Trend plot for the last segment at the receiving end of the pipeline in the stabilized operational mode (12 hours / 43200 seconds since the start-up)
Figure B.11 ≡ Figure 29	Precise maximum liquid surge volume and maximum liquid surge rate calculated by OLGA's Surge Volume interface (steady operational conditions; $2{,}64 \cdot 10^6$ m^3/day)
Figure B.12 ≡ Figure 30	Distribution of pressure and holdup liquid within the system in its stabilized state & liquid flow data (11,75 hours since the start-up; $2{,}64 \cdot 10^6$ m^3/day)
Figure B.13 ≡ Figure 31	Pig run, part 1 of 3 (0,75 hour since the pig launch; $2{,}64 \cdot 10^6$ m^3/day)
Figure B.14 ≡ Figure 32	Pig run, part 2 of 3 (2,00 hours since the pig launch; $2{,}64 \cdot 10^6$ m^3/day)
Figure B.15 ≡ Figure 33	Pig run, part 3 of 3 (4,50 hours since the pig launch; $2{,}64 \cdot 10^6$ m^3/day)
Figure B.16 ≡ Figure 34	After-run distribution of pressure and holdup liquid in the system & changes in the accumulated and current liquid volume flow ($2{,}64 \cdot 10^6$ m^3/day)
Figure B.17 ≡ Figure 35	Liquid trend plot in the end-point for the entire simulation timespan ($2{,}64 \cdot 10^6$ m^3/day)

Figure B.18 ≡ Figure 36	Precise maximum liquid surge volume and maximum liquid surge rate calculated by OLGA's Surge Volume interface (pig run simulation for the $2{,}64 \cdot 10^6$ m^3/day)
Figure B.19 ≡ Figure 37	Pressure & holdup liquid distribution within the system in the stabilized state & liquid flow data (11,75 hours since the start-up; $3{,}5 \cdot 10^6$ m^3/day)
Figure B.20 ≡ Figure 38	Pig run, part 1 of 3 (0,5 hours since the pig launch; $3{,}5 \cdot 10^6$ m^3/day)
Figure B.21 ≡ Figure 39	Pig run, part 2 of 3 (1,25 hours since the pig launch; $3{,}5 \cdot 10^6$ m^3/day)
Figure B.22 ≡ Figure 40	Pig run, part 3 of 3 (2,5 hours since the pig launch; $3{,}5 \cdot 10^6$ m^3/day)
Figure B.23 ≡ Figure 41	After-run distribution of pressure and holdup liquid in the system & changes in the accumulated and current liquid volume flow ($3{,}5 \cdot 10^6$ m^3/day)
Figure B.24 ≡ Figure 42	Liquid trend plot in the end-point for the entire simulation timespan ($3{,}5 \cdot 10^6$ m^3/day)
Figure B.25 ≡ Figure 43	Precise maximum liquid surge volume and maximum liquid surge rate calculated by OLGA's Surge Volume interface (pig run simulation for the $3{,}5 \cdot 10^6$ m^3/day)
Figure B.26 ≡ Figure 44	Pig launch and removal time, simulation for the $2{,}64 \cdot 10^6$ m^3/day flow
Figure B.27 ≡ Figure 45	Pig launch and removal time, simulation for the $3{,}5 \cdot 10^6$ m^3/day flow

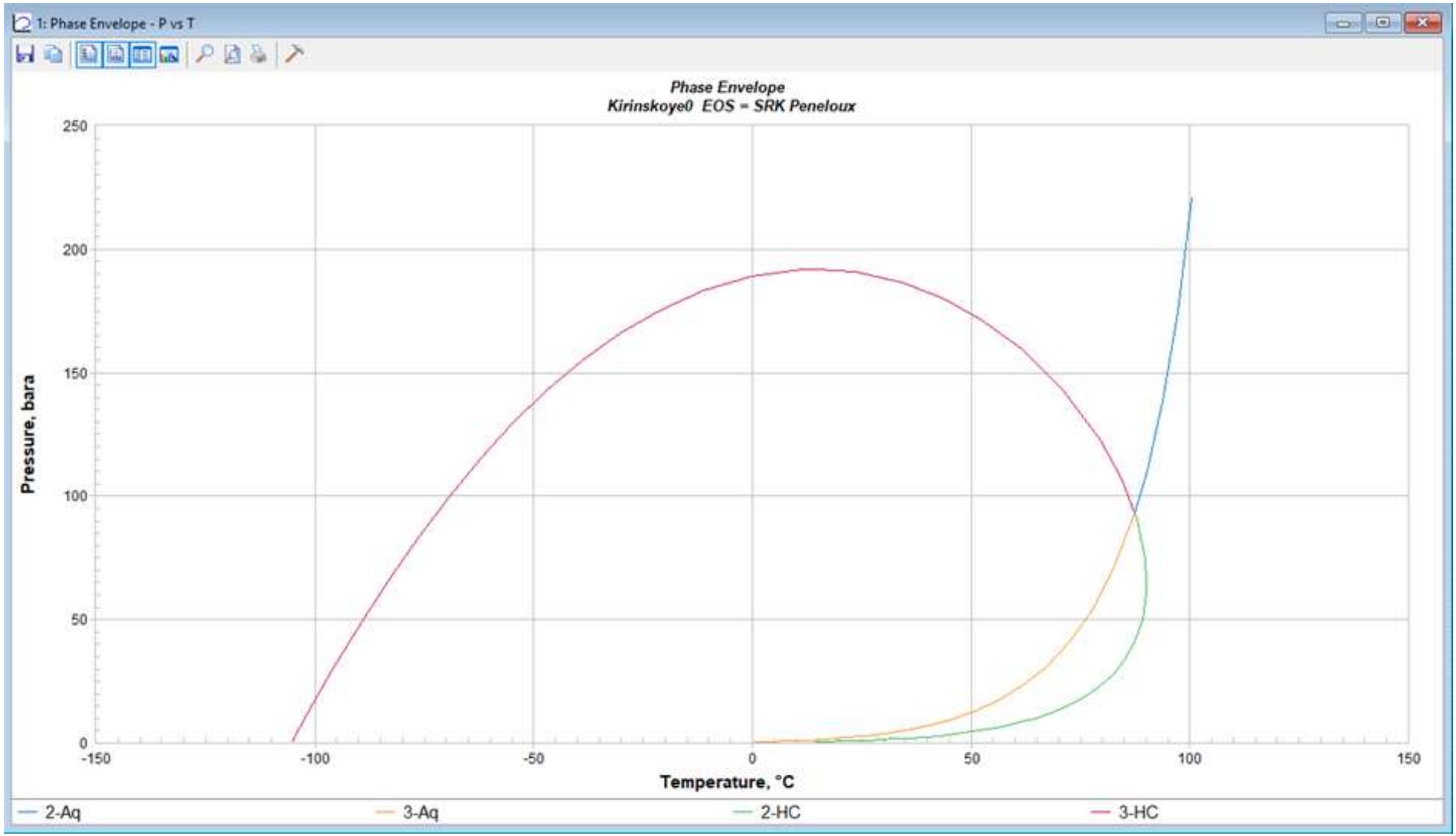

Figure B.1. Phase envelope for the initial fluid composition with 0,854 mol% water and no hydrate inhibitors added

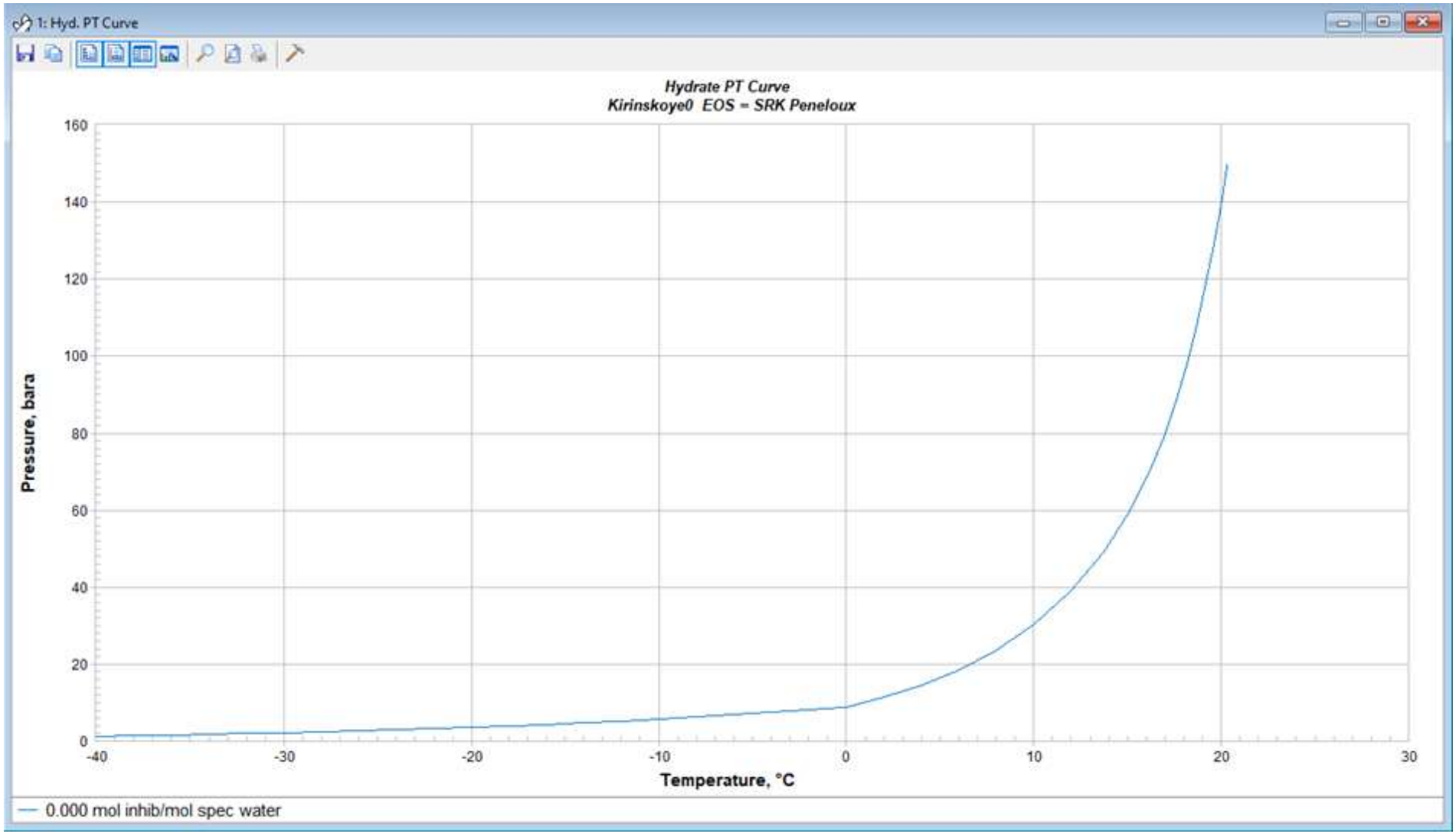

Figure B.2. Hydrate curve for the initial fluid composition with 0,854 mol% water and no hydrate inhibitors added

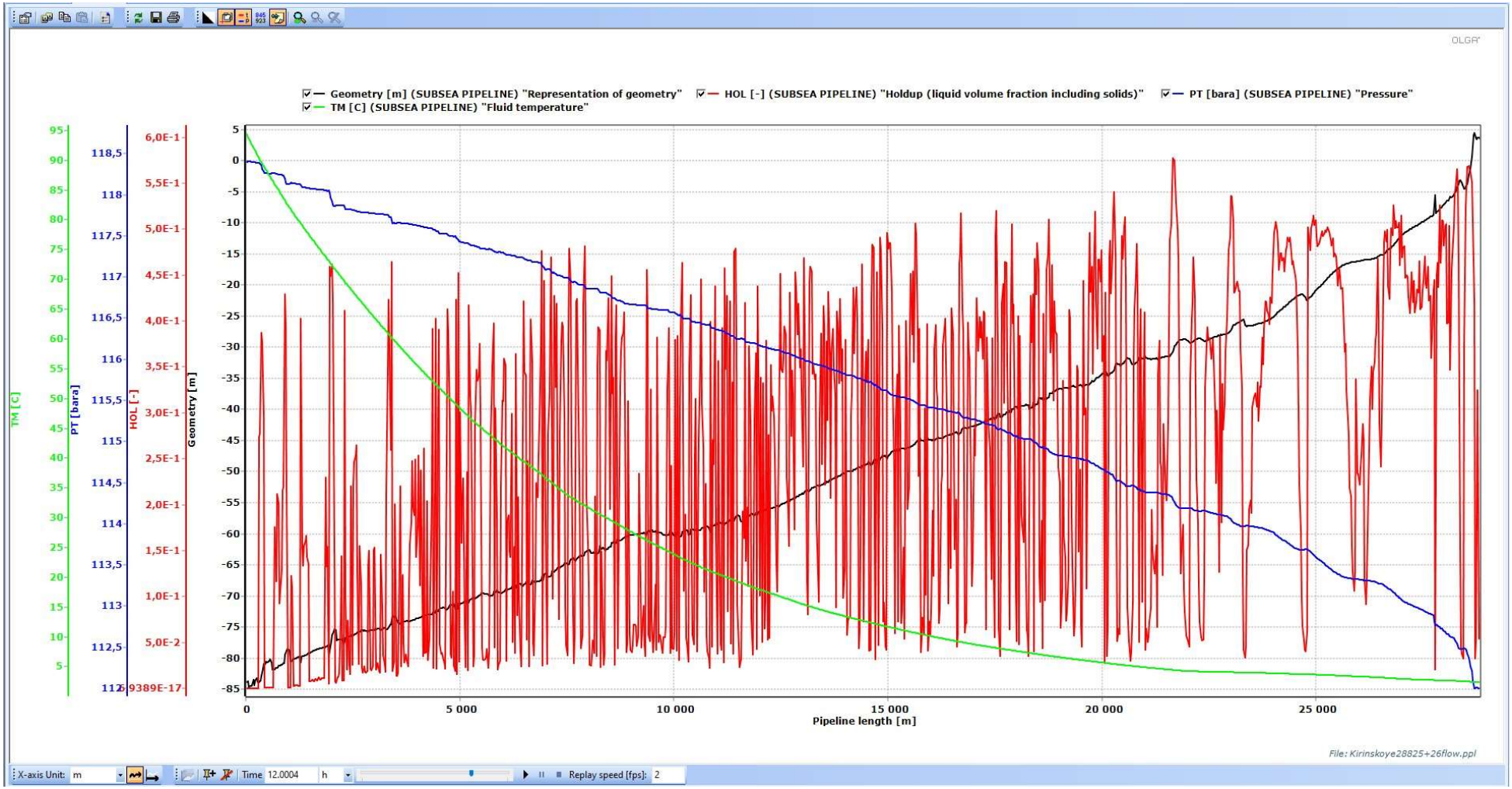

Figure B.3. Pressure, fluid temperature, and liquid volume fraction holdup distribution along the pipeline in the stable operational mode (12 hours since the start-up)

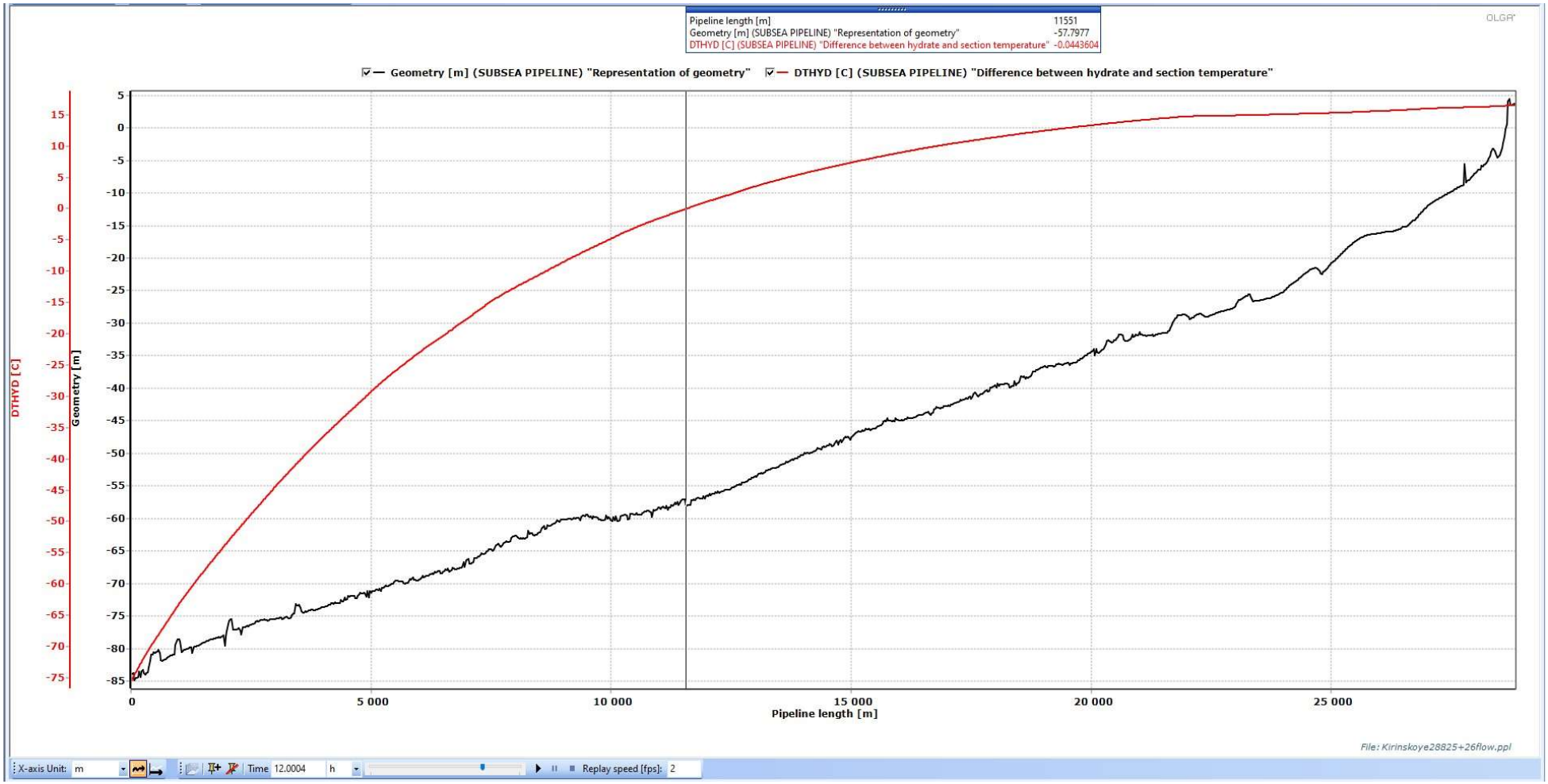

Figure B.4. DTHYD value distribution along the pipeline in its operational mode and without any hydrate inhibitor injection in the pipeline system

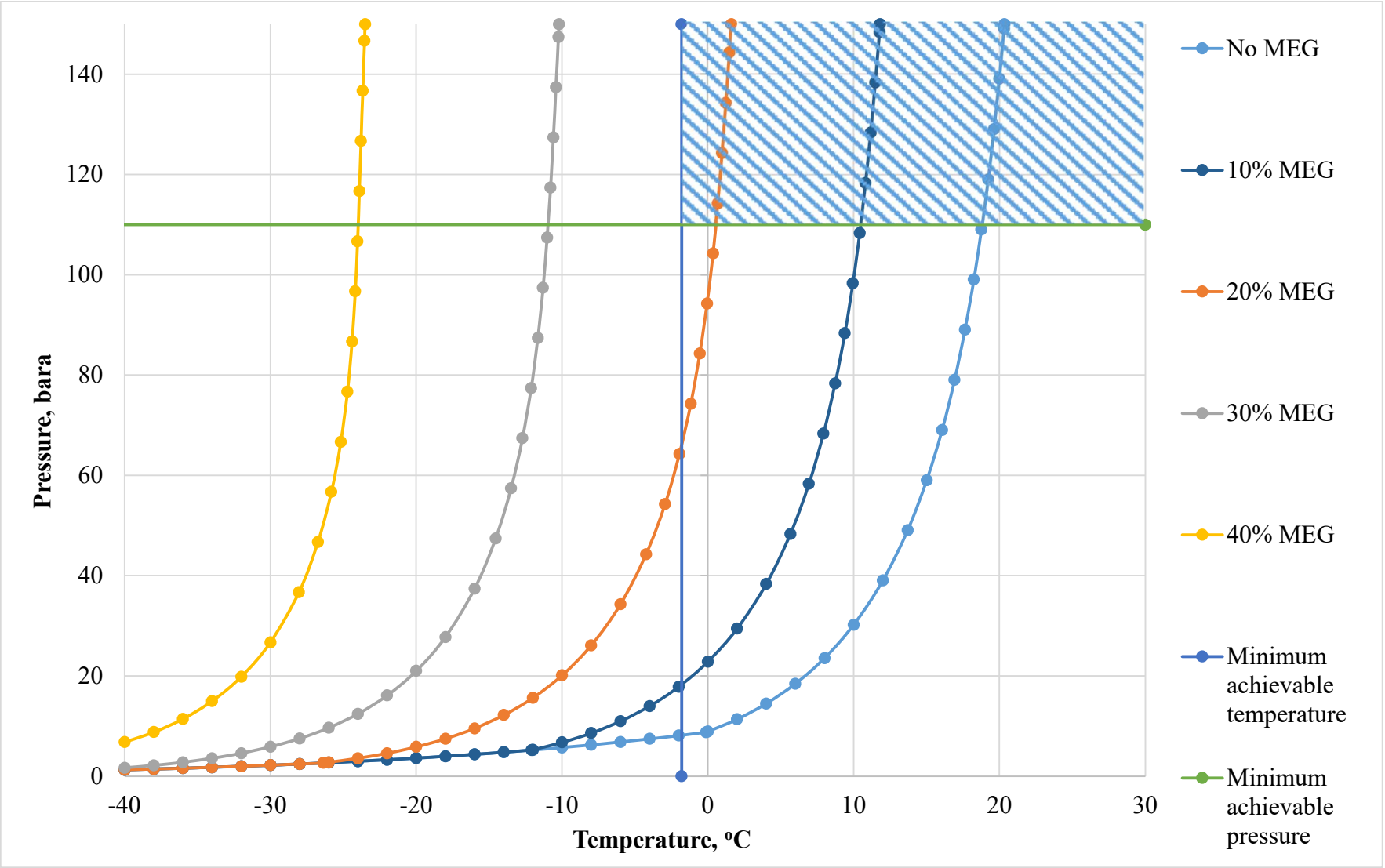

Figure B.5. The first iteration of the hydrate formation curves plotting to find the optimum MEG content: 0, 10, 20, 30, and 40% concentrations are plotted

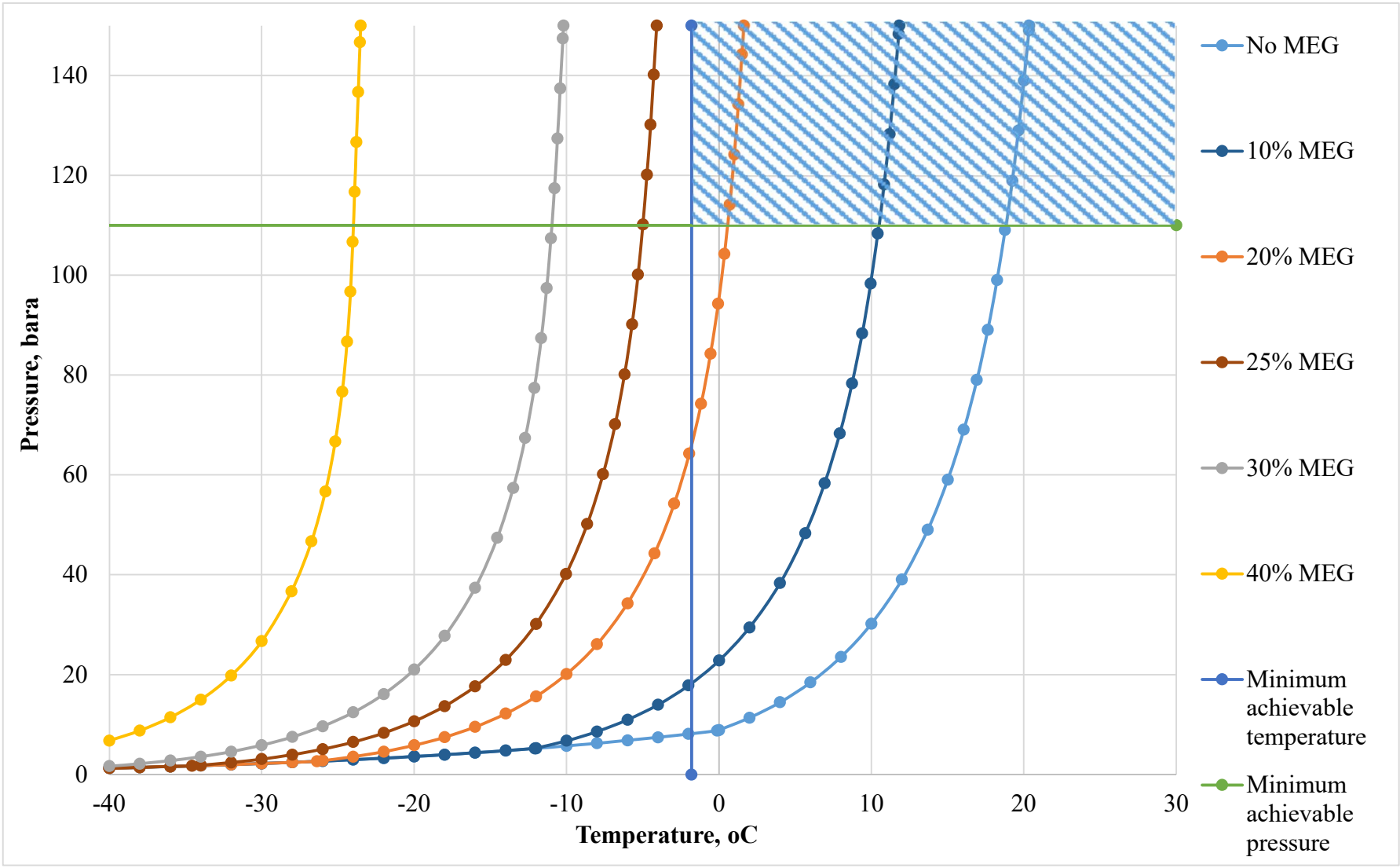

Figure B.6. The second iteration of the hydrate formation curves plotting to find the optimum MEG content: 25% concentration is added to the plot

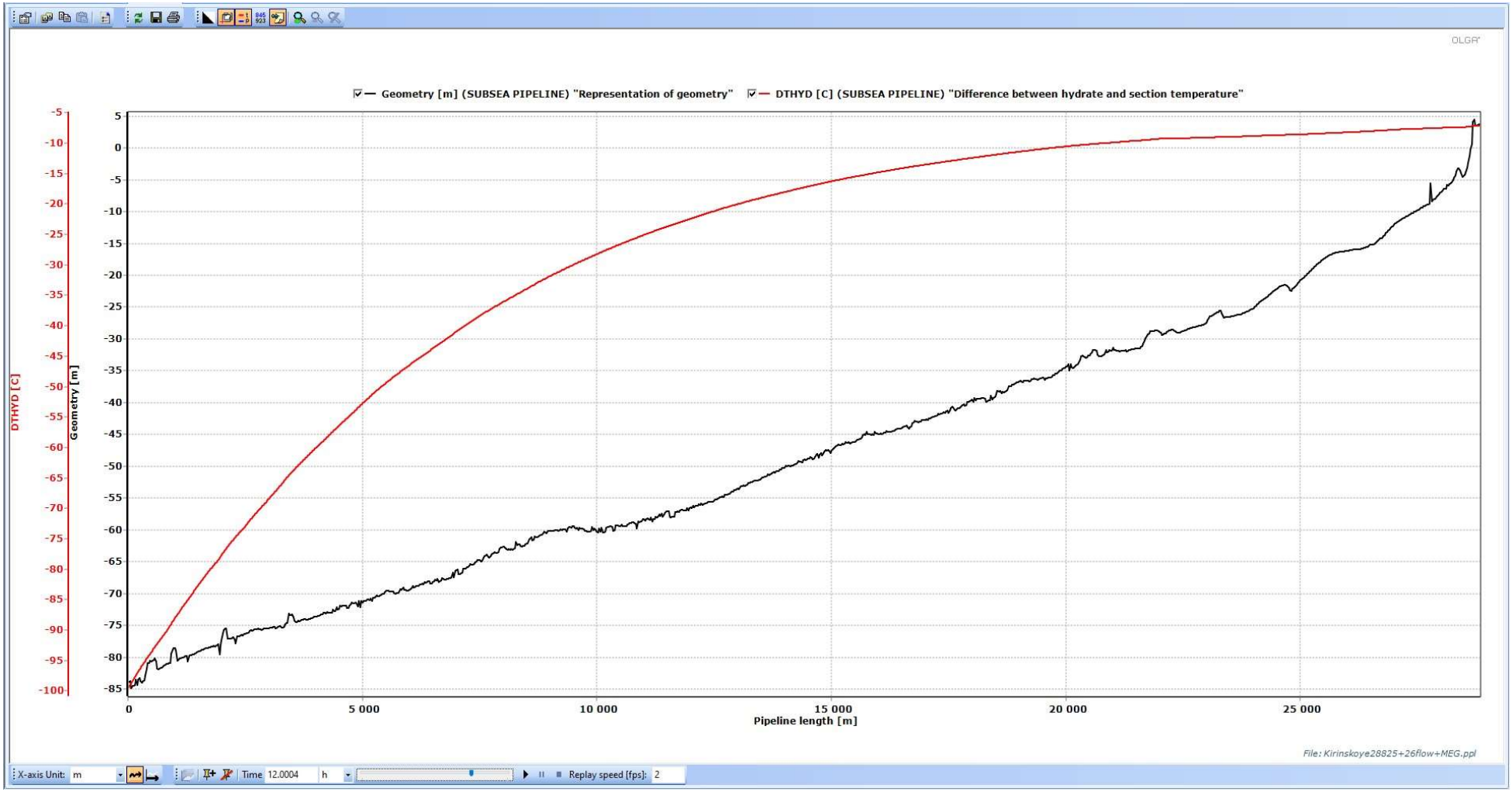

Figure B.7. DTHYD value distribution along the pipeline in its operational mode with continuous injection of hydrate inhibitor (25% MEG solution in the system)

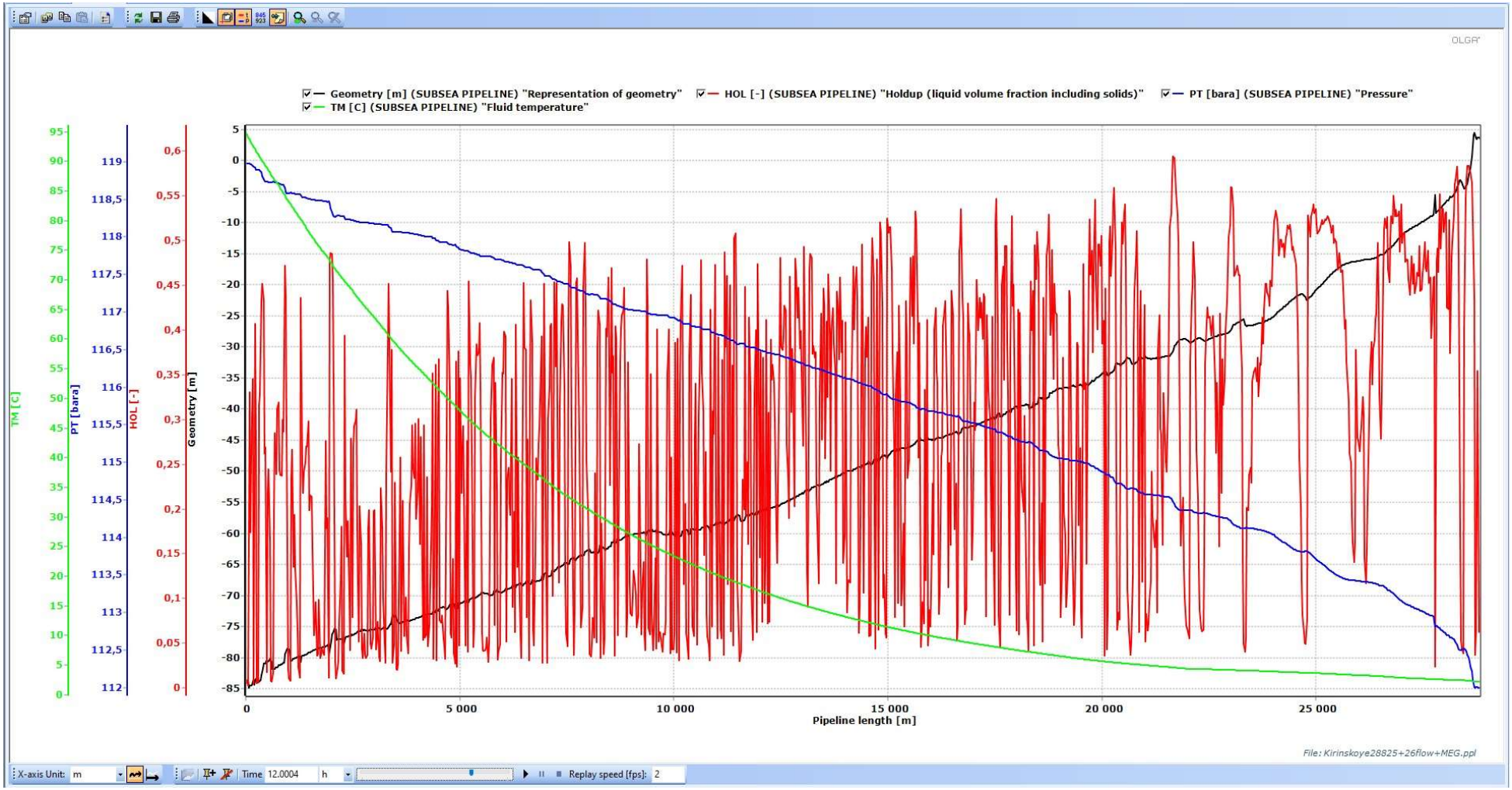

Figure B.8. Pressure, temperature, and liquid volume fraction holdup distribution along the pipeline in the stable and hydrate-free operational mode (12 hours since the start-up, continuous injection of hydrate inhibitor: 25% MEG)

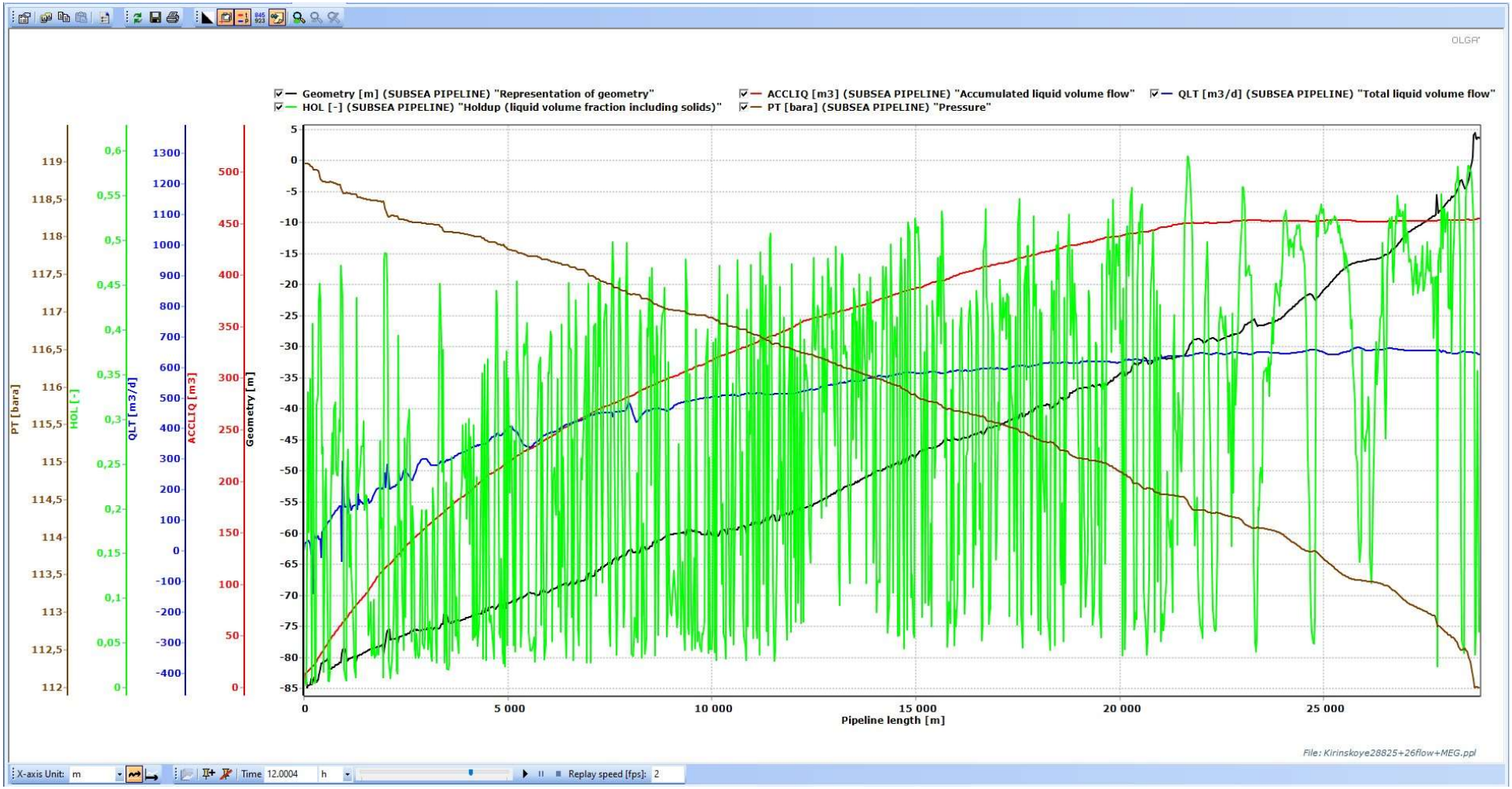

Figure B.9. Pressure and holdup liquid volume fraction distribution along the pipeline & accumulated liquid volume / volume flow parameters for the pipeline (12 hours since the start-up, continuous injection of hydrate inhibitor: 25% MEG)

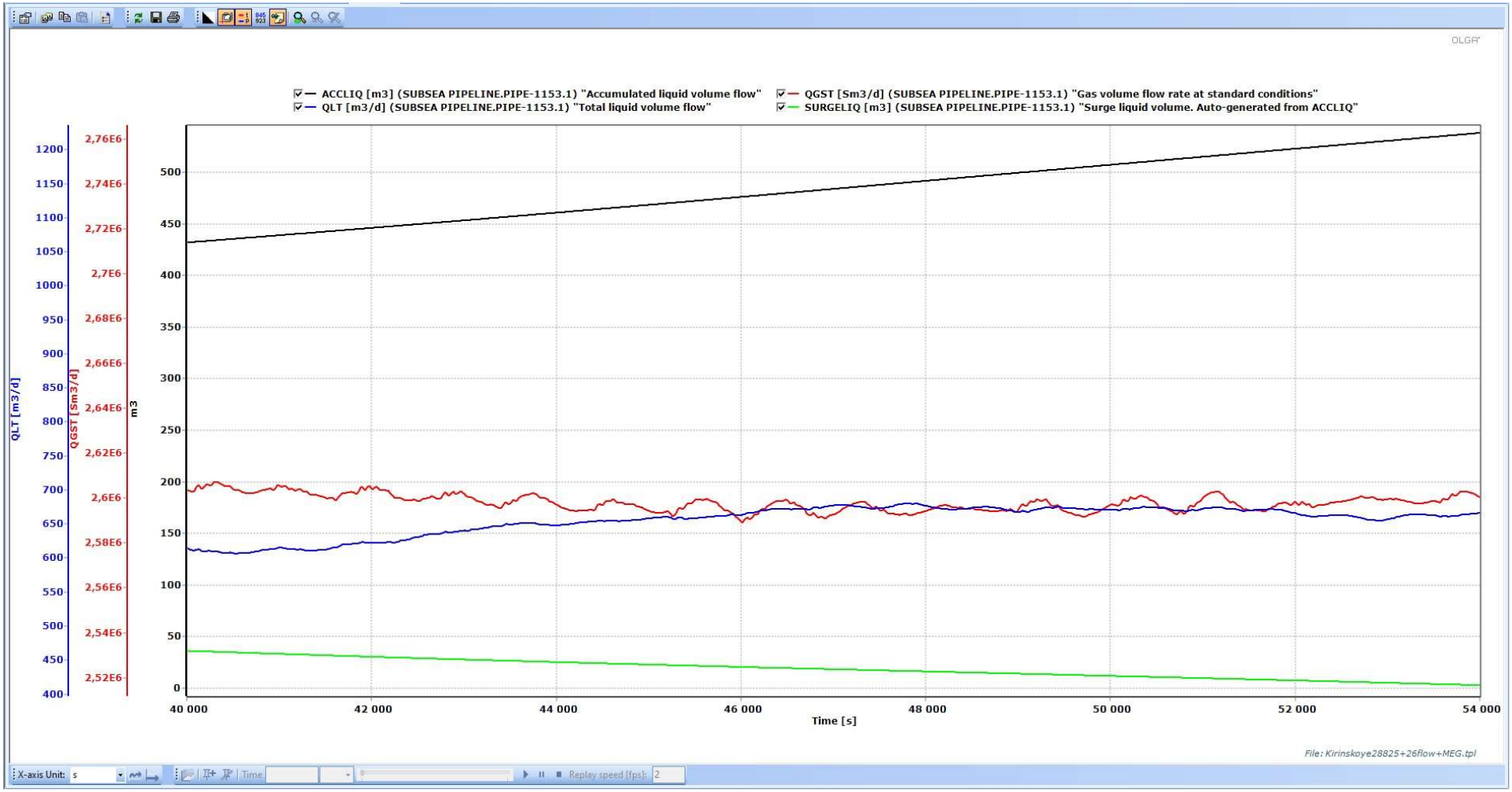

Figure B.10. Trend plot for the last segment at the receiving end of the pipeline in the stabilized operational mode (12 hours / 43200 seconds since the start-up)

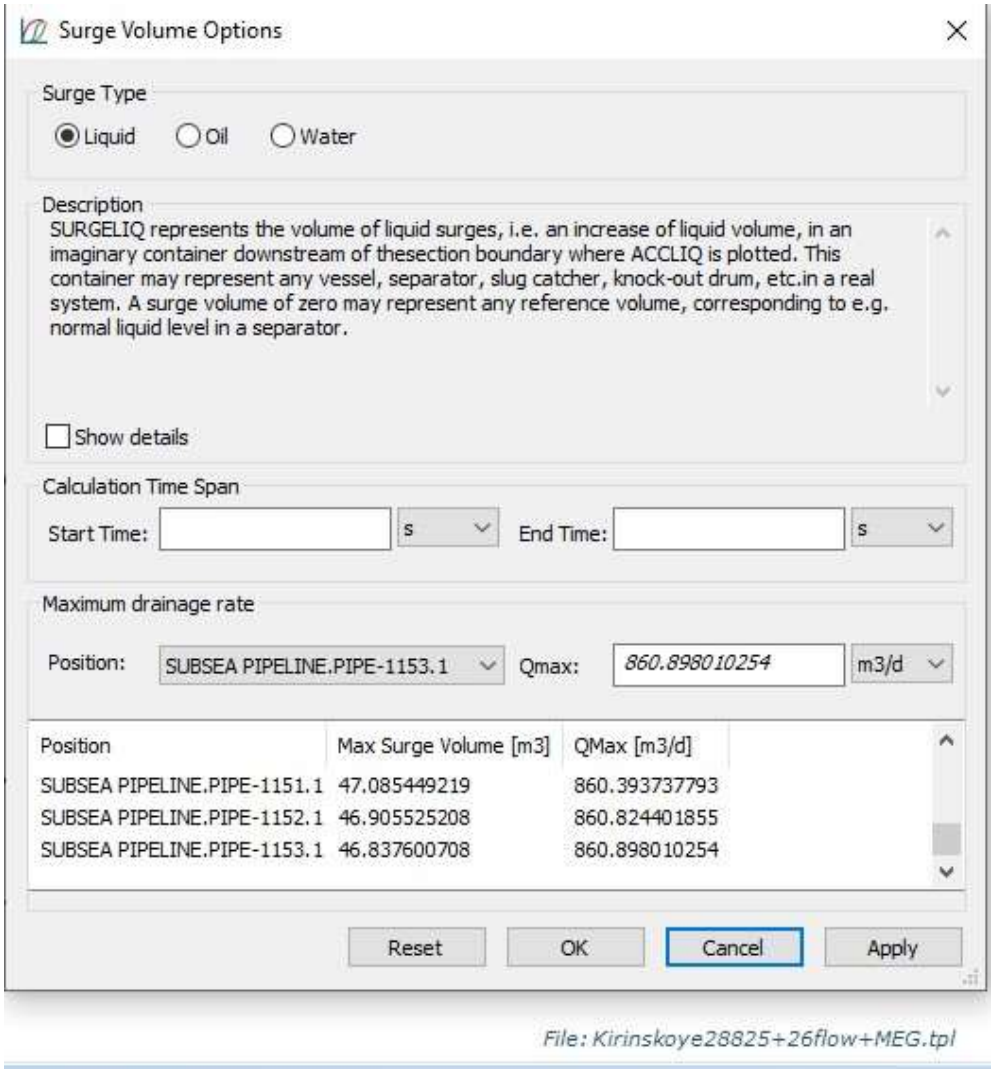

Figure B.11. Precise maximum liquid surge volume and maximum liquid surge rate calculated by OLGA's Surge Volume interface (steady operational conditions; $2{,}64 \cdot 10^6$ m^3/day)

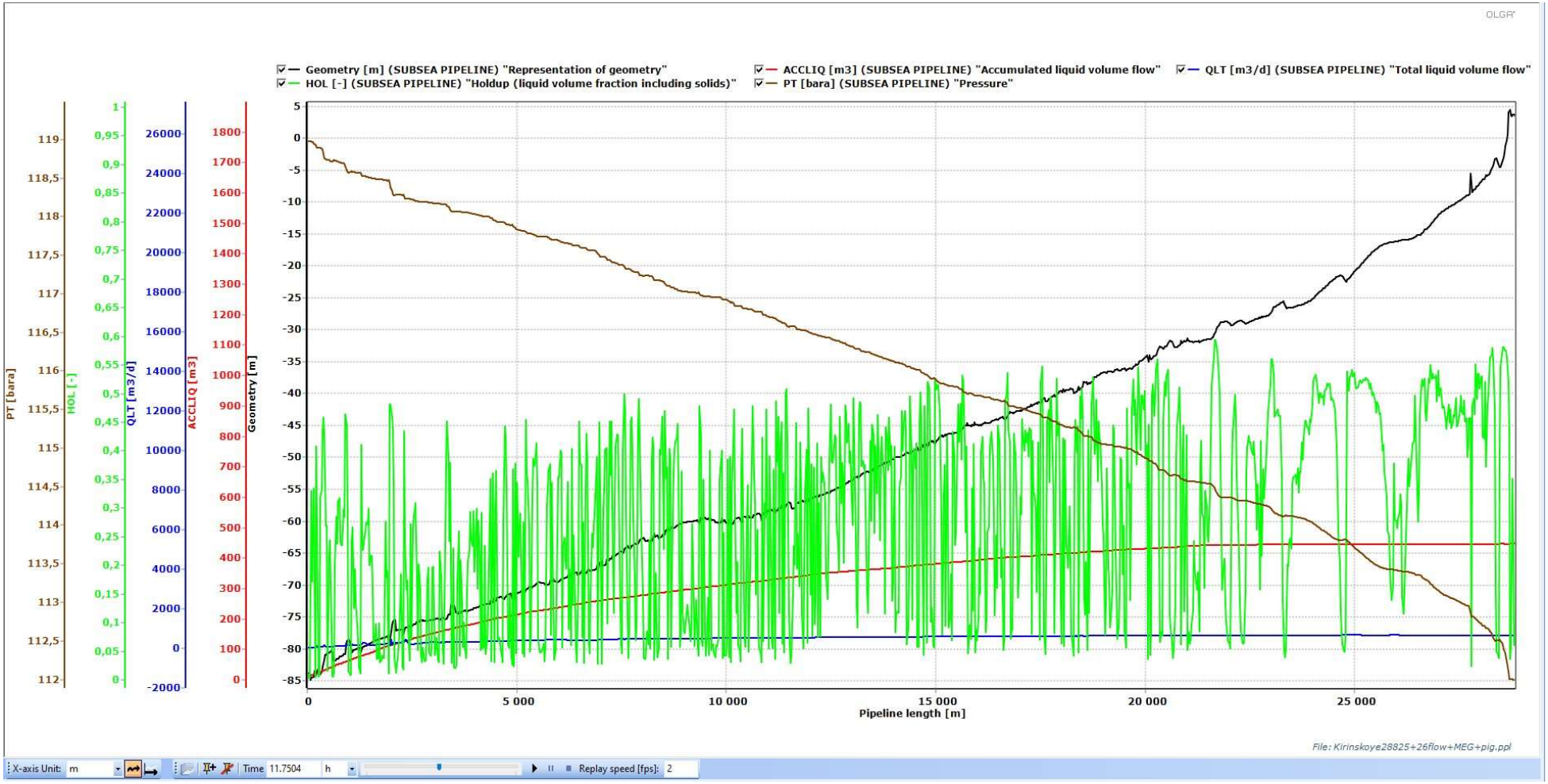

Figure B.12. Distribution of pressure and holdup liquid within the system in its stabilized state & liquid flow data (11,75 hours since the start-up; $2{,}64 \cdot 10^6$ m^3/day)

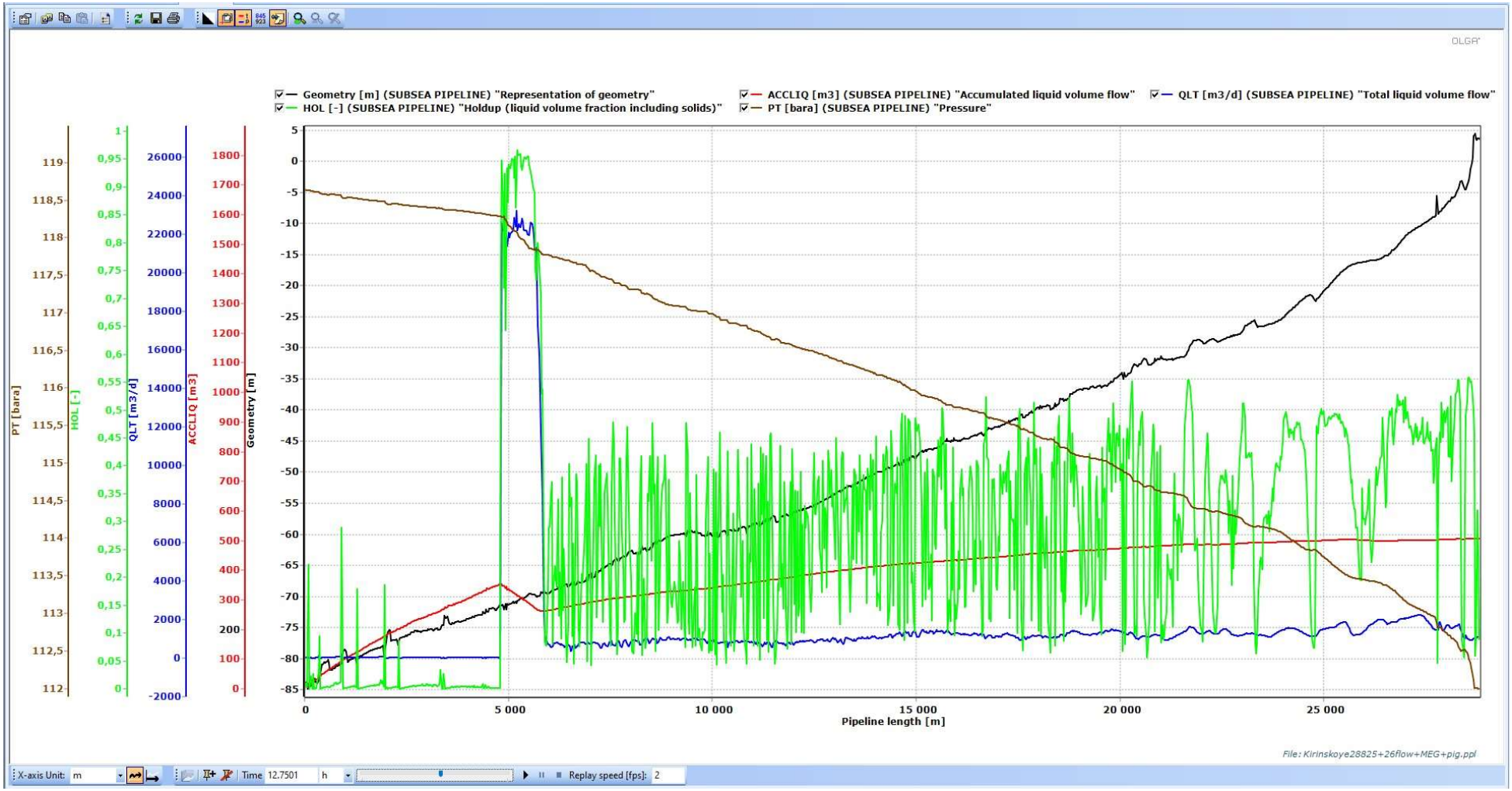

Figure B.13. Pig run, part 1 of 3 (0,75 hour since the pig launch; $2{,}64 \cdot 10^6$ m^3/day)

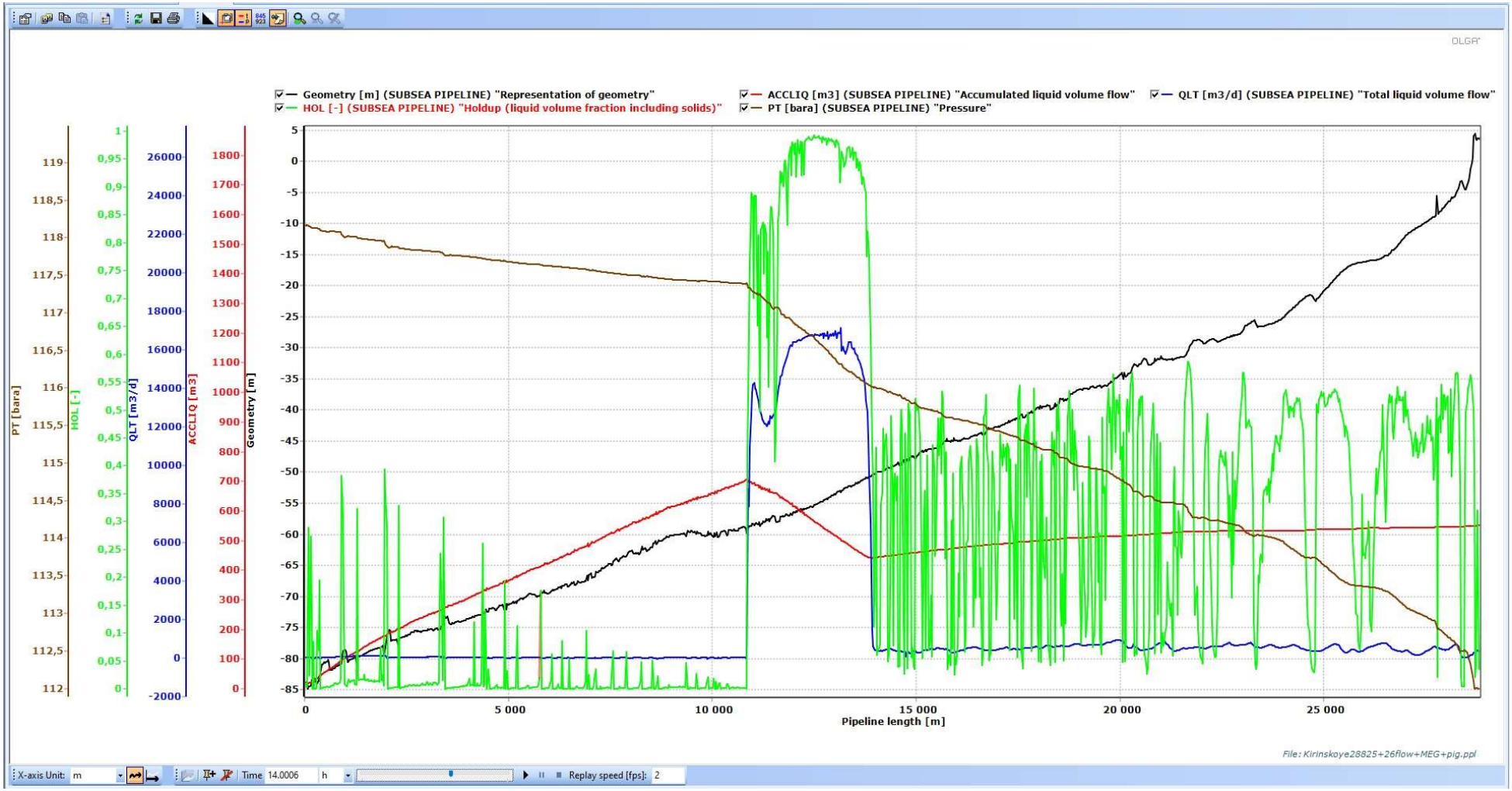

Figure B.14. Pig run, part 2 of 3 (2,00 hours since the pig launch; $2{,}64 \cdot 10^6$ m^3/day)

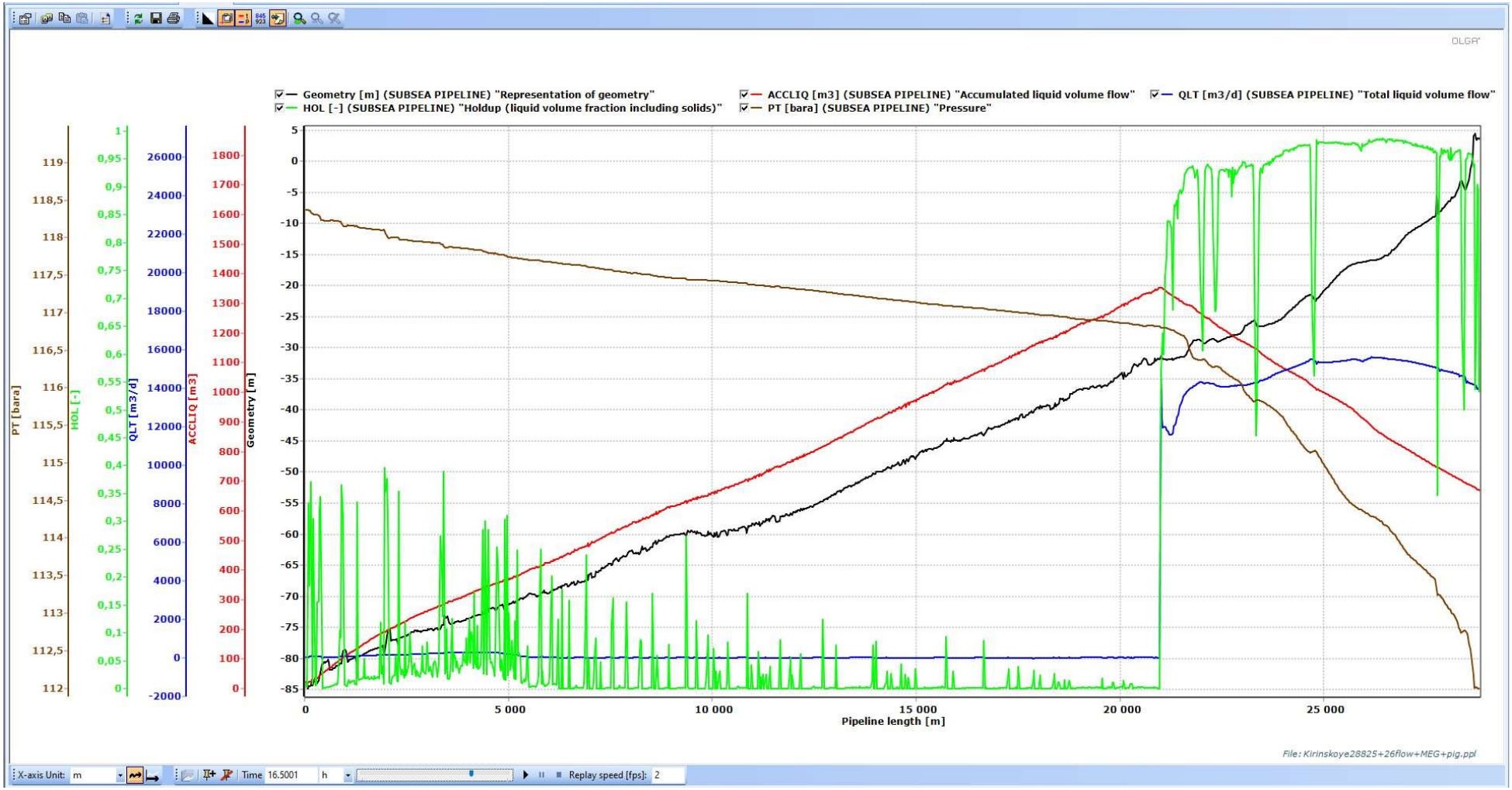

Figure B.15. Pig run, part 3 of 3 (4,50 hours since the pig launch; $2{,}64 \cdot 10^6$ m^3/day)

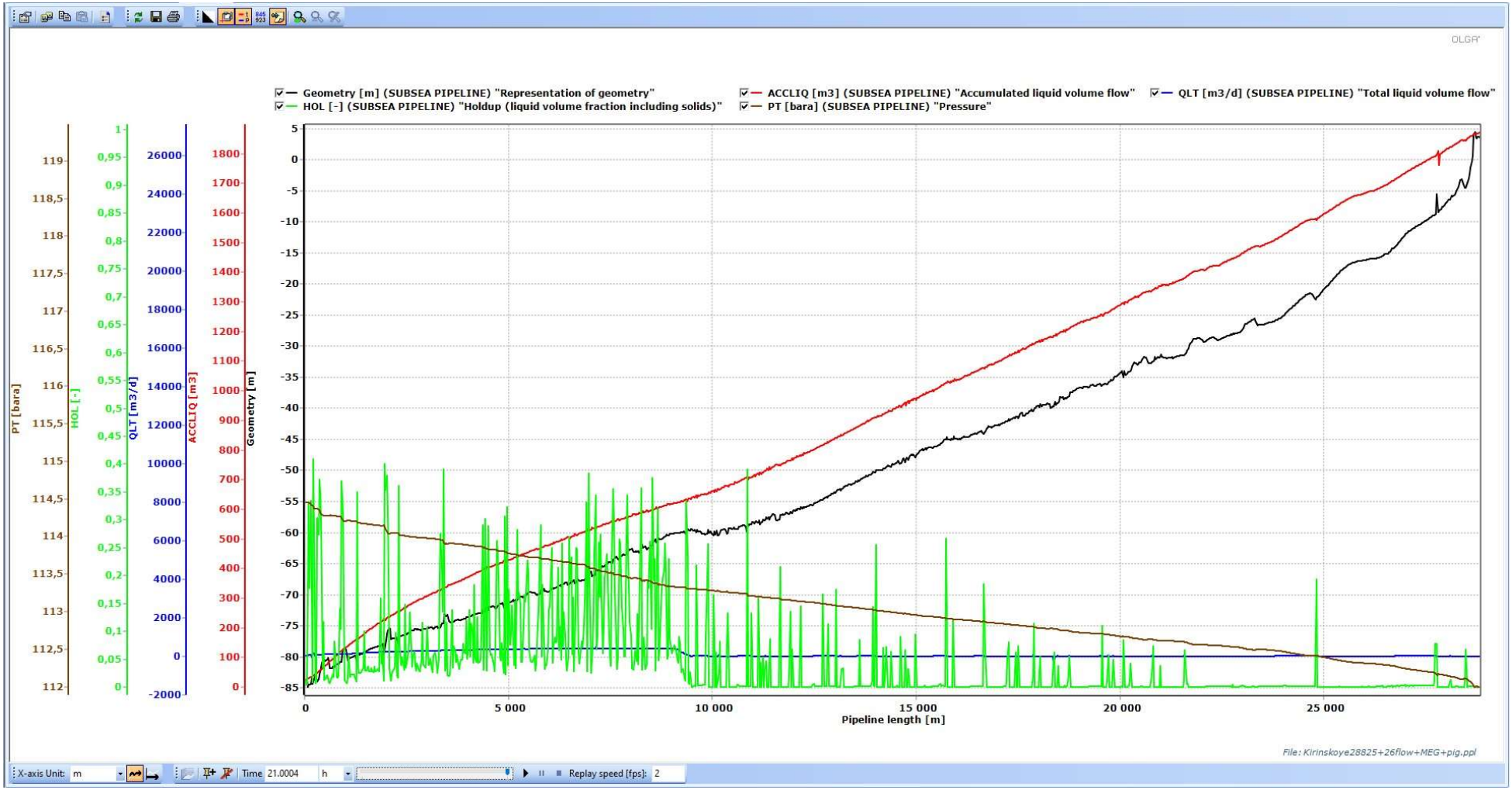

Figure B.16. After-run distribution of pressure and holdup liquid in the system & changes in the accumulated and current liquid volume flow ($2{,}64 \cdot 10^6$ m^3/day)

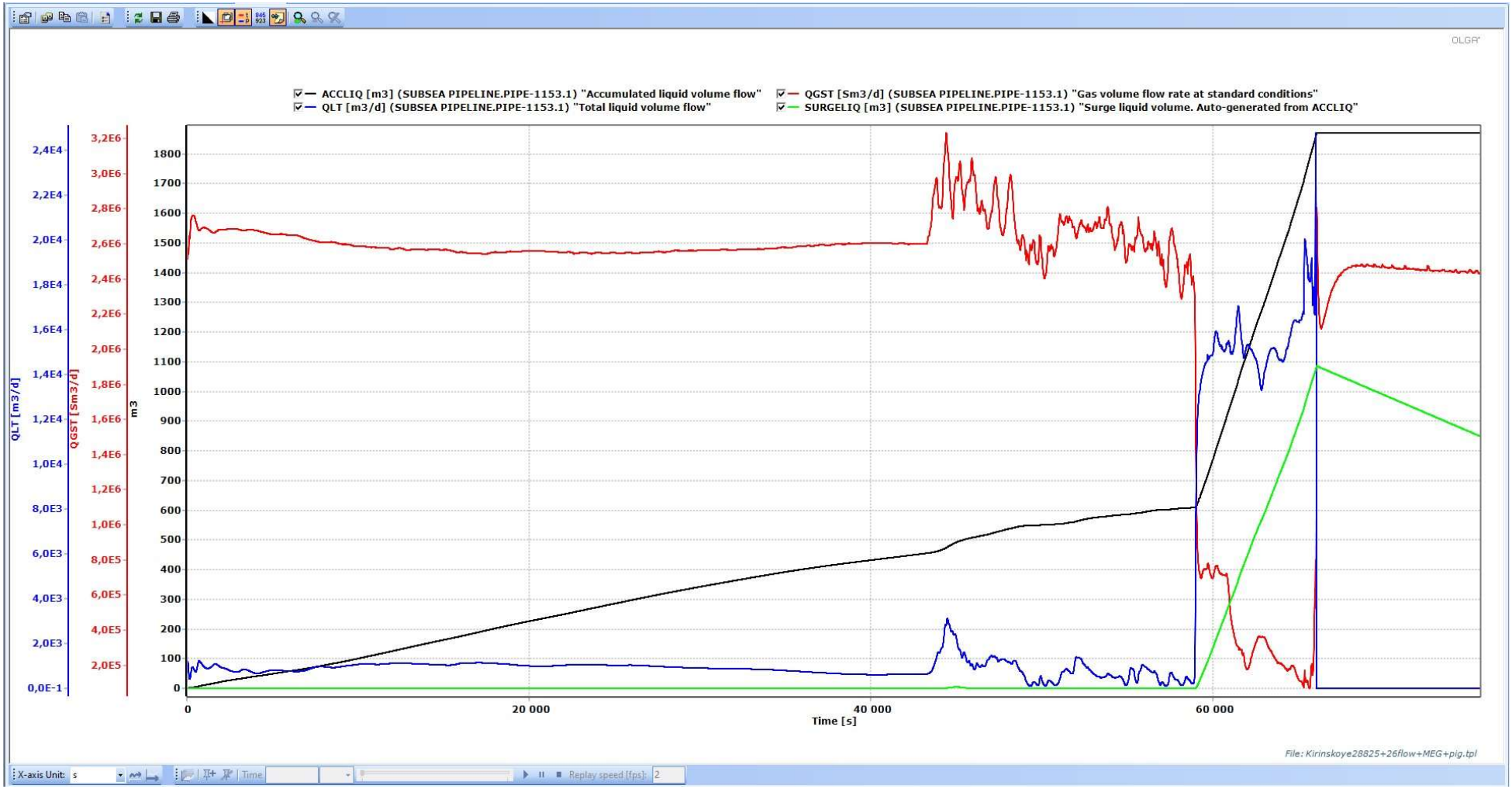

Figure B.17. Liquid trend plot in the end-point for the entire simulation timespan ($2{,}64 \cdot 10^6$ m^3/day)

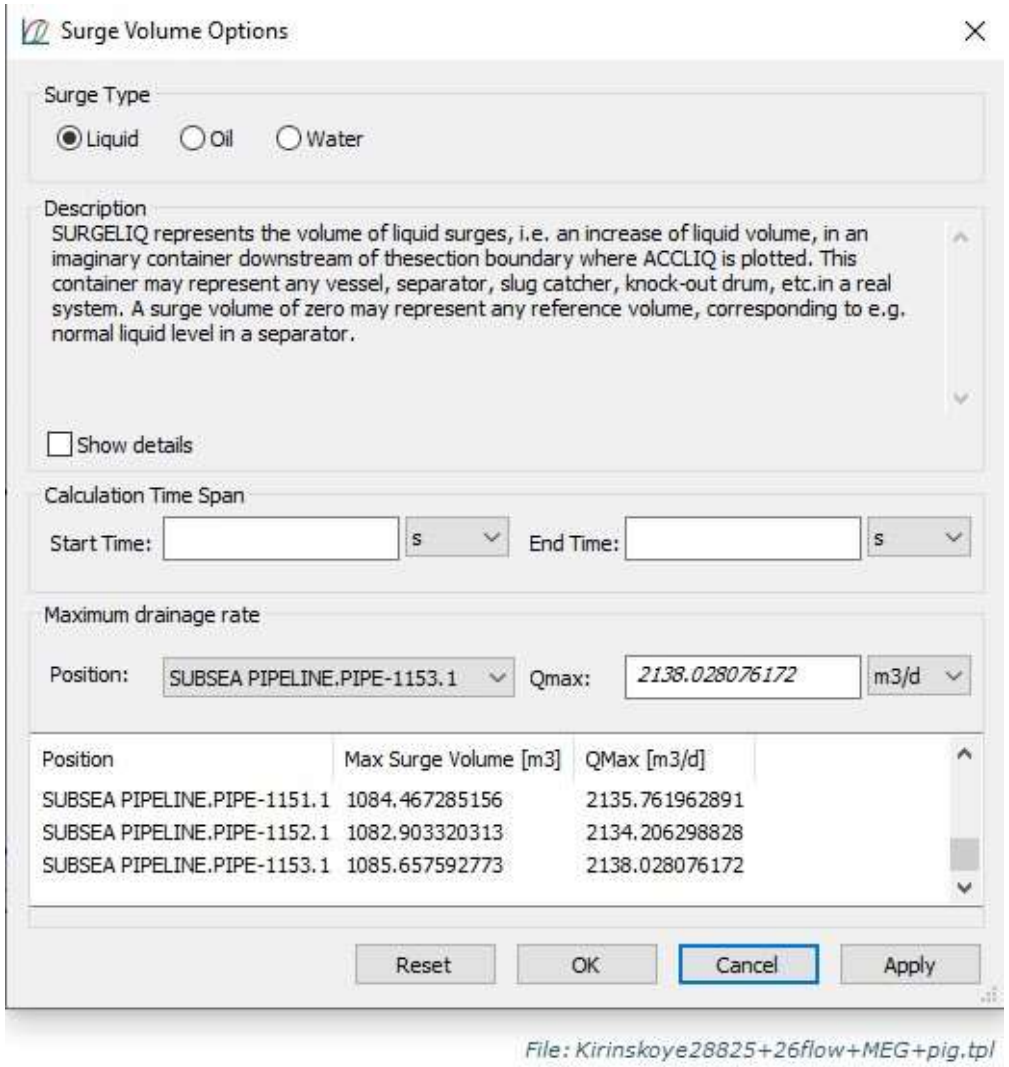

Figure B.18. Precise maximum liquid surge volume and maximum liquid surge rate calculated by OLGA's Surge Volume interface (pig run simulation for the $2{,}64 \cdot 10^6$ m^3/day)

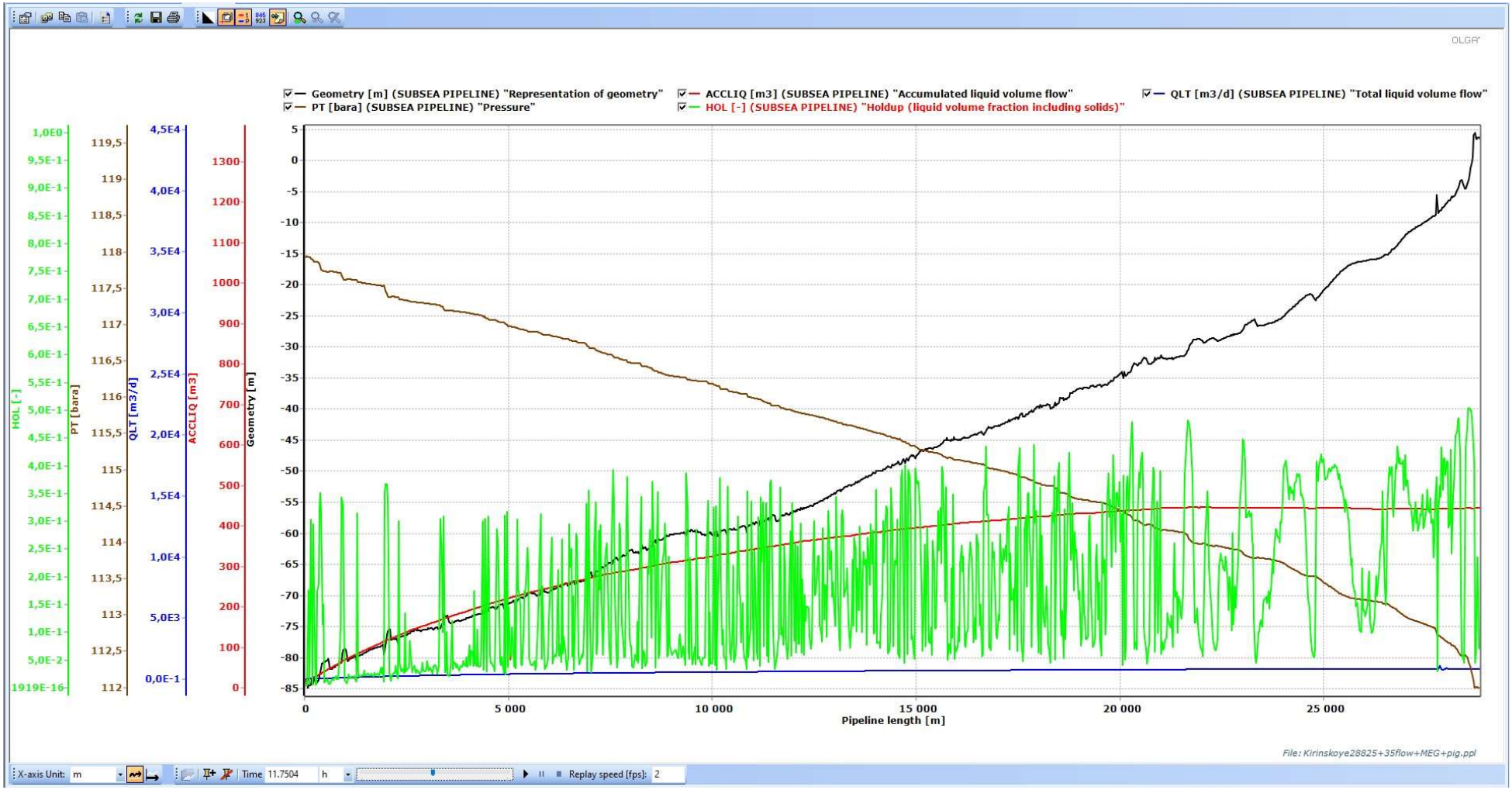

Figure B.19. Pressure & holdup liquid distribution within the system in the stabilized state & liquid flow data (11,75 hours since the start-up; $3{,}5 \cdot 10^6$ m^3/day)

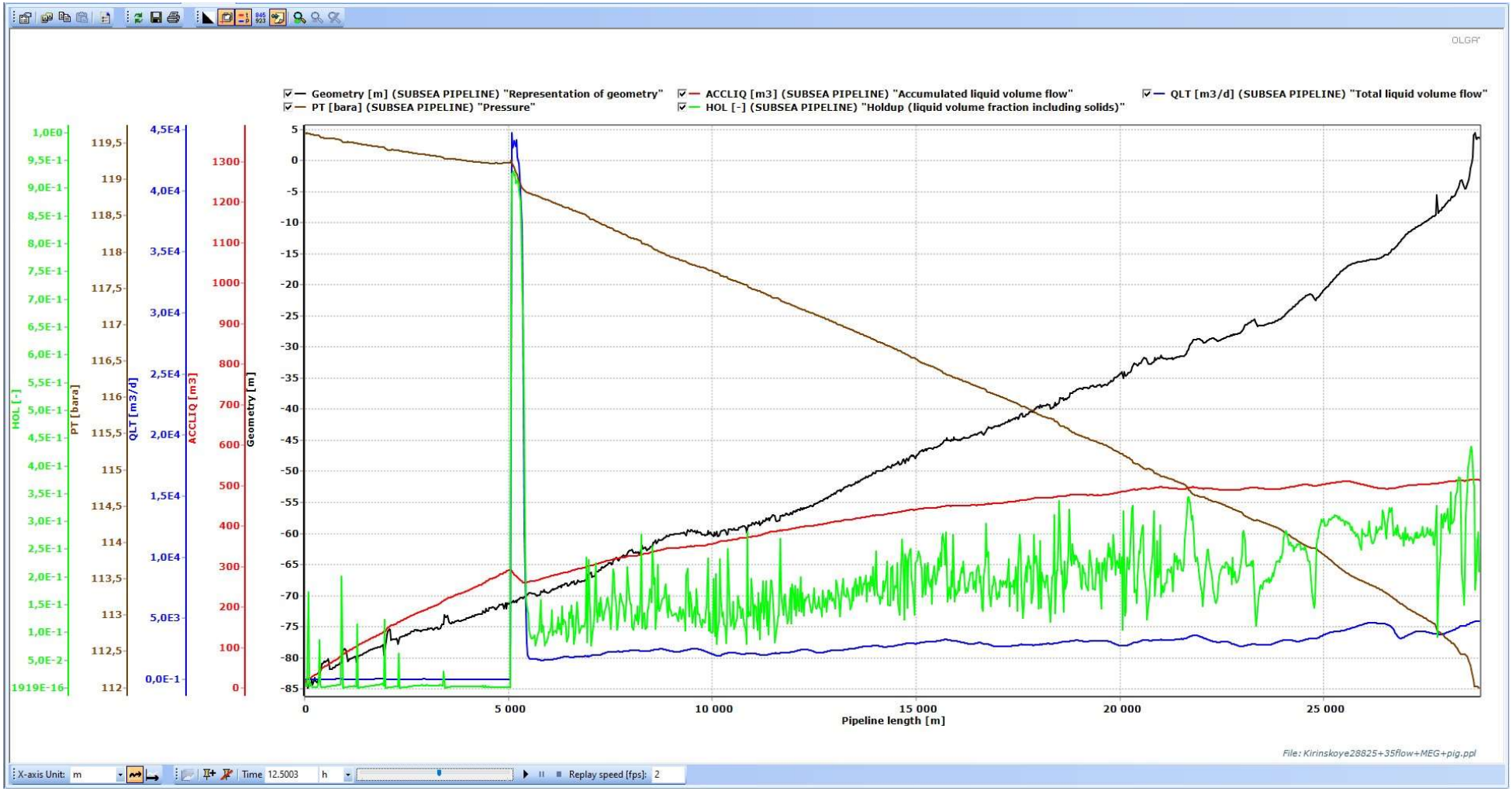

Figure B.20. Pig run, part 1 of 3 (0,5 hours since the pig launch; $3{,}5 \cdot 10^6$ m^3/day)

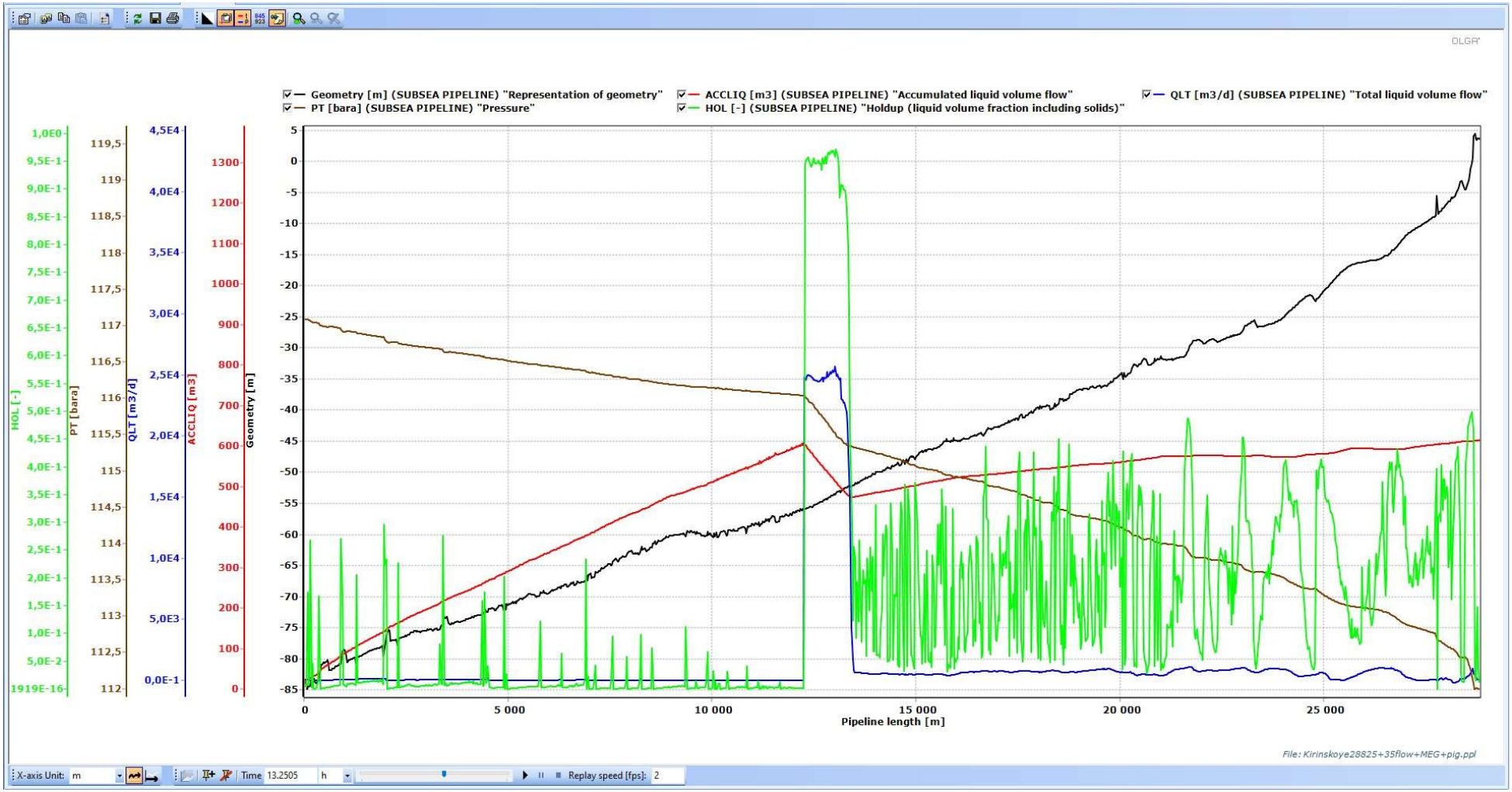

Figure B.21. Pig run, part 2 of 3 (1,25 hours since the pig launch; $3{,}5 \cdot 10^6$ m^3/day)

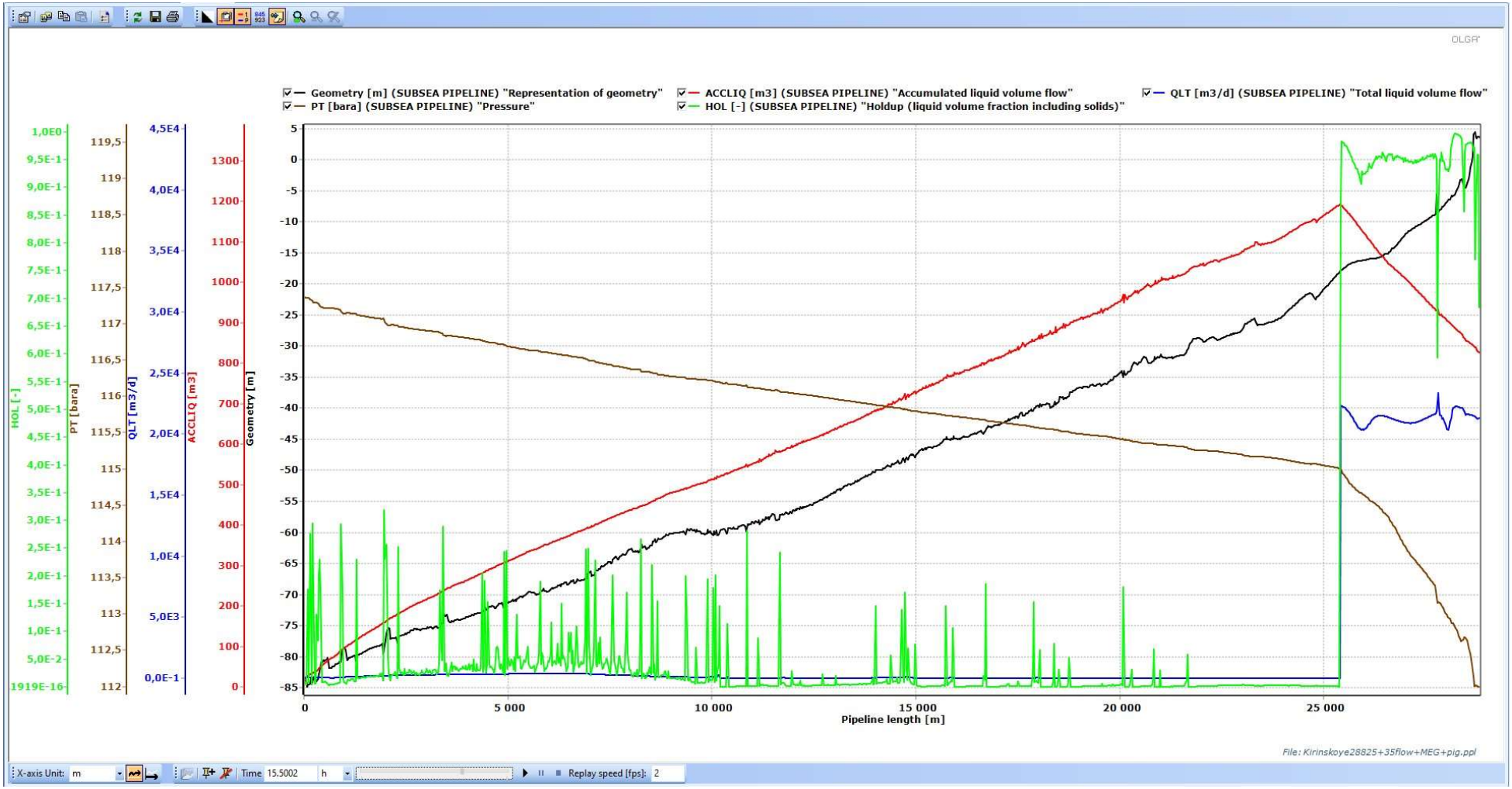

Figure B.22. Pig run, part 3 of 3 (2,5 hours since the pig launch; $3{,}5 \cdot 10^6$ m^3/day)

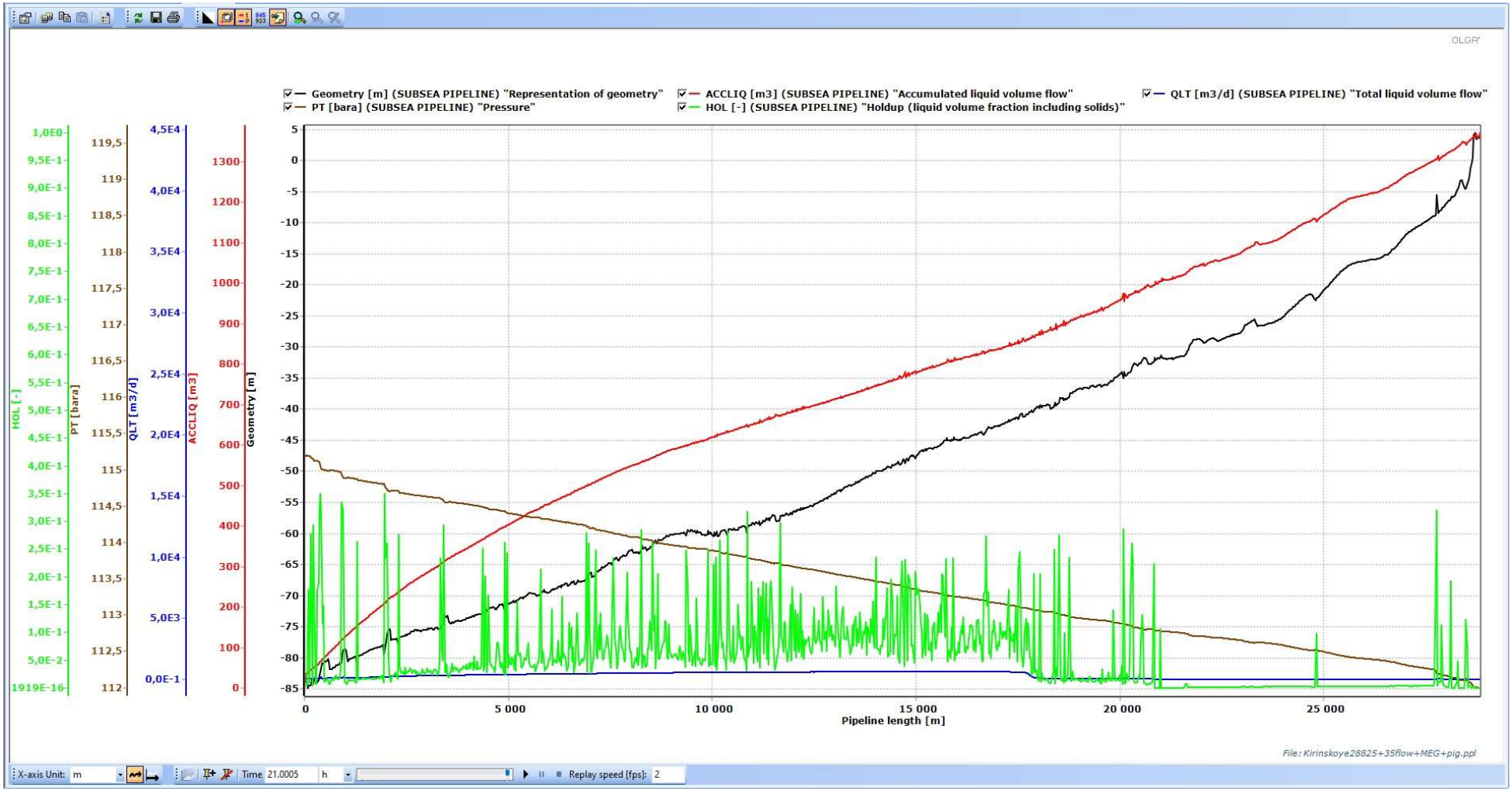

Figure B.23. After-run distribution of pressure and holdup liquid in the system & changes in the accumulated and current liquid volume flow ($3{,}5 \cdot 10^6$ m^3/day)

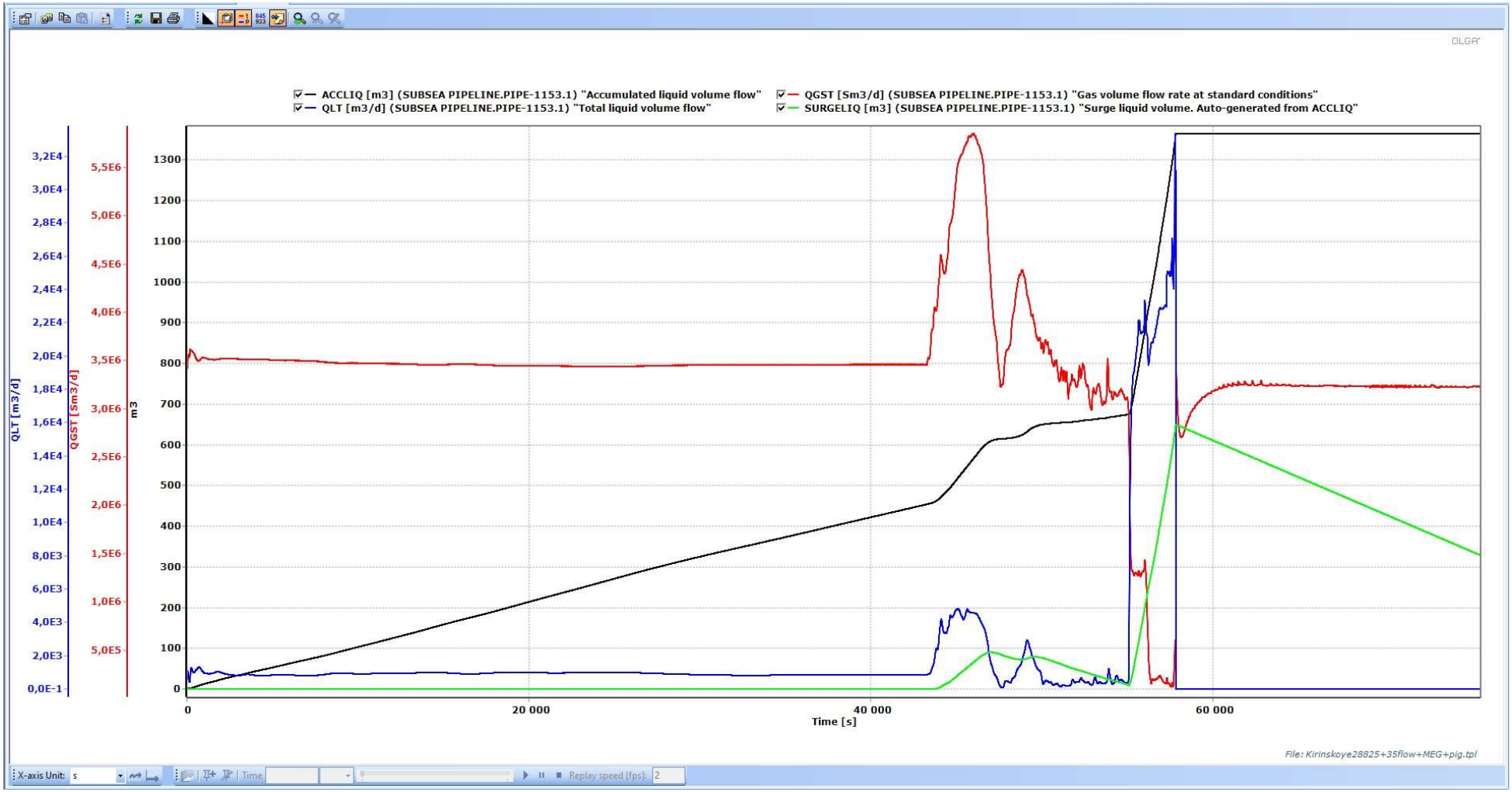

Figure B.24. Liquid trend plot in the end-point for the entire simulation timespan ($3{,}5 \cdot 10^6$ m^3/day)

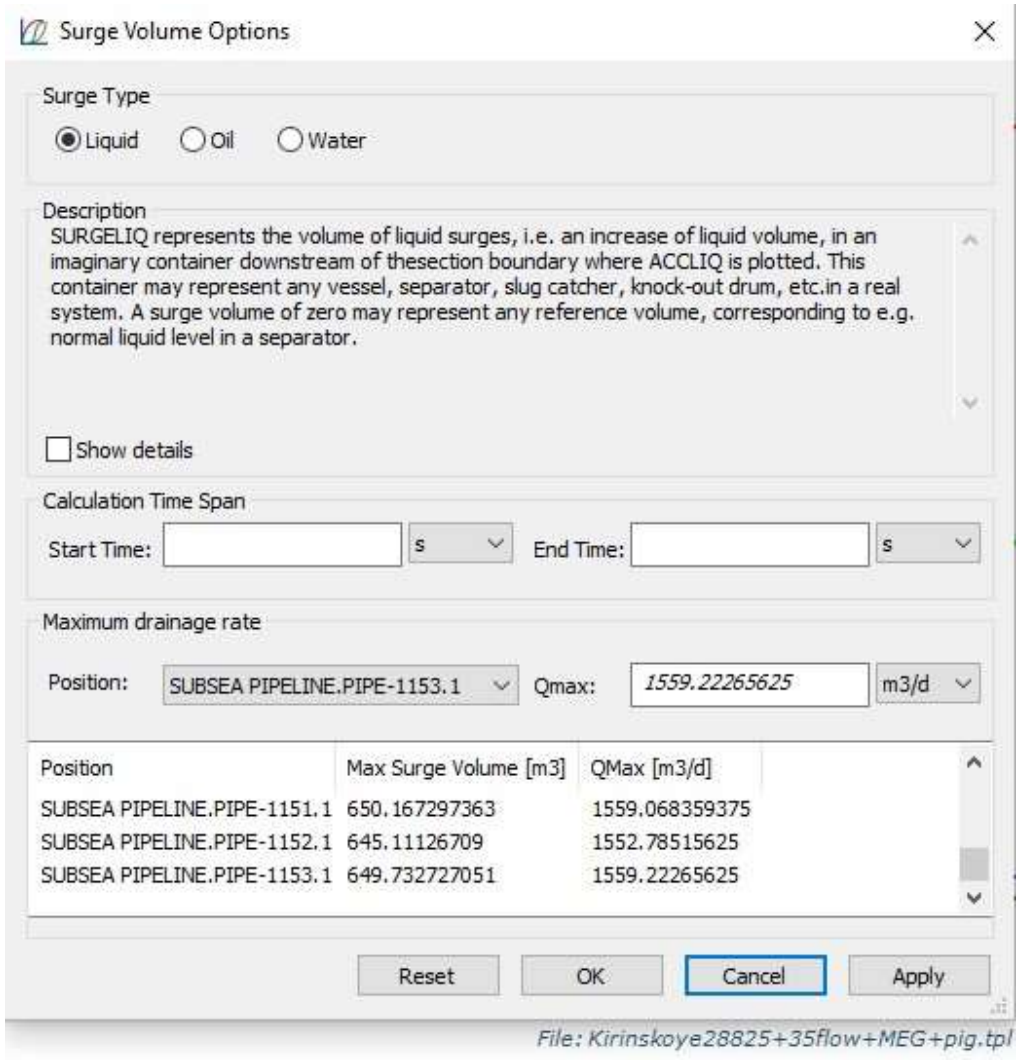

Figure B.25. Precise maximum liquid surge volume and maximum liquid surge rate calculated by OLGA's Surge Volume interface
(pig run simulation for the $3{,}5 \cdot 10^6$ m^3/day)

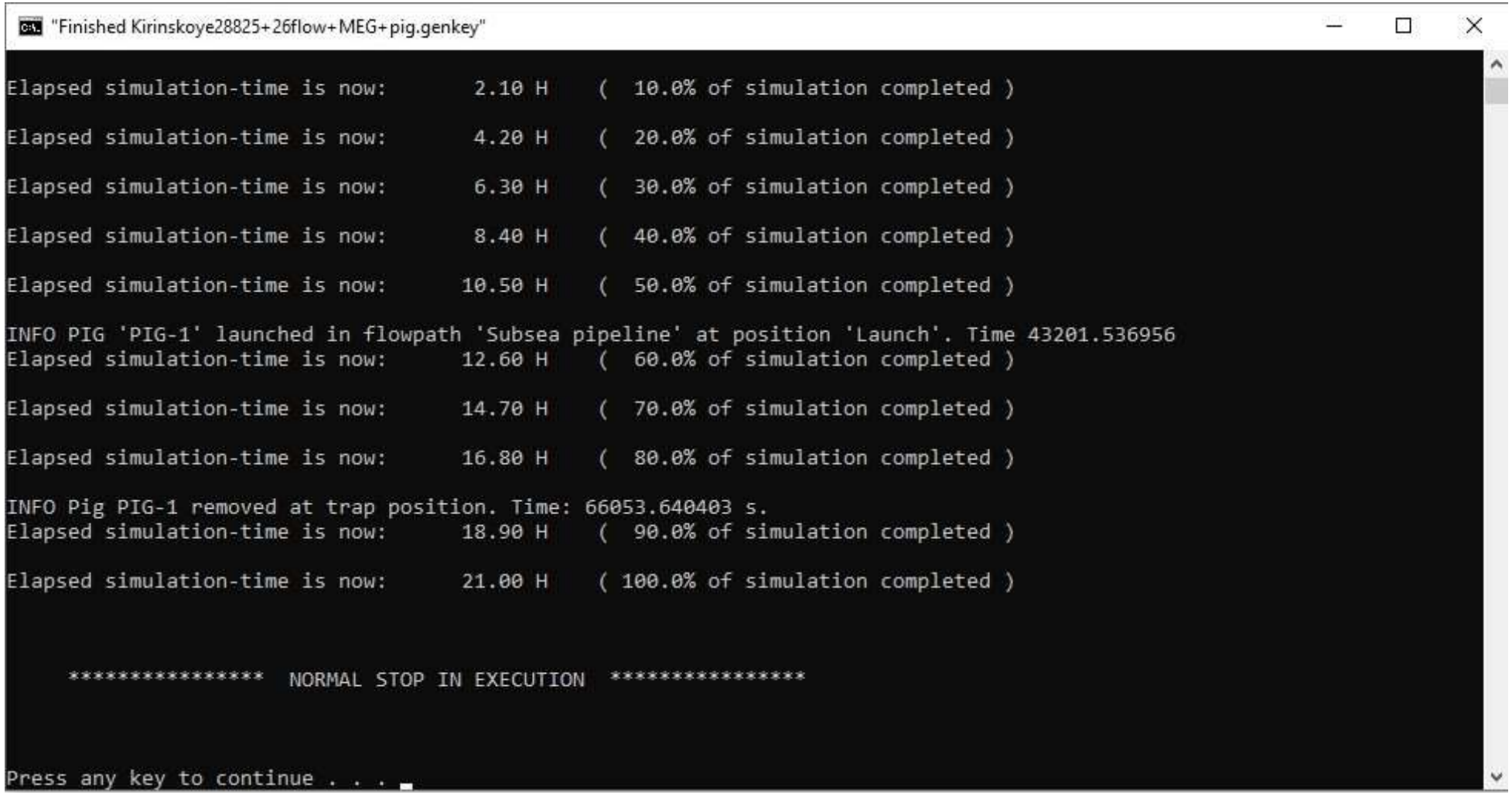

Figure B.26. Pig launch and removal time, simulation for the $2{,}64 \cdot 10^6$ m^3/day flow

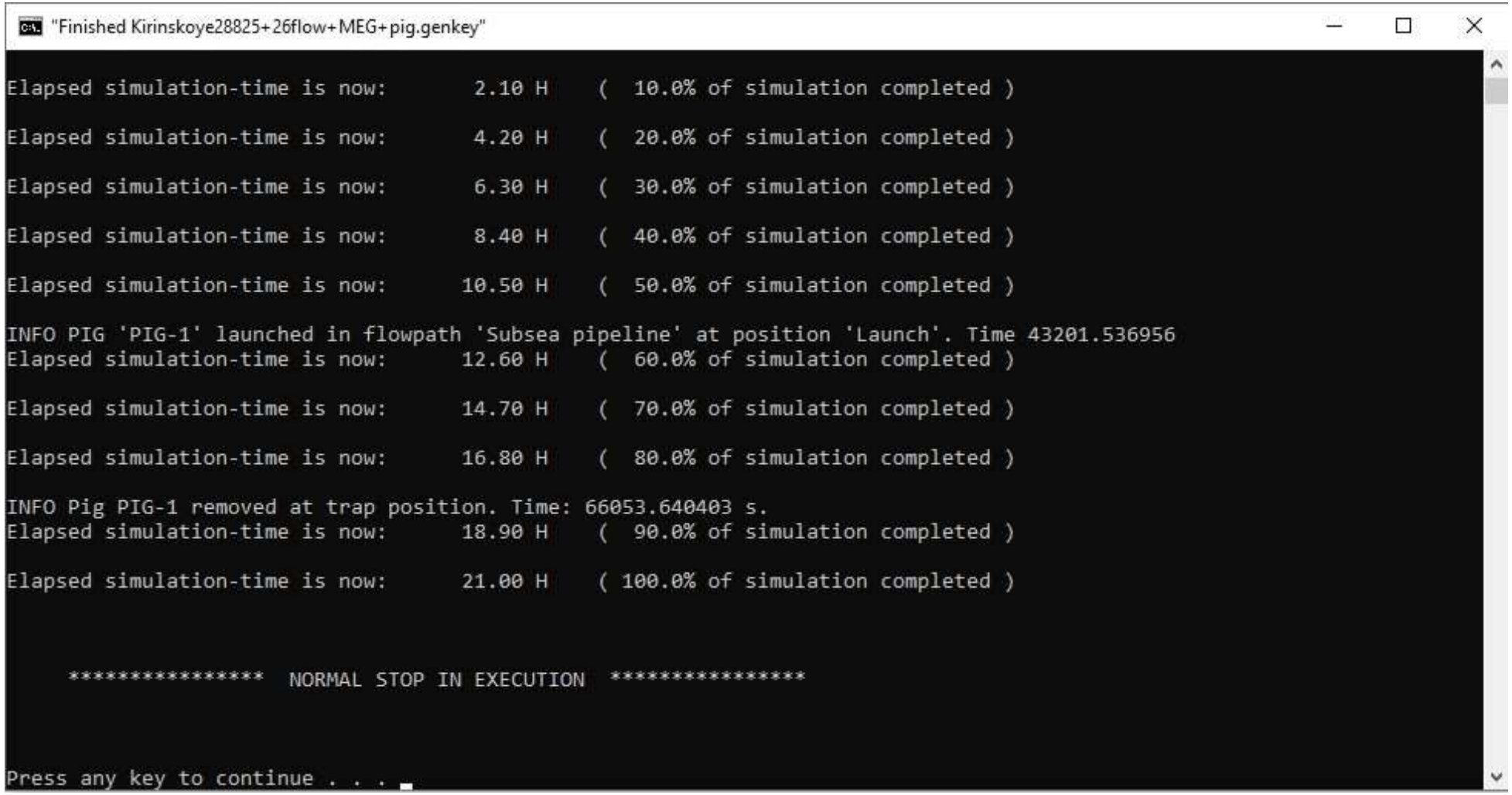

Figure B.27. Pig launch and removal time, simulation for the $3{,}5 \cdot 10^6$ m^3/day flow